VALIDATION OF THE OR103-1/5 INTERGENIC SEQUENCE AS A MOLECULAR TOOL TO PROMOTE BI-CISTRONIC TRANSLATION IN ZEBRAFISH

by

Kerem Uzel

B.S., Molecular Biology and Genetics, İstanbul Technical University, 2011

Submitted to the Institute of Graduate Studies in

Science and Engineering in partial fulfillment of

the requirements for the degree

Master of Science

Graduate Program in Molecular Biology and Genetics

Boğaziçi University

2014

ABSTRACT

VALIDATION OF THE OR103-1/5 INTERGENIC SEQUENCE AS A MOLECULAR TOOL TO PROMOTE BI-CISTRONIC TRANSLATION IN ZEBRAFISH

Sensory neuron in the olfactory system, typically expresses only a single olfactory receptor (OR) gene from a large and diverse genomic repertoire. In zebrafish, a violation of this 'one neuron – one receptor rule' has been identified with the systematic coexpression of two linked ORs. In previous studies we have provided evidence that coexpression of OR103-1 and OR103-5 genes results from a failure to terminate transcription at the end of the upstream OR103-1 gene. We hypothesized that this unusual situation may lead to cotranslation of both OR genes by the same OSN through the presence of an internal ribosome entry site (IRES) within the OR103-1/5 intergenic region. The hypothesis was tested *in vitro* and *in vivo* by using dual-reporter constructs that contain renilla and firefly luciferase or two fluorescent reporter genes linked by the 1.4 kb intergenic region. Strong firefly and renilla luciferase activity in transfected HeLa cells suggests that the intergenic sequence may contain IRES activity in addition to cryptic promoter activity in the heterologous system. In transient transgenic zebrafish embryos injected with dual-reporter constructs a high correlation of GFP and mCherry fluorescence was observed in individual cells. Reporter gene coexpression was not restricted to olfactory tissue and was observed in other tissues when appropriate promoters were used. Colabeling was severly reduced when the reporter genes resided on different plasmids or when a polyadenylation signal was placed downstream of the first reporter. Substitution of the intergenic region with a different promoter equally abolished colabeling. In a final experiment we tried to coexpress OR proteins and fluorescent markers with the help of the bi-cistronic expression system. Forced overexpression of an OR gene in OSNs resulted in convergence of transgenic axons within the olfactory bulb. Under the influence of a strong enhancer, a subpopulation of axons converged onto novel glomeruli that were not present in control constructs that did not contain an OR sequence. In summary, the OR103-1 / 5 intergenic region promotes cotranslation of two linked gene coding sequences from a single transcript and can be used for successful coexpression of a marker gene and a gene of interest.

ÖZET

ZEBRABALIĞINDA OR103-1/5 GENLERİ ARASINDAKİ DİZİNİN İKİ SİSTRONLU PROTEİN ÇEVRİMİNİ SAĞLAYAN BİR ARAÇ OLARAK DOĞRULANMASI

Koku alma sisteminde mevcut olan her bir sinir hücresi geniş ve çeşitli bir yelpazeden yalnızca bir tane koku almaç genini ifade eder. Ancak zebrabalığı koku alma sisteminde bu kurala istisna teşkil eden bir vaka OR103-1 ve OR103-5 genlerinin eşzamanlı ifade edilmesinin tespitiyle ortaya çıkarılmıştır. İki gen arasındaki eşzamanlı ifadenin dizgeli tabiatından dolayı bu düzenin iki gen arasındaki dizilimden kaynaklandığı varsayımını oluşturduk. Tek bir diziden çift gen ifade edilmesine imkan tanıyan vektörler vasıtasıyla varsayımımız öncelikli olarak hücre kültüründe sınandı. HeLa hücrelerinde gerçekleştirilen deneylerin sonuçları OR103-1/5 genleri arasındaki dizinin IRES (dahili ribozom giriş mevki) işlevine sahip olduğunu gösterdi. Ardından, iki muhbir protein arasına klonlamak suretiyle OR103-1/5 genleri arasındaki dizinin zebrabalığı embriyolarında OR103-1 ve OR103-5 gen bölgesinin davranışını tekrar edebilme yeteneği sınandı. Koku alma sistemi içerisinde ve dışarısında mevcut sinir hücresi kümelerinde, muhbir proteinler arasında görülen yüksek eşzamanlı etiketlenme oranları OR103-1/5 genleri arasındaki bölgenin aynı dizi üzerindeki iki adet proteini birlikte ifade ettirme kabiliyetini doğruladı. Muhbir proteinlerin farklı DNA parçalarına bölünmeleri veya RNA dökümünün polyA (çoklu adenilleme) dizisi ile zoraki sonlandırılması muhbir proteinler arasında görülen eşzamanlı etiketlenme oranlarını önemli ölçüde tahrip etti. Öte yandan, aynı deney düzeneğinde OR103-1/5 genleri arasındaki dizinin bir başka promotör bölgesi ile takası, benzer düzeyde eşzamanlı etiketlenme oranları temin edemedi. Ardından vektörlere koku almaç proteini kodlayan diziler eklendiğinde zebrabalığı beyninde muhbir proteinlerce görselleştirilen nöronların bir kısımının oluşturduğu yeni küresel yapılar meydana geldi. Nihai olarak, transgenik koku almaç proteinlerinin koku alma sinirlerindeki mevcudiyeti, Myc-etiketine karşı yapılan boyama deneyleriyle ispat edildi. Böylelikle, transgenik koku almaç proteinlerinin belirli bir koku alma siniri kümesine takdimi OR103-1/5 genleri arasındaki dizinin kullanılması ile gerçekleştirildi.

TABLE OF CONTENTS

LIST OF FIGURES

LIST OF TABLES

LIST OF ACRONYMS / ABBREVIATIONS

BAC	Bacterial Artificial Chromosome
bp	Base Pair
cAMP	Cyclic Adenosinemonophosphate
cDNA	Complementary Deoxyribonucleic Acid
DNA	Deoxyribonucleic Acid
EMCV	Encephalomyocarditis Virus
Gap43	Growth Associated Protein-43
GFP	Green Fluorescent Protein
GPCR	G-protein-coupled Receptor
IRES	Internal Ribosome Entry Site
kb	Kilobase Pair
mRNA	Messenger Ribonucleic Acid
OB	Olfactory Bulb
OE	Olfactory Epithelium
OMP	Olfactory Marker Protein
OR	Odorant Receptor
OSN	Olfactory Sensory Neuron
PBS	Phosphate Buffered Saline
PCR	Polymerase Chain Reaction
RNA	Ribonucleic Acid
UTR	Untranslated Region

1. INTRODUCTION

1.1. The Olfactory System

Chemosensation is one of the fundamental sensory processes that is found in almost all organisms, present from bacteria to the most complex life forms. In its more primitive forms such as chemotaxis it functions as a means of survival by regulating the organisms' response to external stimuli. In higher organisms, chemosensory systems evolved to transform chemical information from their environment into signals that can be consciously and unconsciously interpreted by the nervous system. This interpretation allows organisms to identify food, mates, prey and predators (Prasad and Reed, 1999). The vertebrate chemosensory system, olfaction, is specialized for the detection of odorants and pheromones.

The first layer of olfactory information processing is the detection of olfactory cues, represented by a diverse array of environmental chemicals, through olfactory receptors (ORs), which are members of the seven transmembrane domain G protein-coupled receptor superfamily (Buck and Axel, 1991). The large number and chemical diversity of candidate odor molecules exerted a strong positive evolutionary pressure and resulted in a dramatic evolutionary expansion of OR genes. OR genes, typically, are among the largest gene families found in the genome of almost all organisms (Shi and Zhang, 2009). However, the size of the OR gene repertoire alone does not directly correlate with greater sensitivity and a better ability to discriminate odorants. For instance, known for their rich sense of smell, dogs were shown to have a limited OR gene repertoire when compared to mice or rats. The superiority of their olfactory abilities are thought to be related to the larger surface of their olfactory epithelium (OE) which harbors a larger number of olfactory sensory neurons (OSNs; Olender *et al.,* 2004; Malnic *et al.,* 2010). Similarly, behavioral tests revealed that primates, including humans, have good olfactory sensitivity in spite of their limited OR repertoire and OE surface (Laska *et al.*, 2000; Verbeurgt *et al.*, 2014). The underlying reason behind the elevated sense of smell in primates is suggested to be due to the comparably

higher number of glomeruli in their olfactory bulbs and larger brain regions that are involved in olfactory processing (Shepherd, 2004; Maresh *et al.*, 2008).

The high discriminatory power of the olfactory system mainly lies in the combinatorial coding scheme through which odor information is encoded by ORs. It has been demonstrated that a single OR typically detects multiple odorants (Zhao *et al.*, 1998) and that the same odorant may interact with multiple ORs. Thus, different odorants are recognized by different combinations of OR activation (Friedrich and Korsching, 1997; Malnic *et al.*, 1999). Consequently, the combinatorial use of ORs allows the identification of many different odorants/odorant mixtures by the olfactory system and drastically increases its sensitivity (Buck, 2005).

1.1.1. Anatomy of the Olfactory System

Odorants are detected in specialized structures of the peripheral olfactory organs. In vertebrates the peripheral olfactory organs are located in the nasal cavity, in close functional relationship with the respiratory system (Song *et al.*, 2013). The sensory tissue, that lines the nasal cavity is sensitive to inhaled chemicals and called the olfactory epithelium (OE). Bipolar neurons that are specialized in the detection of odorant chemicals are called olfactory sensory neurons (OSNs), which constitute the majority of cells in the OE. OSNs contain cilia on their apical dendrites, which extend into the nasal cavity and the interaction between ORs and odorants takes place at the surface of the cilia. Although the OR repertoire is very large and diverse, each individual OSN expresses only a single OR (refer to Section 1.3.1. for further details). OSNs project an unbranched axon to the olfactory bulb (OB), the first relay station in the brain. Critically, the axons of OSNs that express the same OR coalesce to form spherical structures, which are called the glomeruli, inside the OB (Buck, 2000). Thus, the internal representation of the external stimuli in the brain is generated through the expression of only a single OR per OSN and the specific convergence of axons from OSNs with different ORs into a large glomerular array.

In rodents, another peripheral chemosensory organ, called the vomeronasal organ (VNO), is thought to be specialized in the detection of pheromones and kairomones (Firestein *et al.,* 2001). Neurons in the VNO express receptors that belong to vomeronasal receptor families and project their axons to the accessory olfactory bulb (AOB; Belluscio *et al.,* 1999). The zebrafish peripheral olfactory system, on the other hand, does not possess two anatomically distinct neuronal pathways such as the main olfactory system and accessory / vomeronasal olfactory system, which are specialized for the detection and processing of two different types of behaviorally relevant chemicals: odorants and pheromones, respectively. Instead, its single peripheral olfactory organ contains different types of OSNs that differ from each other in terms of cell morphology, relative positions in the OE, and molecular marker gene expression. The peripheral olfactory organ of the adult zebrafish has a rosette-like appearance, which is formed through the folding of several lamella along the midline raphe (Hansen and Zeiske, 1998).

There are at least four different types of OSNs that reside in the zebrafish OE: ciliated, microvillus, crypt and kappe neurons (Hansen and Zeiske, 1998; Hamdani and Doving, 2007; Ahuja *et al.,* 2014). All of these cells project their axons to the same OB through the tightly bundled olfactory nerves (Yoshiara, 2009). Although these cell types are intermingled within the sensory surface of the olfactory rosette, each can be distinguished by their unique morphology and spatial position within the apical-basal dimension of the OE. With respect to their contribution to the entire OSN population, ciliated and microvillus OSNs are the major groups and more numerous, while crypt cells and kappe neurons are minor groups with less sensory neurons. Ciliated OSNs are located in the more basal layer of the OE and project a long dendrite bearing long cilia that reach to the lumen of nasal cavity, while microvillus OSNs have a more apical position of their soma, shorter dendrites and microvilli that extend from their apical dendrites (Thommesen *et al.,* 1983; Yamamoto and Ueda, 1978; Hamdani *et al.,* 2001; Hansen *et al.,* 2003; Sato *et al.,* 2005; Oka *et al.,* 2011). Crypt cells are located in the most apical layer and have large, globose cell bodies equipped with both cilia and microvillae (Hansen and Zeiske, 1998). Most recently, a new OSN population in zebrafish has been identified with the kappe neurons which are morphologically related to crypt neurons but with a slightly different morphology and spatial distribution compared to crypt cells (Ahuja *et al.,* 2014).

Different types of OSNs express different families of chemosensory receptors. Ciliated OSNs express receptors of the OR and TAAR families, while microvillous OSNs express V1R and V2R genes (Mombaerts *et al.,* 1996; Wagner *et al.,* 2006). Crypt cells express a single V1R-related ORA4 gene (Oka *et al.,* 2011) and project to a single dorso-medial glomerulus. Kappe neurons have also been shown to project to a single, distinct glomerulus in the dorso-medial cluster, suggesting that they also express a single chemosensory receptor gene (Ahuja *et al.,* 2014). In addition, specific molecular markers for each type of OSNs have been described. Mature ciliated OSNs are known to express the zebrafish homologue of the olfactory marker protein (OMP; Celik *et al.,* 2002), while microvillous OSNs express the transient receptor potential channel C2 (TRPC2; Sato *et al.,* 2005). Crypt cells are shown to be immunoreactive to TrkA and S-100 calcium binding protein (Catania *et al.,* 2003, Germana *et al.,* 2004) while kappe neurons are identified by their G_o-like immunoreactivity (Ahuja *et al.*, 2014). However, neither of these cells appear to express the related antigen and specific labeling might arise from cross-reactivity with as of yet unidentified markers.

The organization of the zebrafish OB is very stereotyped, similar to its vertebrate counterpart. The initial study to identify glomeruli in the adult zebrafish OB was conducted in 1994 by Baier and Korsching using DiI tracing from the OE, a neuronal tracer dye that is retained in lipid bilayers. The dye is transported anterogradely from the OE to the OB and thereby reveals the entire population of glomeruli. Approximately 80 glomeruli were consistently identified by their stereotyped position and morphology and their bilateral symmetry in the left and right OB. In a more recent study, Braubach *et al.* (2012) labeled different OSN types using specific antibodies against general neuronal markers, such as G-protein α subunits and calcium binding proteins. The approach mentioned above, allows them to identify approximately 140 glomeruli in each adult zebrafish OB by their anatomical distribution of in specific regions of the olfactory bulb. Those glomeruli can be classified into two groups: a small subset, 27 glomeruli, that are clearly distinguishable in all of the individuals, and a larger group that is made up of smaller, anatomically non-identifiable glomeruli within larger clusters of glomeruli, which seems to have imprecise boundaries and display overlapping innervation.

1.2. Odorant Receptor Repertoire

1.2.1. Types of Odorant Receptors

As previously described, there are two anatomically distinct organs in peripheral olfactory system named as main olfactory epithelium (MOE) and the vomeronasal organ (VNO). Initially, it was thought that the VNO and MOE have distinct functions, such as detecting odorants and pheromones, respectively (Dulac, 1997; Buck, 2000). Later, however, it has been shown that both systems can detect both types of ligands (Malnic *et al.*, 2010). The MOE and VNO both express their own characteristic type of chemoreceptors to recognize different chemicals. Odorant receptors (ORs) and trace amine-associated receptors (TAARs) are expressed in sensory neurons in the MOE (Buck and Axel, 1991; Liberles and Buck, 2006), while detection in VNO is mediated through two different gene families of vomeronasal receptors: V1Rs and V2Rs (Dulac and Axel, 1995). Consequently, the repertoire of olfactory receptor genes currently includes four different gene families: ORs, TAARs, V1Rs and V2Rs; all of which belong to the larger family of G protein-coupled receptors (GPCRs). Interestingly, early vertebrates that lack a separate VNO, such as fish, all of four receptor families are expressed in the same peripheral OE, suggesting the separation of these distinct chemosensory subsystems later in evolution.

The odorant receptors were initially discovered in 1991 through groundbreaking studies by Linda Buck and Richard Axel and their characterization of 18 rat odorant receptor genes (Buck and Axel 1991). New approaches in genome sequencing and bioinformatic gene identification have revealed the full extent of the OR gene repertoire and confirmed the findings by Buck and Axel. It is now beyond doubt that the OR gene family constitutes the largest gene family in vertebrate genomes (Alioto and Ngai, 2005; Niimura and Nei 2005; 2006; 2007; Grus *et al.*, 2007). ORs belong to the rhodopsin-like subclass of GPCRs, class A, which have short N- and C- termini outside seven-transmembrane domain. Similar to other class A GPCRs, ligand binding is thought to take appear in pockets formed by the transmembrane helices. One candidate pockets is formed by the third, fifth and sixth transmembrane domains (Emes *et al.*, 2004) while a second one is formed by TM3 through

TM7 (Liu *et al.,* 2003). The coding region of ORs is contained within a single large exon and consists of approximately 1000 nucleotides. The overall number of functional OR genes varies significantly between species. In mammals the size of the expressed OR repertoire ranges between 262 and 1207 for platypus and rat, respectively (Grus *et al.,* 2005; Niimura and Nei, 2007). The OR repertoire of the mouse comprises 1035 intact and 356 nonintact (truncated & pseudogenes) genes (Niimura and Nei, 2007). The proportion of intact and pseudogenes also varies across species, pseudogenes constitute 13.1% of the total mouse OR repertoire (Zhang *et al.,* 2007); however, any correlation between pseudogenes to repertoire proportion and the ability of discriminating odorants across species could not be found (Zhang and Firestein, 2009). OR genes can be found on all chromosomes of the mouse genome in forms of isolated genes and tight clusters, except chromosome 12 and the Y chromosome (Zhang and Firestein, 2002). Among the 43 identified clusters, the largest one is located on chromosome 2 comprising 344 ORs (Zhang *et al.,* 2007) while isolated genes occur very rarely and make up only 1.5% of the OR repertoire (Zhang and Firestein, 2009). The size of the OR gene repertoire is smaller in fishes compared to birds and mammals. The zebrafish OR repertoire comprises 161 intact and 18 pseudogenes (Alioto and Ngai, 2005; Niimura and Nei, 2005). In fish, the genomic distribution of OR genes resembles the situation in mammals: most OR genes are organized in clusters on most chromosomes and isolated single genes are rare (Alioto and Ngai, 2005). Subfamily members of ORs generally have the same transcriptional orientation within clusters, indicating tandem duplication as a possible gene expansion mechanism (Korsching, 2009).

The second type of chemosensory receptors that are expressed in MOE are TAARs. Like ORs, TAARs also belong to class A GPCRs. TAARs resemble OR genes in their lack of introns within the coding sequence and similar nucleotide lengths. In addition, the expression profile of TAARs also resemble OR expression patterns (Liberles and Buck, 2006). However, even though the two types of chemosensory receptors are coexpressed in the same sensory epithelium, they are not coexpressed at the level of individual neurons (Liberles and Buck, 2006). In the mouse, 15 intact and 1 pseudo TAAR genes have been identified (Grus *et al.* 2007). On the other hand, the TAAR gene repertoire of the zebrafish consists of 119 members (109 intact and 10 nonintact genes; Hashiguchi and Nishida, 2007). Interestingly, different from other odorant receptor gene families, the TAAR gene family is

the only one which has a larger repertoire in zebrafish when compared to mammals, suggesting a strong selective pressure which may be related to the elevated importance of biogenic amine odorants, the general ligand for TAARs, for fish compared to tetrapods (Shi and Zhang, 2009).

In rodents, two different chemosensory receptor families are expressed in the VNO. One of them, the V1R family, is not formally classified but resembles to class A receptors. Similar to ORs and TAARs, V1Rs contain intronless coding regions. Interestingly, the size of the V1R gene family shows great variation among species; the repertoire size can vary up to 34-fold among mammals with functional VNOs (Grus *et al.*, 2007). 191 intact and 117 nonintact V1R genes have been identified in the mouse genome (Zhang *et al.*, 2007). In fishes, contrary to mammals, the size of the V1R-like repertoire as well as its variation among species decrease drastically (Hashiguchi and Nishida, 2006; Saraiva and Korsching, 2007; Shi and Zhang, 2007). Since zebrafish do not have a separate VNO structure, homologs of V1Rs, the ORA genes, are expressed in the same olfactory epithelium as ORs and TAARs. The class term ORA is an abbreviation for “olfactory receptor gene related to class A of GPCRs”. The zebrafish ORA gene family is relatively small and comprises only 6 members (Saraiva and Korsching, 2007).

The second type of vomeronasal receptors, the V2Rs, belong to class C GPCRs with their class-specific large, extracellular N-terminal domain that most likely forms the ligand binding pocket (Korsching, 2009). Unlike the other three receptor families, the coding sequence of V2Rs is spread out on multiple exons (Dulac and Axel, 1995; Matsunami and Buck, 1997). The V2R repertoire is found to be frequently lost in terrestrial vertebrates; at least three independent losses of the entire V2R gene repertoire have been detected in mammals, which typically go along with a parallel loss of the entire VNO (Shi and Zhang, 2007). However, the repertoire is large in rodents, the mouse V2R repertoire comprises 121 intact and 158 pseudogenes (Shi and Zhang, 2007; Young and Trask, 2007). Interestingly, the family is also expanded in teleosts. The closest relatives of mammalian V2Rs in zebrafish belong to the family of OlfC receptors, which are also class C of GPCRs. With 44 intact genes and 8 pseudogenes, the OlfC repertoire of zebrafish is the largest known among

teleosts (Alioto and Ngai, 2006; Hashiguchi and Nishida, 2006) and is in the range of mammalian V2R repertoires.

1.2.2. Class Distinction in Odorant Receptors

ORs can be phylogenetically separated into two broad classes based on amino acid sequence differences: the Class I ORs and the Class II ORs. The class I ORs were initially identified in fish (Ngai *et al.*, 1993) and in frog (Freitag *et al.*, 1995) and their presence in the mammalian genome was considered an evolutionary remnant (Freitag *et al.*, 1998). However, Class I ORs in human and mouse genomes make up a significant proportion of the entire OR gene repertoire (Glusman *et al.*, 2001; Zhang and Firestein, 2002) indicating an important function of these genes in mammalian olfaction. Class I ORs constitute approximately 10% of the OR repertoire in mammals and are found in a single large cluster in mouse and humans (Zhang and Firestein, 2002), suggesting an ancient evolutionary origin. The OR gene repertoire of zebrafish almost entirely comprises Class I ORs or ORs that are phylogenetically close (Alioto and Ngai, 2005).

Class II ORs are thought to be unique to terrestrial vertebrates: they make up 90% of the mammalian OR repertoire, are similar in number as Class I ORs in semiaquatic animals (Freitag *et al.*, 1998), and are very rare in teleosts (Korsching, 2009). There might only be a single class II-related OR gene in the zebrafish genome (Alioto and Ngai, 2005; Niimura and Nei, 2005; Tınaztepe, 2009). Therefore, a specialization between Class I and Class II ORs seems to exist at detecting water-soluble and volatile odorants, respectively. As a matter of fact, Class I ORs were shown to be responsive to water soluble odorants such as aliphatic acids, aldehydes and alcohols (Malnic *et al.*, 1999; Kobayakawa *et al.*, 2007).

1.3. Expression of Odorant Receptors

1.3.1. Odorant Receptor Gene Choice

1.3.1.1. Monogenic Expression. One key feature of the the mammalian olfactory system is that every single OSN that expresses only one OR gene from the entire repertoire (Malnic *et al.,* 1999). This feature is referred as the one receptor – one neuron rule (Mombaerts, 2004). Over the past decades different studies using various approaches are conducted which directly or indirectly confirmed this hypothesis.

One of the evidences of 'one receptor – one neuron' rule stems from absolute and relative cell counts of OSNs expressing a given OR after their visualization by *in situ* hybridizations. The OR gene repertoire is around 1000 and 1200 genes in mouse and rat, respectively (Nimura and Nei, 2007), while the reported number of mature OSNs that express olfactory marker protein (OMP) in three-week old and adult rats amounts to 22 and 15 million cells, respectively (Meisami, 1989; Youngentob *et al.,* 1997). So, if one neuron expresses only one OR gene, the expected absolute cell counts for each OR gene should be around several thousands of OSNs per organism, comprising on average 0.1% of the total number of OSNs. This is indeed the case for several OR genes in both mouse and rat (Ressler *et al.,* 1993; Strotmann *et al.,* 1994; Kubick *et al.,* 1997; Royal and Key, 1999; Iwema *et al.,* 2003).

OSNs that express a given OR are found to be scattered within a confined zone in MOE (refer to Section 1.3.3. for further details). There are four larger zones; and theoretically, approximately one-fourth of the total repertoire should be expressed in each quadrant of the OE. One fourth of the OR repertoire would amount to approximately 250 and 300 genes in mouse and rat, respectively (Niimura and Nei, 2007). Thus, the expected frequency of cells expressing a given OR gene among all of the mature OSNs in one of the defined zones should be around 0.4%. Interestingly, the observed frequencies are around 0.3-0.7% for two mouse genes (Ressler *et al.,* 1993) and around 1.3 to 1.9% for two rat genes (Strotmann *et al.,* 2004). Similarly, the number of OSNs expressing a single OR

approximately constitute 0.1% of all OSNs in mouse (Vassar *et al.,* 1994) and around 0.5-2% in zebrafish (Chess *et al.,* 1992) supporting the singular OR expression of OSNs.

In addition, results of double *in situ* hybridization assays, visualizing the expression patterns of two OR genes simultaneously also support the 'one neuron – one receptor rule. When sequential OE sections are exposed to gene-specific and degenerate family-specific probes at the same time, the total number of cells that stain positive for family-specific probes are equal to the sum of the cells that are labeled with gene-specific probes (Kubick *et al.,* 1997). Additionally, three mouse OR genes within the same cluster are shown to be expressed in a mutually exclusive manner through double *in situ* hybridizations (Tsuboi *et al.,* 1999). A systematic and comprehensive test of the 'one neuron- one receptor' rule by these means is difficult because of the very large number of possible combinations of OR genes that could potentially be coexpressed.

A direct approach to test the one receptor – one neuron rule was conducted by reverse transcription polymerase chain reaction (RT-PCR) on individual OSNs. While the experimenters could not amplify any OR gene in around 50% of the cells, they could only detect a single receptor in the other half (Malnic *et al.,* 1999). In line with this observation, the responsiveness of the OSN to odorants matches the OR gene that was amplified by RT-PCR (Touhara *et al.,* 2000; Kajiya *et al.,* 2001). If an OSN expresses only a single OR gene, then it should only respond to the set of odorants that is capable of binding to that specific OR. Consequently, by changing the OR that a single neuron expresses, a shift of the set of odorants that could excite the neuron should be expected. Bozza and his colleagues were able to alter the responsiveness of OSNs from acetophenone and benzaldehyde to octanal and aliphatic aldehydes by changing the expressed odorant receptor in that set of OSNs from M71 to I7, thereby indirectly confirming the one receptor – one neuron rule (Bozza *et al.* 2002). Additionally, the number of glomeruli that are specific for each OR within the MOB correlates with the number of OR genes in the mouse genome providing indirect support to the rule (Bozza *et al.* 2009). Each OSN population that is defined by the expression of a given OR typically converges their axons onto two glomeruli per OB and there are roughly two times the number of glomeruli per OB as there are OR genes expressed in the OE.

1.3.1.2. Monoallelic Expression. Odorant receptor genes have also been shown to be expressed in a monoallelic fashion. The initial observation of monoallelic expression of ORs originated from reverse transcription polymerase chain reaction (RT-PCR) using various OSN pools (Chess *et al.*, 1994). Polymorphisms were identified in cDNA sequences of the I7 OR gene from two different strains of mice. When these two mouse strains were crossed and OSN pools isolated from the progeny, RT-PCR using primers that target polymorphic region of the I7 gene could amplify only one polymorphic allele, thereby indicating monoallelic expression of ORs (Chess *et al.*, 1994). The principle on monoallelic expression was directly demonstrated by DNA/RNA *in situ* hybridizations in OSN nuclei which revealed the mutual exclusion of endogenous MOR28 alleles at the transcriptional level (Ishii *et al.*, 2001). Moreover, when each allele of M71 gene is tagged with different fluorescent proteins in a transgenic mouse, colocalization of marker expression could not be observed in any OSN, providing further evidence for monoallelic expression as well as indicating its strict regulation (Li *et al.*, 2004). Typically, both alleles are expressed at equal rates: cell counts of tagged ORs show a 2:1 ratio between homozygous and heterozygous mice, respectively; confirming the monoallelic expression of ORs in an indirect way (Mombaerts *et al.*, 1996).

1.3.2. Coexpression of Odorant Receptors

Although very few in number, it was shown in several studies that exceptions to the 'one neuron – one receptor' rule exists and that some OSNs express multiple ORs. These studies rely on single cell RT-PCR or *in situ* hybridizations and were able to detect coexpression at the RNA level. Therefore it is still unclear whether multiple ORs are translated into functional proteins in exceptional OSNs mentioned above.

The first systematic coexpression was reported in the rat with the I9 and HGL-SL2* OR genes. A modified 3'-RACE protocol was conducted on single OSNs and I9 and HGL-SL2 mRNAs are found to coexist in the very same OSN; coexpression of these genes was then confirmed by the detection of double-positive OSNs in double-label in situ

hybridization assays directed against the I9 & HGL-SL2 coding sequences (Rawson *et al.*, 2000). All of the OSNs that are HGL-SL-positive were also double-positive for I9, while, in contrast, a subpopulation of I9-positive neurons did not express the HGL-SL receptor. Another incidence of OR coexpression in OSNs was reported for the mouse septal organ. In order to track the development of OSNs in the septal organ; Tian and Ma conducted *in situ* hybridization assays targeting all 9 ORs that are dominantly expressed at different time points ranging from embryonic day 16 to postnatal 3 months (2008). Interestingly, a fraction of MOR256-3 expressing OSNs were found to be double positive for at least one of the other eight ORs. The portion of double-positive cells among MOR256-3 expressing OSNs was 2% and 0.2% at P0 (postnatal day 0) and in one month old mice, respectively (Tian and Ma, 2008). This decrease in the ratio of double positive cells from P0 to P30 disappeared when noses of mice were kept under sensory deprivation or in Bax null mutant backgrounds, in which apoptosis is disturbed. These results suggest neuronal activity as the reason and apoptosis as the underlying mechanism for the elimination of neurons that express more than one OR.

To date, only a single case of coexpression of OR genes has been reported in the zebrafish olfactory system (Sato *et al.,* 2007). In this study, double *in situ* hybridization assays were performed using probes that target different ORs belonging to two different subfamilies. Among these combinations, colocalization of signals was detected between OR 103-1 and OR103-5/2. The probes used in this study were not suitable to discriminate between the OR103-5 and OR103-2 genes due to the high sequence similarity (96.3%) of these genes. Interestingly, only a fraction of OR103-5/2-positive neurons were double positive for OR103-1, while every single OR103-1-positive OSN was also found to label for OR103-5/2 (Sato *et al.,* 2007). This systematic coexpression between two genomically linked OR genes suggests a possible regulatory involvement of the OR103-1/5 intergenic region which is the subject of this study.

However, the reported incidences of coexpression between OR genes remain rare in number and are typically regarded as exceptions to the rule. One reason for the rarity of identified examples may be related to the difficulty of their detection. The most informative

way to detect coexpression between two ORs is by double *in situ* hybridization with probes targeting two different ORs. But, the high number of OR genes is a formidable challenge for testing each combination of OR pairs, even in teleosts where the OR gene number is comparably limited. Consequently, identification of systematic coexpression between OR genes depends on chance. However, systematic coexpression that breaks the one neuron – one receptor rule could provide an interesting experimental window into the general mechanism of OR gene choice and monogenic expression of OR genes.

1.3.3. Zonal Expression of Odorant Receptors

As already described, a single OSN expresses only one OR gene out of a large and diverse repertoire (refer to Section 1.3.1. for further details). However, the probability of OR gene choice for a given OR is not identical for all OSNs that reside in MOE. Instead, OR gens are expressed in a zonal fashion. Initially, the existence of four different expression domains throughout MOE was shown. An OSN in a given zone may only express a subset of OR genes that are specific for this zone (Ressler *et al.*, 1993; Vassar *et al.*, 1994). However, recently it was shown that more than only four individual expression patterns exist for OR genes (Miyamichi *et al.*, 2005). It was suggested that a restricted zonal expression domain exist for each individual OR and that these domains are organized throughout the OE in a continuous and overlapping fashion (Norlin *et al.*, 2001a; Iwema *et al.*, 2003; Miyamichi *et al.*, 2005). In zebrafish, using 4 ORs, overlapping expression rings are revealed as the counterpart of zonal restriction mechanism identified in MOE (Weth *et al.*, 1996).

Although the molecular mechanisms underlying the zonal expression of OR genes are far from being understood, zone specific expression of various proteins have been identified. For instance, the axonal surface glycoprotein, olfactory cell adhesion molecule (OCAM), is expressed in the OE in a zone specific manner in the dorsal OE (Yoshiara *et al.*, 1997). It was also demonstrated in the same study that Zones II, III and IV are OCAM-positive, while the neurons that reside in the most dorso-medial part of the OE, zone I, lack OCAM expression. Furthermore, neurons in the OCAM-negative part of OE express O-MACS, a member of the medium-chain acyl-CoA synthetase (Oka *et al.*, 2003). Moreover, it is

suggested that O-MACS may be involved in the zonal segregation of OE due to the fact that it is expressed not only in neural populations in the dorsal part of OE but also in the supporting and basal cell layers unlike any other zone-specific genes. In another report a semaphorin receptor, Neuropilin-2, was shown to have a graded expression pattern in the OE (Norlin *et al.,* 2001b). Because most ORs are expressed in an overlapping and continuous manner throughout the dorsomedial/ventrolateral axis of the OE (Miyamichi *et al.,* 2005), graded Neuropilin-2 expression may be involved in patterning OR expression (Miyamichi *et al.,* 2005). Finally, it was reported that Class I OR's are confined to a subzone in the dorsal MOE and OSNs located in the dorsal zone differ by lineage and by cell type, which may lead to restricted choice of ORs: either Class I or Class II OR genes (Bozza *et al.,* 2009).

1.3.4. Transcriptional Regulation of OR Gene Expression

The establishment of monogenic and monoallelic expression of OR genes are not fully understood, and different models have been proposed over the past decades. One of the models comprised irreversible DNA alterations to express a single OR in analogy to immunoglobulin and T-cell receptor genes expressed in lymphocytes (Tonegawa, 1983; Jung and Alt, 2004). However, elegant experiments that utilized cloning a mouse by nuclear transfer from nuclei of M71-expressing OSNs rejected this hypothesis (Li *et al.,* 2004; Eggan *et al.,* 2004). Contrary to the expectation, the cloned mice did not have a monoclonal nose containing only M71-expressing OSNs. Rather, the expression pattern and organization of ORs in cloned mice was indistinguishable from wild-type animals. Therefore, it was concluded that the mechanism of OR gene choice does not involve irreversible DNA rearrangements (Eggan *et al.,* 2004; Li *et al.,* 2004).

1.3.4.1. Locus Control Regions. A study in 2002 revealed a 2 kb homology region while comparing mouse and human genomes which is located 75kb upstream of MOR28 cluster (Nagawa *et al.,* 2002). This homology region (H region) was then shown to be essential for expression of the MOR28 gene. When deleted from a yeast artificial chromosome transgenic construct expression of OR genes from the adjacent MOR28 cluster was abolished from the transgenic construct (Serizawa *et al.,* 2003). In the same study, when the H region was

relocated more closely to the MOR28 cluster, the number of OSNs expressing the proximal OR genes increased drastically, demonstrating a cis-acting effect of the H region on the MOR28 cluster similar to a locus control region (LCR; Serizawa *et al.,* 2003). Subsequently, another study proposed a trans-acting role of the H region on OR gene loci on different chromosomes. The authors demonstrated an apparent association of the H region with various olfactory receptor genes located on other chromosomes by the chromosome conformation capture technique (Lomvardas *et al.*, 2006). However, targeted deletions of the H region in knockout mice disproved the pan-enhancer model of H region by showing that it is not necessary for the expression of OR genes outside the MOR28 cluster. The deletion resulted in abolished expression of only three genes MOR28, MOR10 & MOR83, and reduced expression of MOR29A, MOR29B, MOR30A & MOR30B genes -all of them within the MOR28 cluster, demonstrating that H region only acts in cis but not in trans (Fuss *et al.*, 2007, Nishizumi *et al.*, 2007). In 2011, another candidate cis-acting LCR, the P Region, was identified and demonstrated to regulate expression of OR genes in P2 cluster in mouse (Bozza *et al.*, 2009; Khan *et al.*, 2011). Additionally, regions with similar LCR properties were found in zebrafish with the E-15-1 & E15-2 regions on chromosome 15 (Nishizumi *et al.*, 2007). Moreover, fusion of the mouse H region with proximal OR promoters in transgenic constructs was shown to dramatically increase the number of OSNs that are transgene-positive in zebrafish (Nishzumi *et al.*, 2007; Tastekin, 2012) suggesting the conservation of the mechanism which controls the OR gene choice probability across species.

1.3.4.2. Proximal Promoter Elements. In addition to LCRs, proximal promoter elements were also shown to be involved in regulation of OR gene expression. In the mouse, short transgenic constructs comprising 6.7 kb, 405 bp, 161 bp, 306 bp, or 298 bp upstream of different OR coding sequences are able to drive transgenic expression for M4, MOR23, M71, P3 & M72 genes, respectively, suggesting a regulatory roles of short-range cis-acting elements contained within these promoter sequences (Qasba and Reed, 1998; Vassalli *et al.*, 2002; Rothman *et al.*, 2005; Vassalli *et al.*, 2011; Plessy *et al.,* 2012). A bioinformatic analysis of these proximal promoter regions has demonstrated the presence of conserved regulatory motifs such as homeodomain (HD) and O/E transcription factor binding sites (Hoppe *et al.*, 2006; Michaloski *et al.*, 2006; Vassalli *et al.*, 2011; Plessy *et al.,* 2012).

Moreover, two homeodomain transcription factors, LHX2 and EMX2, were then shown to be critically involved in OR gene expression. In the mouse, a knockout mutation of Lhx2 resulted in a virtually complete loss of expression of all Class II OR genes while having only a minor impact on expression of Class I OR genes with two exceptions (Hirota *et al.*, 2007). Additionally, EMX2 was shown to be critical for transcription for a large but specific group of OR genes that were affected by Emx2 knock-out (McIntyre *et al.*, 2008). Transcription factors that bind to O/E like sites in OR gene promoters, such as Olf-1, and Lhx2 / Emx2, which bind to homoeodomain sites, are not exclusively involved in the regulation of OR gene expression but also have a wider impact on proper OSN development (Hirota and Mombaerts 2004, Kolterud *et al.*, 2004; Hirota *et al.*, 2007). Interestingly, identical regulatory sequence motifs that can be found within proximal promoter regions also appear to exist in LCRs. When the mouse H and P regions were analyzed, HD binding sites and an O/E site were identified (Vassalli *et al.*, 2011).

1.3.5. Negative Feedback Mechanism

A study in 2003 proposed a negative feedback model for monogenic OR gene expression, which claims that the expressed functional OR gene has a negative regulatory impact on other OR genes in order to maintain the one receptor - one neuron rule within OSNs (Serizawa *et al.*, 2003). In this study, the replacement of the MOR28 gene with a fluorescent reporter gene resulted in the coexpression of a large number of other OR genes in transgene-expressing OSNs. A similar phenotype was detected when the the MOR28 gene contained a frame-shift mutation instead of complete deletion of the coding sequence, suggesting that expression of a functional OR protein is a prerequisite to generate the negative-feedback signal (Serizawa *et al.*, 2003). The model is further supported by previous observations of coexpression between endogenous M4 gene and lacZ transgene -driven by M4 promoter- in 1% of OSNs (Qasba and Reed, 1998). Removal of the start codon from another OR coding sequence was also shown to be unable to produce the negative feedback signal, strengthening the concept that the origin of feedback signal is somehow linked to the OR protein instead of RNA transcription from an OR gene locus alone (Lewcock and Reed, 2004).

Thus, OSNs that are unable to produce a functional OR protein because the OR coding sequence has been deleted or otherwise rendered unfunctional could not produce a negative feedback signal to suppress expression of other OR genes. Instead, those cells undergo another round of OR gene selection, called 'second OR gene choice'. As a consequence of this heterogeneity in OR gene expression following second choice, the axons of those OSNs target different glomeruli in the OB, most likely to glomeruli that represent the ORs that were chosen as second choice (Serizawa *et al.*, 2003; Feinstein *et al.*, 2004; Bozza *et al.*, 2009). From the restricted pattern of axonal convergence of OSNs that undergo second choice, it is has been suggested that second choice is not random (Feinstein *et al.*, 2004). Later, it was shown in 2009 that second choice of OR is class restricted for class I and class II ORs. Axons of OSNs that are positive for a reporter gene that substitutes either a Class I and Class II OR innervated mutually exclusive and non-overlapping OB regions that are populated by either class I or class II-expressing OSN axons (Bozza *et al.*, 2009). Interestingly, when transgenic OSNs were forced to express β2 adrenergic receptor instead of an OR they form a new but specific glomerulus within the OB, suggesting that b2-AR can substitute for the OR in transgenic OSNs. However, replacing the ORs with V1R sequences did not lead to the formation of glomeruli (Feinstein *et al.*, 2004).

To further elucidate the target of the negative feedback signal, expression of OR proteins was driven under the control of TetO promoter which became active only in the presence of tetracycline transactivators (TTA). When TTAs was expressed in different subpopulations of OSNs with various promoters, no coexpression between endogenous and transgenic ORs could be observed, indicating that endogenous ORs can prevent the expression of transgenic ORs regardless of the nature of the promoter that drives their expression (Nguyen *et al.*, 2007). Thus, the presence of an OR coding sequence itself may be sufficient for the inhibition of transgenes by the negative feedback signaling.

Recently, it was proposed that the negative feedback signal produced by ORs is mediated by the activation of the unfolded protein response (UPR) in OSNs. The proposed model is based on the halt of translation initiation in immature OSNs through activation of

Perk and phosphorylation of eif2α following OR gene expression in the cell. It is followed by the selective translation of activating transcription factor 5 (ATF5) and transcription of Adcy3 which will abolish the UPR while locking in OR gene choice (Dalton *et al.*, 2013). Adcy3 expression also results in downregulation of lysine-specific demethylase 1 (LSD1), a protein which was previously shown to be involved in stochastic initiation of OR transcription (Lyons *et al.*, 2013).

In zebrafish, a bacterial artificial chromosome transgenic line carrying an OR gene cluster was generated to gain insight into the OR gene choice mechanism. The transgenic OR gene cluster comprises 16 OR genes from three different subfamilies and the coding regions of two OR genes from different subfamilies, OR 103-1 and OR 111-7, were replaced by fluorescent proteins. Similar to the observations in the mouse, substitution of the OR coding regions with fluorescent protein sequences forced the fluorescently tagged OSNs to undergo a second round of OR gene selection. Through *in situ* hybridizations, the OR genes expressed by reporter gene-positive OSNs are found to be restricted to OR members within the same subfamily of the cluster. This observation is different from the mouse where expression of OR, predominantly from other chromosomes was observed (Sato *et al.*, 2007).

1.4. Axonal Targeting of OSNs

1.4.1. Zone-to-zone Projection

One of the main features in the formation and maintenance of axonal connections between the OE and the OB is a zone-to-zone projection. Olfactory cell adhesion molecule (OCAM) which is differentially expressed in the ventral MOE (refer to Section 1.3.3. for further details); is also shown to exist in a divergent pattern in MOB. The first evidence of zone-to-zone projection was found in 1997. Axons of the OSNs found in OCAM-negative zone of MOE coalesce and form glomeruli within the domains of MOB that are OCAM negative (Yoshiara *et al.*, 1997). A similar case could be found in AOE; the targets of axons that originate from OSNs located in OCAM-positive and OCAM-negative zones of the vomeronasal organ, segregated within rostral and caudal zones in the AOB, respectively

(Yoshiara *et al.,* 1997). OCAM, however, is not the only factor which contributes to zone-to-zone projection. Through *in situ* hybridization and DiI staining experiments, Miyamichi and his colleagues reported that the expression pattern of ORs in the MOE along the dorsomedial/ventrolateral axis correlates with the location of corresponding glomeruli in the MOB along the dorsal/ventral axis (2005). One of the factors that regulate the correlation between DM/VL axis of MOE and D/V axis of MOB could be the axon guidance molecules Robo-2 and its ligands Slit-1 & Slit-3. Robo-2 expression in the MOE forms a gradient along the dorsomedial/ventrolateral axis from high to low, respectively. In addition, Robo-2's ligands Slit-1 & Slit-3 are also differentially expressed in the MOB along D/V axis, from low to high, respectively (Cho *et al.*, 2007), suggesting an important role of the Slit-Robo pathway in OSN axon pathfinding and zonal projection. Further evidence is provided for zone-to-zone projection from three OR genes within the same cluster: MOR28, MOR10 and MOR83. These OR genes have a random distribution pattern in the same zone within MOE; and via *in situ* hybridizations, axons of OSNs expressing these genes are found to project to distinct but proximal glomeruli (Tsuboi *et al.*, 1999).

1.4.2. Role of ORs in Axonal Guidance

Apart from their primary function of recognizing odorants, OR proteins themselves appear to have a role in axonal wiring of OSNs. The OR protein is present on axons and axon terminals of OSNs during the formation of glomeruli in OB (Barnea *et al.*, 2004; Mombaerts, 2006). The axonal guidance function of OR proteins was shown by swapping the coding regions of the P2 and M12 OR genes in gene-targeted mice (Mombaerts *et al.*, 1996). OR-swapped OSNs project their axons to topographically fixed glomeruli that are distinct from their wild-type P2 & M12 counterparts. The expansion of the same approach to different OR genes in various reports also resulted in the formation of novel, ectopic glomeruli (Wang *et al.,* 1998; Bozza *et al.,* 2002; Feinstein *et al.,* 2004). However, axonal projection towards the endogenous glomerulus was reported in gene swap experiments at the M71 & M72 gene loci (Feinstein and Mombaerts, 2004), indicating that OR protein is involved in the axon guidance process but is not the sole determinant.

The introduction of a transgenic OR many times produces novel glomeruli that are distinct from their endogenous analogues, especially when the transgenic OR is expressed in a zone that is different from endogenous expression of this OR. Critically, the shift in the D/V axis that is observed between transgenic and endogenous glomeruli correlates with the shift between expression zones in OE. For instance, the axons of transgenic M71-positive OSN that show a ventral shift in the OE converge onto more ventral glomeruli compared with their endogenous equivalents (Vassalli *et al.*, 2002). More interestingly, axons appear to reroute as axons expressing the endogenous M71 OR were found to target ectopic glomeruli predominantly formed by the coalescence of transgene expressing OSNs (Vassalli *et al.*, 2002).

The expression level of the OR has also been shown to affect axonal guidance of OSNs. When an internal ribosome entry site (IRES) was introduced directly upstream of the M71 coding region in order to decrease its expression level changes in the glomerular position were observed (Feinstein *et al.*, 2004). Since the IRES-mediated translation has a lower efficiency compared with the cap-dependent translation mechanisms (Weber and Koster, 2013), M71 protein level is expected to be reduced in OSNs which expresses the modified IRES:M71 allele. The overall reduction is estimated to be tenfold decrease, which could be validated from the signal intensity of reporter proteins. Decrease of OR expression levels resulted in the formation of a novel glomerulus which was located more anterior and more ventral when compared to the endogenous M71 glomerulus (Feinstein *et al.*, 2004), suggesting that the same OR can produce different axonal identities that depend on OR expression levels and which will lead to axon coalescence at alternative locations in the olfactory bulb.

A potential mechanism for the effect of OR expression levels was recently reported. Imai et al. showed that cAMP signals produced by the OR instruct axonal targeting of OSNs. Mutation of a conserved Asp-Arg-Tyr (DRY) tripeptide motif which is located within intracellular loop 5 of the OR protein and which mediates G protein binding results in a failure of glomerulus formation and axonal convergence (Imai *et al.*, 2006). The blockage of OR's initiation of cAMP cascade through the mutation is restored by the introduction of

PKA regulated transcription factors, signifying the role of G proteins in axonal targeting. It appears that baseline cAMP levels generated by GPCRs are determinants of axonal projections of OSNs (Nakashima *et al.*, 2013). Using activity mutants of the β2-adrenergic receptor, which can function as a surrogate OR (Omura *et al.*, 2013), it is shown that alterations in baseline GPCR activity resulted in differential expression of axon-targeting molecules and consequently changed glomerular positions along the anterior/posterior axis (Nakashima *et al.*, 2013).

1.4.3. Axonal Guidance Cues

In addition to the OR protein itself, classical axon guidance molecules have also been shown to affect glomerulus formation and position. In the mouse, the axon guidance receptor Neuropilin-2 (Nrp2) and its repulsive ligand Semaphorin-3F (Sema3F) were reported to influence the topographical order in MOB along the dorsal/ventral axis (Takeuchi *et al.*, 2010). It was shown that both, the receptor and the ligand, are differentially expressed by projecting OSN axons. During development, early formed glomeruli are located in the dorsal region of the MOB (Bailey *et al.*, 1999). Axons of early arriving neurons in dorsal zone of the OE secrete Sema3F in the anterodorsal part of MOB and eventually repel late arriving axons, which express Nrp2, from penetrating the dorsal OB (Takeuchi *et al.*, 2010). Thus, graded and complementary expression of Nrp2 and Sema3F guides the segregation of axons within the D/V axis. A different set of axon guidance molecules may regulate axonal interactions along the anterior/posterior axis. The genes coding for the homophilic adhesive molecules Kirrel2 & Kirrel3 and for the repulsive molecules ephrin-A5 and EphA5 were shown to be differentially expressed in an activity-dependent manner (Serizawa *et al.*, 2006). In agreement with activity-dependent sorting of OSN axons, the cyclic nucleotide-gated channel subunit OCNC1, is needed for proper formation of glomeruli and axon trajectories (Zheng *et al.*, 2000). Recently, it was also shown that in Robo1 knockout mice OSNs from the dorsal zone fail to project their axons to the dorsal OB. Thus, another set of repulsive signaling molecules, Robo1 and its ligand Slit, contribute to axonal targeting of OSNs. Interestingly, OSNs do not express Robo1 but olfactory ensheating cells (OECs) do, suggesting that neurons targeting the dorsal OB are innervated through OEC-guided OSN projection (Aoki *et al.*, 2013).

In zebrafish, live imaging of OSNs and their axonal projection was performed with single-cell resolution. Interestingly, the migration of axons seems to be direct, reaching their glomerular target without any detour or a stalling in a glomerulus along their path (Dynes and Ngai, 1998). These findings suggest that guidance cues may exist throughout the OB that guide OSN axons along their path (Miyasaka *et al.*, 2013). So far, three intercellular signaling pathways were found to affect projecting axons in zebrafish. Among the identified cues, the first one that is active in a chronological manner is Cxcl12/Cxcr4 chemokine signaling. The chemokine receptor *cxcr4b* is expressed in the olfactory placode during the initial phase of OSN axon pathfinding while its ligand, *cxcl12a*, is expressed along the telencephalon-placode border and the anterior part of the telencephalon (Miyasaka *et al.*, 2007). Similar to the mouse, Robo2/Slit-signaling has been shown to be another factor that during formation of neural circuitry in zebrafish. Robo is a transmembrane glycoprotein which is transiently expressed in the olfactory placode during early development. The repulsive ligand, Slit, which has 4 homologues in zebrafish, is expressed in a pattern that lines the trajectories of OSN axons. In *robo2* mutant fish, early projecting axons mistarget to ventromedial and posterior regions of the OE without penetrating into the OB (Yoshihara, 2009). Additionally, when endogenous Slit gradients were abolished through misexpression of Slit2 in transgenic fish, a misrouting phenotype was observed that was similar to the robo2 mutants (Miyasaka *et al.*, 2005). Finally, a recent study demonstrated that Netrin/DCC-mediated attraction is involved in axonal targeting to the OB of zebrafish (Lakhina *et al.*, 2012). A subpopulation of OSNs express DCC and their target glomeruli are mainly located in medioanterior part in the ventral OB which correlates with the netrin1a and netrin1b expression pattern. Loss of Netrin/DCC signaling produced mistargeting of axons and in some cases abolished their ability to penetrate the OB. Least, depletion of the cell matrix protein anosmin-1a, which can be found in OSNs from 22 hours post fertilization onward, perturbs fasciculation of olfactory axons and their glomerular targeting to OB (Yanicostas *et al.*, 2009).

1.5. Glomerular Map in Zebrafish Embryos

The glomerular pattern in the OB of adult zebrafish was initially described in 1994 using the lipophilic tracer DiI. A follow-up study in 2012 used a combination of DiI tracing and antibody staining to provide a more detailed description of the map (refer to Section 1.1.1. for further details; Baier and Korsching, 1994; Braubach *et al.*, 2012). The glomerular pattern in the fish is bilaterally symmetric and invariant between organisms and starts to develop at 3.5 days post fertilization. Glomerular positions can be classified into lateral, medial, central, dorsal and ventral zones (Dynes and Ngai, 1998). In the embryo, the glomerular pattern consists of nine isolated peripheral structures including four different lateral glomeruli, four medial glomeruli and a single ventral posterior glomerulus. It also comprises two large zones, the central and dorsal zone, which could further be subdivided into individual protoglomeruli. In 2005, different classes of OSNs were visualized through expression of fluorescent proteins under the control of cell type-specific promoters, such as OMP and TRPC2 gene promoters, in transgenic fish and it was shown that axons of ciliated and microvillous OSNs target different glomerular regions in a mutually exclusive manner (Sato *et al.*, 2005). All of the protoglomeruli in central and dorsal zones, the medial glomeruli and one of the lateral glomeruli (LG3) is formed by axons of ciliated OSNs, whereas the ventral posterior glomerulus and three of the lateral glomeruli (LG1, LG2, LG4) arise from microvillous OSNs (Lakhina *et al.*, 2012). Another study based on transgenic fish line expressing Ca^{2+} indicator protein also focused on early development of the OB and asserted that first odor responses in the OB can be detected around 3 days post fertilization, confirming that protoglomeruli are functional (Li *et al.*, 2005). Furthermore, responses to amino acids and bile acids generate specific activity patterns in different parts of the OB, indicating a topographic organization of glomeruli, which is not only anatomical but also functional even in embryonic stages (Li *et al.*, 2005).

1.6. Internal Ribosome Entry Sites

In 1991 an alternative translation initiation mechanism was discovered for the encephalomyocartidis virus (EMCV) that is independent of Cap-mediated translation and

utilization internal ribosome entry sites (IRESs; Ghattas *et al.*, 1991). Canonical translation initiation in eukaryotes is mediated through recognition of the m7G-cap at 5' terminus, which is typical for eukaryotic cellular mRNAs, by the 43S pre-initiation complex. The pre-initiation complex comprises 40S ribosomal subunits, initiation factors eIF2 and eIF3, and the methionine initiator tRNA (Mokrejs *et al.*, 2006). The complete ribosome assembly is concluded once the initiation complex attaches to the cap and then scans the 5'-UTR for the first initiation codon to initiate polypeptide synthesis (Kozak, 1991).

Some viruses lack the m7G-cap in their RNAs and, as a result, have evolved a different translational initiation strategy in order to synthesize viral proteins. The alternative translational initiation mechanism depends on the recruitment of the 43S ribosomal complex to the 5' UTR of a mature mRNA through secondary structures called IRES. The docking of the ribosome at the IRES bypasses the need of a m7G-Cap, thus, it is referred as the cap-independent translation mechanism (Hellen and Sarnow, 2001).

IRES sequences not only allow their species of origin to initiate translation in a cap-independent manner, they also provide additional advantages to the virus in host cells. Polioviruses could block cap dependent translation of host cell RNAs while diverting the translational machinery to the production of viral proteins (Spriggs *et al.*, 2010). The same principle is later adopted by eukaryotic cells to regulate the expression of several proteins that are involved in stress responses, development, apoptosis, cell cycle control, and neuronal function; conditions where conventional protein synthesis is inhibited (Gilbert, 2010). In addition, the usage of IRESs to regulate protein expression at the translational level provides a swift alternative resulting in short response times for cells to external stimuli (Holcik and Sonenberg, 2005).

To date, more than 500 IRESs have been identified from both viral and eukaryotic origins, with an average length of 474 bp (Mokrejs *et al.*, 2006). However, no universal consensus sequences could be identified from the known IRES sequences making bioinformatic identification of new IRES regulated proteins difficult. Therefore, identification of secondary structures on mRNA that could harbor IRESs relies solely on

empirical data (Thompson, 2012). Some of the characterized IRES sequences from eukaryotic systems were found to contain weak or cryptic promoters upon further investigation, thereby lowering the overall number of IRESs proposed in early reports (Bert *et al.*, 2006). Finally, highly structured viral IRES sequences have shown to be far more efficient than their eukaryotic counterparts (Mokrejs *et al.*, 2006).

1.6.1. Coexpression via IRES Sequences

Besides their interesting mechanism, IRES sequences have proven to be valuable tools in transgenic experiments. Coexpressing a fluorophore along with the protein of interest is an essential approach to visualize expression of a specific protein *in vivo*. Different strategies can be applied: (i) direct genetic fusion of a fluorescent protein to the N- or C- terminus of the coding region; (ii) utilization of bidirectional promoters that occur naturally in the mammalian genome in Janus vectors (Trinklein *et al.*, 2004); (iii) insertion of self-cleaving peptides of the 2A-family between the coding regions of two proteins in same orientation (protein of interest and reporter protein) to generate two individual proteins from a single open reading frame (Provost *et al.*, 2007); (iv) translation of two independent proteins with an IRES sequence that exists between coding regions of two proteins with same orientation and recruits a second ribosome to the mRNA between two cistrons (Weber and Koster, 2013). The latter two approaches are favorable, because independent proteins are expressed for the gene of interest and the reporter while maintaining the natural expression pattern of the gene of interest.

1.6.1.1. Use of IRES Sequences in the Olfactory System. IRES sequences have been valuable tools in studying OR gene expression because of the direct role that the OR protein plays in axon targeting and OR gene expression, and which could be affected by protein fusions. Similarly, because of monogenic and monoallelic expression, transgenes that utilize OR gene promoters cannot be used to reveal OR gene expression without abolishing expression of the OR. Pioneered in 1996, IRES sequences were used in the mouse olfactory system to direct coexpression of a mouse OR gene (P2) and a marker protein (lacZ; Mombaerts *et al.*, 1996); an approach that is now a standard in the field. To date, it has been

used in at least fourteen other mouse OR genes: M71, M72, P3, P4, M50, I7, MOR23, mOR37A, mOR37B, mOR37C, M5, MOR28, SR1, and MOL2.3 (Serizawa *et al.,* 2000; Strotmann *et al.,* 2000; Zheng *et al.,* 2000; Potter *et al.,* 2001; Zou *et al.,* 2001; Bozza *et al.,* 2002; Treloar *et al.,* 2002; Vassalli *et al.,* 2002; Weber *et al.,* 2002; Cuthforth *et al.,* 2003; Feinstein & Mombaerts 2004; Feinstein *et al.,* 2004; Shykind et al. 2004). This strategy was instrumental in identifying and studying aspects of olfactory function, such as zonal expression of ORs, their role in axonal convergence, and to elucidate their ligand spectrum (refer to Sections 1.3.3. and 1.5.2. for further details).

Attempts to adopt the OR-IRES-marker strategy to visualize specific subpopulations of OSNs in the zebrafish olfactory system have failed (Sato *et al.,* 2007). Although IRES sequences of viral origin are reported to drive two fluorescent proteins in various tissues other than the OE in zebrafish (Fahrenkrug *et al.,* 1999), the level of EMCV IRES driven proteins was demonstrated to be low (Kwan *et al.,* 2007). The underlying reason behind this failure may be the differential efficiency of viral IRES sequences to initiate translation in different species or their temperature dependence. An attractive opportunity to bypass this caveat might be the utilization of cellular IRES sequences that are derived from the zebrafish genome directly.

1.6.2. IRES Sequences Identified in the Zebrafish Genome

In zebrafish, candidate IRES sequences have been identified in the coding region of the connexin Cx55.5 gene (Ul-Hussain *et al.,* 2008). The carboxy-terminal domain of the protein has been demonstrated to be internally translated via a putative IRES in *in vitro* assays. Another IRES was identified, which is located between two open reading frames of wnt8; the efficiency of the described IRES was very low according to *in vitro* assays, and and its *in vivo* activity is still elusive (Lekven *et al.,* 2001).

Here, I examined the systematic coexpression of two OR genes and tested whether the intergenic region between these two linked genes has IRES activity. The IRES activity that is supported by *in vitro* assays is then used for bi-cistronic translation in the zebrafish olfactory system. Using various approaches, the achievement of high double expression rates between two reporter genes are confirmed to originate from bi-cistronic constructs. Finally, the OR103-1/5 intergenic region is used as a molecular tool to visualize OSN subpopulations that express specific ORs.

2. PURPOSE

The initial aim of this study is to elucidate the regulatory roles of OR103-1/5 intergenic region at the coexpression of OR103-1 and OR103-5 genes. Because of the systematic nature of the detected coexpression, we hypothesized that the intergenic region could possess IRES function. It is primarily tested in HeLa cells using bi-cistronic expression vectors. The supportive *in vitro* results lead to further investigation of our hypothesis in the zebrafish olfactory system. Here, we tested the intergenic region's ability to recapitulate the OR103-1 and OR103-5 gene locus with reporter genes and achieved coexpression in high levels both in OE and other tissues. Then, using multiple approaches we confirmed the origin of colabeling as co-translation from a bi-cistronic transcript instead of independent expressions from two independent promoters. Our final objective is to use bi-cistronic translation from the intergenic region as an alternative method to the OR-IRES-Marker strategy for the introduction of transgenic OR proteins to subpopulations of OSNs in zebrafish.

3. MATERIALS AND METHODS

3.1. Materials

3.1.1. Fish

The Zebrafish (*Danio rerio*) used in this study includes AB/AB, Ab/Tü, Tü/Tü strains obtained from the Zebrafish International Resource Center (ZIRC), at the University of Oregon, Eugene, USA, and wild-type fish obtained from a local pet shop (referred to as PS-WT). Both adults and embryos are raised at the Boğaziçi University Life Sciences Center (Vivarium).

3.1.2. Equipment and Supplies

The list of equipment, chemicals and consumables are provided in Appendix A and Appendix B.

3.1.3. Buffers and Solutions

The buffers and solutions for molecular biology procedures, such as polymerase chain reaction, ligation of DNA fragments and others were either obtained directly from the manufacturer of molecular reaction kits or prepared according to Sambrook and Russell (1989). Zebrafish specific solutions were prepared according to Westerfield (1997).

3.2. Methods

3.2.1. Fish Maintenance

Zebrafish of the AB/AB, AB/Tü, Tü/Tü, and PS-WT strains were kept at 28ºC under a 14/10 hours light / dark cycle. Five to fifteen adult zebrafish were kept in 3 liter tanks and larger groups in 10 liter tanks. Individual Tanks were connected to a professional zebrafish housing system with aeration, temperature control and 5 stage filtration (Stand Alone System, Aquatic Habitats, FL). Adult Zebrafish were fed three times a day, twice with live brine shrimp (*Artemia sp.*) and once with flake food. Artificial fish water was prepared by mixing 2 g sea salt, 7.5 g sodium bicarbonate 0.84 g calcium sulfate in 100 liters of reverse osmosis water.

Matings to obtain fertilized oocytes for microinjection were set up in static water in special mating tanks after the third feeding slot of the day (afternoon or early evening) and fish were left undisturbed until the following morning. The mating tanks include an inserted container with a perforated bottom, and this design protects the freshly fertilized eggs from predation by the parents. Imitation plastic plants were placed into the tanks to provide artificial spawning sites for females. Fertilized eggs sink to the bottom of the outer tank and were collected with Pasteur pipettes. Microinjection of plasmid DNA was performed on fertilized oocytes at the one cell stage. Because of the short time span between early cleavages (10 to 15 minutes) a plastic divider to separate males and females in the mating tank was removed immediately before injection to induce timed matings. The divider was removed in the morning (usually shortly after onset of light cycle) before spawning. Fertilized eggs were transferred into a petri dish, rinsed and kept in E3 medium which is prepared according to Westerfield (1993).

3.2.2. Microinjection into Zebrafish Oocytes

The night prior to injection of plasmid DNA, fish were set up in mating tanks and spawning was induced the following morning at the beginning of the light cycle by removing the separators. Fish eggs were collected immediately after spawning and unfertilized eggs and other debris were removed. Fertilized eggs were lined up in an agarose injection mold. Glass capillary needles used for microinjection were filled with injection solution including 100 ng/µl plasmid DNA, 10mM KCL and 0.01% Phenol Red. Co-injection solutions contained 50 ng/µl plasmid DNAs of each transgenic construct (100 ng/µl in total) in 10mM KCL and 0.01% Phenol Red. Using a FemtoJet® Express pressure injector (Eppendorf), 4 nanoliters of injection solution was injected to the yolk of each one-cell stage embryos. After injection, embryos were transferred into E3 medium, and kept in 28ºC until expression analysis at 3 and 4 dpf. E3 medium was renewed and dead embryos removed daily.

3.2.3. Polymerase Chain Reaction (PCR)

Polymerase Chain Reactions (PCRs) were performed using GoTaq Flexi DNA Polymerase (Promega) according to the manufacturer's instructions. Taq DNA Polymerase (Fermentas, USA) was used for colony PCRs according to the manufacturer's protocols. Standard PCR protocol includes 50-100 ng DNA template, 0,5 µM forward and reverse primers, 1X reaction buffer, 1.5 mM $MgCl_2$ (if not supplied in the reaction buffer), 0.2mM dNTP mix and 1-3 Units of Taq polymerase. Generally, a standard PCR protocol comprises 4 minutes of an initial denaturation step at 95ºC, followed by 25 to 36 cycles of 30 seconds at 95ºC, 30 seconds at the annealing temperature (equivalent to lowest TM of the primers minus 4ºC) and 1minute (min) /1 kilobase (kb) target amplicon at 72 °C. The reaction was terminated by 10 min of a final elongation step at 72ºC followed by 30 min at 4ºC. For colony PCR reactions, which were performed for identification of positive transformants after ligation of DNA fragments, the cycle number was increased up to 36 cycles and the initial denaturing step was adjusted to 10 minutes to allow for sufficient lysis of bacteria.

3.2.4. Restriction Endonuclease Digests of DNA

Restriction digestions were performed with endonuclease enzymes from New England Biolabs, Promega or Fermentas. Reactions contain 1-5 units of restriction enzymes per microgram of DNA and 1X concentration of the buffer that is recommended and supplied by the manufacturer. If necessary 1X BSA was added to the reaction. Digestion reactions were incubated at 37ºC for 1 to 8 hours.

3.2.5. Agarose Gel Electrophoresis and DNA Extraction from the Gel

DNA samples were run in 1% agarose gel containing ethidium bromide (0.5µg/ml) until DNA fragments were separated as desired. The 1kb DNA ladder (NEB, USA) was used as a molecular weight marker. Agarose gels were visualized under UV light and documented as electronic TIF files.

Extraction of DNA fragments from agarose gels after separation was performed using the Roche High Purification kit. Agarose blocks containing the fragment of interest were cut out from the gel using a scalpel. Then 100 µl of binding buffer per 0.01g of agarose gel was added and the mixture was incubated at 56ºC for 10 minutes to allow the gel to dissolve in buffer. Next, 50 µl of isopropanol per 0.01g of agarose gel was added and the mixture was loaded to spin columns provided with the kit, washed, and eluted using Tris/EDTA. Eluted DNA was quantified with NanoDrop® Spectrometer or visualized on agarose gel.

3.2.6. PCR Purification

High Pure PCR Purification Kit (Roche,USA) was used according to the manufecturer’s instructions to purify PCR products and plasmids.

3.2.7. Ligation of DNA Fragments to Vectors

For ligation reactions, typically a 1:3 molar ratio of vector to insert was used. Estimation of the DNA amount was done considering the relative intensities of vector and insert after gel electrophoresis, concentrations measured by Nanodrop® Spectrophotometer and the size of the DNA fragments. Ligation reactions include vector and insert DNA (up to 100 ng), 1 µl of T4 DNA ligase (NEB), 2 µl of 10x Ligase Buffer and dH_2O was added up to a final volume of 20 µl. The reaction mixture was incubated at 25ºC for 1 hour, followed by transformation into competent cells.

For direct ligation of PCR products into vector plasmids, the pGEM-T Easy (Promega) vector system was used. Ligation reaction included 3 µl of purified PCR product, 0.5 µl pGEM-T Easy vector, 5 µl of 2x ligase buffer, 1 µl of T4 DNA ligase (NEB) and dH_2O to adjust the reaction volume at 10 µl. The reaction mixture was incubated at 25ºC for 1 hour and transformed into competent cells.

3.2.8. Preparation of Competent Cells (Rubidium Chloride Method)

First, a single colony of the Top10 MRF' bacteria strain was picked and inoculated overnight at 37ºC in 5 ml LB medium. 500 µl of the overnight culture was used to inoculate 500 ml of fresh LB medium and incubated at 37ºC on a shaker until the OD_{550} reached a reading of 0.6. Then the bacteria culture was chilled on ice for 15 minutes and centrifuged at 3000 rpm for 10 minutes at 4ºC. The supernatant was removed and bacteria were resuspended gently in the remaining supernatant. 500µl of CT1 (30 mM potassium acetate, 10 mM $CaCl_2$, 50 mM $MnCl_2$, 100 mM RbCl and 15% glycerol) solution was added and incubated on ice for 30 minutes. Another centrifugation step was performed at 3000 rpm for 10 minutes at 4ºC, the supernatant removed and 20µl of CT2 solution (10 mM MOPS, 75 mM $CaCl_2$, 10 mM RbCl and 15% glycerol) was added to resuspend the pellet. Finally the bacteria suspension was divided in 50 µl aliquots and immediately shock frozen in liquid nitrogen. Aliquots were stored in -80ºC until transformation.

3.2.9. Transformation of Plasmid DNA into Competent Cells

50 µl of competent cells were thawed on ice for 5 minutes. Plasmid DNA or ligation reaction was added to the cells and mixed (10 µl of ligation reaction mix is used in standard transformation and 10-50 ng of plasmid DNA is used for re-transformation). The mixture was incubated on ice for 30 minutes and heat shocked in a water bath at 42ºC for 90 seconds and the mixture was immediately transferred to ice for 5 minutes. Then 500-1000 µl of fresh LB was added and the transformation mixture was incubated for 60 minutes at 37ºC for recovery. Finally 250-500 µl of the transformation mixture was spread on appropriate selection plates.

3.2.10. Plasmid Isolation

Plasmid isolation was performed using the Plasmid MiniGeneJet Isolation kit (Thermo Scientific) according to manufacturer's instructions.

3.2.11. Whole Mount Antibody Staining of Zebrafish Embryos

Embryos (3 dpf) were anesthetized in 1x MS222 solution and fixed in 4% formaldehyde in PBS at room temperature for 3 hours. Following fixation embryos were transferred into 100% MetOH in a stepwise manner by increasing the MetOH concentration by 25% increments in PBS. At this stage embryos could be stored in MetOH up to several months before further processed. Embryos were rehydrated by successive incubations in 75% MetOH / 25% PBS, 50% MetOH / 50% PBS and 25% MetOH / 75% PBS at room temperature for 5 minutes per step. Then embryos were transferred into PBX (PBS containing 0.5% Triton X-100) and incubated 3 times 5 minutes at room temperature with rocking agitation. Embryos were transferred into antibody blocking solution (10% goat serum, 0.5%BSA in PBX) and incubated for 2 hours at room temperature with rocking agitation. After blocking the solution was replaced with primary antibody solution (diluted

1/500 in blocking solution). Embryos were incubated overnight at 4ºC with rocking agitation and washed briefly in PBX solution at room temperature. The washing step was repeated 5 times for 5 minutes, and 3 times for 20 minutes with rocking agitation. Embryos were transferred into antibody blocking solution (10% goat serum, 0.5%BSA in PBX) and incubated for 2 hours at room temperature. After the incubation the blocking solution was replaced with secondary antibody solution (diluted 1/800 in blocking solution) and incubated for 2 hours at room temperature on a rocking shaker. Embryos were rinsed in PBX solution very briefly at room temperature and washed in PBX 5 times for 5 minutes, and 3 times for 20 minutes. Finally embryos are transferred to PBS solution and stored at 4ºC until mounting and documentation.

3.2.12. Antibody Staining of Embryonic Sections

Sections were cut on a LEICA CM3050S cryostat and fixed in 4% PFA / 1xPBS solution for 10 minutes. After fixation sections were washed in PBST (1xPBS / Tween 0.05%) for 5 minutes and treated with 0.2M HCl for 10 minutes and again washed in in PBST for 5 minutes. Then, the sections were incubated in blocking solution (10% normal donkey serum, 1% BSA in PBST) at room temperature for 1 hour, followed by overnight incubation in primary antibody (1:250) in 250 ul blocking solution at 4ºC. On the next day, 3 consecutive washing steps were performed in PBST for 10 minutes each. The sections were finally incubated in secondary antibody diluted (1:800) in 250 ul blocking solution in room temperature for 90 minutes. Then three more washing steps were performed in PBST for 10 minutes each. The sections were stored in PBS at 4ºC until imaging by confocal microscopy.

3.2.13. Whole mount *in situ* Hybridization of Embryos

Embryos (3 dpf) were anesthetized in 1x MS222 solution and fixed in 4% formaldehyde in PBS at room temperature for 3 hours and stored in 100% methanol at -20°C. Embryos were treated with 3% H_2O_2 in methanol at room temperature for 20 minutes and rinsed with 100% methanol. The samples were then treated in a methanol series

(methanol in PBT; PBS containing 0.1% Tween 20): 75% 5 minutes, 50% 5 minutes, 25% 5 minutes. Embryos were washed two times with PBST for 5 minutes and then digested with 10 µg/ml proteinase K in PBST at room temperature for 30 minutes. Digestion was stopped by incubating embryos in 4% PFA in PBS at room temperature for 20 minutes. Four consecutive 5 minute washing steps were performed in PBS to remove residual PFA. Embryo were prehybridized with 300 µl hybridization mix (HM contains 50% Formaldehyde, 5x SSC, 0.1% Heparin, 5% yeast RNA 0.1% Tween 20, 1% Citric Acid) at 65ºC in a water bath for 3 hours. HM was discarded and replaced with HM containing 5ng/ml of DIG-labeled RNA probe for overnight hybridization at 65ºC. Next day, HM is replaced with 2x SSC through a 10 minute series of 75% HM / 25% 2x SSC, 50% HM / 50% 2x SSC, 25% HM / 75% 2x SSC and 100% 2x SSC in 70ºC. Embyos were then washed with 0.2% SSC for 30 minutes at 70ºC, followed by a series of 10 minute washes in PBST at rom temperature on a horizontal shaker (40 rpm). Embryos were incubated for three hours at room temperature in blocking buffer followed by overnight incubation at 4ºC with gentle agitation. Next day the samples were washed 3 times for 5 minutes in PBST. The supernatant was removed and 300 µl of tyramide-Cy3 solution was added. Samples were incubated at room temperature for 40 minutes and then washed with PBST. Finally they were stored in PBS until documentation.

3.2.14. Bodipy Staining

Live embryos were transferred into Bodipy solution which contains 100 µM Bodipy in E3 medium and incubated at 28ºC for 45 minutes. The embryos were washed in three consecutive steps with E3 medium which is prepared according to the instructions by Westerfield (1993), and immediately documented using confocal microscopy.

3.2.15. 3D Modeling

Using 3D Slicer®, a 3D reconstruction of the glomerular map was generated based on confocal z-stacks of bodipy-stained embryos. Relevant structures, such as glomeruli, outline

of the head, etc. were maske on every optical section from a z-stack through the first 50 µm of the embryo head and a 3D rendering was generated by the program.

3.2.16. Imaging of Zebrafish Embryos

For live imaging, embryos were anesthetized with 0.04% MS222 (Sigma, USA), mounted in low-melting agarose (2%) and covered with a coverslip. Mounted embryos were then imaged using SP5-AOBS laser scanning confocal microscope (Leica, Germany).

3.2.17. Culture of HeLa Cells and Transfection of Plasmids

HeLa cells were split and seeded in cell culture flasks and incubated at 37ºC and 5% CO_2. For passage, the DMEM/F12 medium was removed and cells were washed in 10 ml of PBS. 10 ml of fresh DMEM/F12 medium was added to 10 cm plates. HeLa cells were detached from the storage plates and mobilized by adding 1 µl of trypsin and incubated for 5 minutes at 37ºC. Detached cells were collected with the medium and centrifuged at 2000 rpm for 2 minutes. The supernatant was removed and 10 ml of fresh medium was added to the pellet, and the cells were gently re-suspended. After re-suspension, 10 µl of the solution was mixed with 10 µl of tryphan blue dye and cells were counted on a hematocytometer. Approximately, 60.000 cells were seeded into each well of 12-well plates and supplemented with 1 ml of fresh medium. Cells were grown for 24 hours until transfection.

For transfection with dual luciferase constructs, three different wells were transfected with the same plasmid/construct. The transfection mixture for each triplicate contains 1 µg of plasmid DNA, 1.25 µl of X-treme GENE Transfection Reagent (Roche) and ~100 µl of transfection medium for each well. The mixture was incubated for one hour at room temperature before 100 µl of transfection mixture was added to each well. Finally 12-well plates were incubated for 24 hours at 37ºC before luciferase assays.

3.2.18. Lysis of Cells and Luciferase Assays

Lysis of HeLa cells was performed 24 hours after transfection and luciferase assays are performed with Dual-Luciferase Reporter Assay (Promega) with buffers provided by the manufacturer according to the instructions. The luminescence was measured in a 96-well plate reader (Thermo Scientific, Fluroskan Ascent Fl). The luminometer was set to dispense 100 µl firefly luciferase substrate, delay 2 seconds and measure luminescence for 1 second. After measurement, 100 µl Stop & Glo® Reagent was added, incubated for 15 minutes and luminescence of renilla luciferase was measured for 1 second.

Table 3.1. List of Antibodies Used in This Study.

Antibody	Company	Catalog No	Working Dilution
Myc-Tag (71D10) Rabbit mAb	Cell Signaling Technology	2278	1:250
Goat Anti Rabbit Alexa 488	Invitrogen	A-11008	1:800

4. RESULTS

4.1. The Intergenic Region May Promote Bi-cistronic Translation

We asked what could be a possible mechanism for the observed co-expression of the genomically linked OR103-1 and OR103-5/2 genes. It could arise from independent transcription of two neighboring OR genes in the same OSN, thus critically violating the 'one neuron – one receptor' rule, or from a failure of termination of transcription at the end of the OR103-1 gene. The reported coexpression has been demonstrated by in situ-hybridization against the two OR genes (Sato *et al.*, 2007), an approach that does not allow to distinguish between these mutually exclusive mechanisms. Using reverse transcription polymerase chain reaction on RNA derived from olfactory tissue we identified a long transcript comprising the OR103-1 and OR103-5 genes, favoring failure of transcriptional termination as the cause of coexpression.

Given that a single long transcript encompassing two linked OR genes may be the cause of coexpression we wondered whether both ORs could be actually translated by the same OSN or if only the first gene is actively translated into protein. The first scenario would resemble the function of an IRES that promotes bi-cistronic translation of two coding sequences from a single messenger. To test this possibility *in vivo* and *in vitro*, we used dual-reporter constructs in cell lines and in living zebrafish embryos, which is a common methods to assess IRES activity (Holcik and Sonenberg, 2005). In those expression vectors, the DNA sequence suspected to contain IRES activity is cloned between two different reporter genes and the correlation of reporter activity is examined. Under this experimental paradigm, if the tested sequence does not contain IRES activity, translation will be terminated at the stop codon of the first coding sequence. Thus, only the reporter gene that is located in the first position of these constructs will be translated. However, if the tested sequence contains IRES activity, cap-independent initiation of translation will result in activity (fluorescence or luciferase activity) of both reporter genes in the same cell (refer to Section 1.7. for further details).

4.1.1. *In Vitro* Characterization of Co-translation

To examine IRES activity of the OR103-1 / OR103-5 intergenic region in vitro, we used the bi-cistronic expression system pRF in cultured HeLa cells. The pRF vector comprises sequences coding for renilla and firefly luciferase in its first and second cistron, respectively (Lang *et al.,* 2002). A multiple cloning site between the reporter genes allows for the insertion of sequences o be tested for IRES activity. Expression of the construct is driven by the SV40 early promoter and enhancer sequences (Coldwell *et al.,* 2001). To test whether the intergenic region contains IRES activity the full 1.4 kb of sequence between OR103-1 and OR103-5 was cloned between the renilla and firefly luciferase genes in a construct termed pR-inter$_{(1.4kb)}$-F. As a positive control, the widely used EMCV IRES sequence (refer to Section 1.7. for further details) was inserted into the multiple cloning site of pRF to generate pR-EMCV-F (Figure 4.1a). Three constructs, pR-inter$_{(1.4kb)}$-F, pR-EMCV-F, and empty pRF vector were transfected in triplicates into HeLa cells and renilla and firefly luciferase activities were measured 24 hours following transfection using a luminometer (refer to Sections 3.12.14. and 3.12.15. for further details).

As expected, the empty pRF vector resulted in high levels of renilla and basal levels of firefly activity, because translation of reporter genes will terminate at the end of the renilla luciferase sequence in this construct. Thus, any change in firefly luciferase activity in the pR-inter$_{(1.4kb)}$-F and pR-EMCV-F constructs relative to pRF may originate from IRES activity of the DNA fragments inserted between the two reporter genes. In both constructs, in pR-inter$_{(1.4kb)}$-F and pR-EMCV-F, firefly luciferase activity was significantly higher when compared to pRF. To express this difference quantitatively, the ratios of firefly to renilla luciferase activity (Fluc/Rluc) were calculated and normalized to pRF (Figure 4.1b). In the positive control construct pR-EMCV-F, as expected, firefly activity was increased with a Fluc/Rluc ratio of 29.2 ± 6.1 compared to the empty vector. This value is consistent with previous findings where an average 14-fold increase in Fluc/Rluc ratio has been reported (Coldwell *et al.,* 2001). Interestingly, when luciferase activity in the pR-inter$_{(1.4kb)}$-F construct was measured, a 116.5 ± 7.2 –fold increase of Fluc/Rluc over pRF was obtained. Thus, the intergenic region promotes an increase of expression of a downstream luciferase reporter gene consistent with IRES activity.

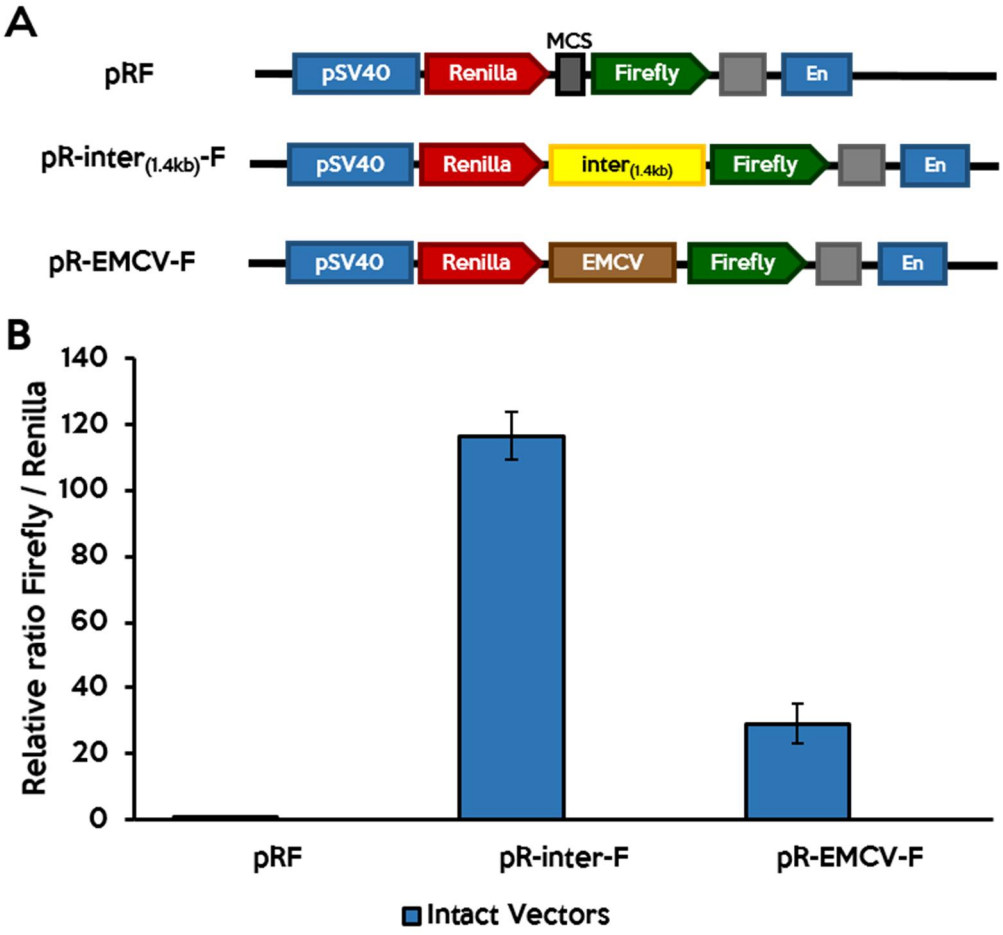

Figure 4.1. Examination of IRES activity using the pRF dual luciferase system. (A) Overview of the pRF, pR-inter$_{(1.4kb)}$-F and pR-EMCV-F constructs. (B) Fluc/Rluc ratios calculated for pRF, pR-inter-F and pR-EMCV-F transfected cells.

The intergenic region comprises sequence upstream of the OR103-5 gene and may contain regulatory elements and promoter sequences which could result in transcriptional activity from the OR103-5 promoter (refer to Section 1.3.4.1. for further details). In theory, the OR103-5 promoter of the intergenic region should only be active in olfactory tissue. However, interaction of the OR103-5 promoter with the SV40 early promoter or the SV40 enhancer that are a component of the pRF vector may induce expression of firefly luciferase in HeLa cells. In order to exclude the possibility that the elevated firefly activity is due to the presence of cryptic promoters in the intergenic region or splice sites in the resulting transcript, the following control experiments were performed. In order to detect any potential

intrinsic promoter activity from the intergenic region, the SV40 promoter was deleted from the constructs (Figure 4.2a). The Fluc/Rluc ratios of the promoterless constructs will reveal the contribution of downstream promoters to of firefly activity.

As expected, removal of the SV40 early promoter from the empty pRF vector abolished renilla firefly activity of this construct. Similarly, renilla activity was largely undetectable in the promoterless pR-inter$_{(1.4kb)}$-F and pR-EMCV-F constructs. Firefly luciferase activity, however, was severely reduced but still detected for cell lysates of cells transfected with pR-inter$_{(1.4kb)}$-F and pR-EMCV-F. Removal of the SV40 promoter decreased the Fluc/Rluc ratio of the pR-inter$_{(1.4kb)}$-F construct by 54%, from 116.5 ± 7.2 to 53.9 ± 4.5, while the Fluc/Rluc ratio of pR-EMCV-F was reduced by 86% from 29.2 ± 6.1 to 4.2 ± 2.6 (Figure 4.2b).

It has been suggested in similar reports that the SV40 enhancer of the pRF vector may interact with cryptic or weak promoters contained within sequences tested for IRES activity (Bert *et al.,* 2006; Vopalensky *et al.,* 2008). A common control experiment is to delete the SV40 enhancer from the constructs to check for this possibility. A new set of constructs was prepared where the SV40 enhancer was removed from the dual luciferase constructs (Figure 4.3a). In these constructs, activity of renilla and firefly luciferase was drastically reduced. The Fluc/Rluc ratio for the enhancerless variant of pR-EMCV-F decreased from 29.2 ± 6.1 to 1.6 ± 0.7. For pR-inter$_{(1.4kb)}$-F a low remaining Fluc/Rluc ratio of 8.7 ± 1.8 was detected, which reflects a 93% decrease in the Fluc/Rluc ratio (Figure 4.3b).

In an additional control experiment, both the SV40 enhancer and the SV40 early promoter were deleted from the dual luciferase constructs (Figure 4.4a) and transfected into HeLa cells. The remaining firefly luciferase activity measured in these constructs represents the background expression of the second reporter from sequences contained within the tested DNA sequence. For the enhancer- and promoterless pR-inter$_{(1.4kb)}$-F construct an increase in the Fluc/ Rluc ratio to 1.879 ± 376.5 was observed (Figure 4.4b). This dramatic increase is most likely an experimental artifact because the simultaneous removal of the SV40 promoter and SV40 enhancer completely abolishes renilla luciferase activity. This significant decrease

in the denominator (Rluc) resulted in excessively elevated Fluc/Rluc ratios which are not meaningful. A similar tendency of the Fluc/Rluc ratio was observed for pR-EMCV-F. However the more pronounced increase in Fluc/Rluc ratio for pR-inter$_{(1.4kb)}$-F may imply basal promoter activity of the OR103-5 promoter in HeLa cells. In order to reflect the absolute contribution of each luciferase, relative luciferase activity graphs were plotted where the activity of each luciferase is separately expressed relative to the activity of the intact construct (Figure 4.4c).

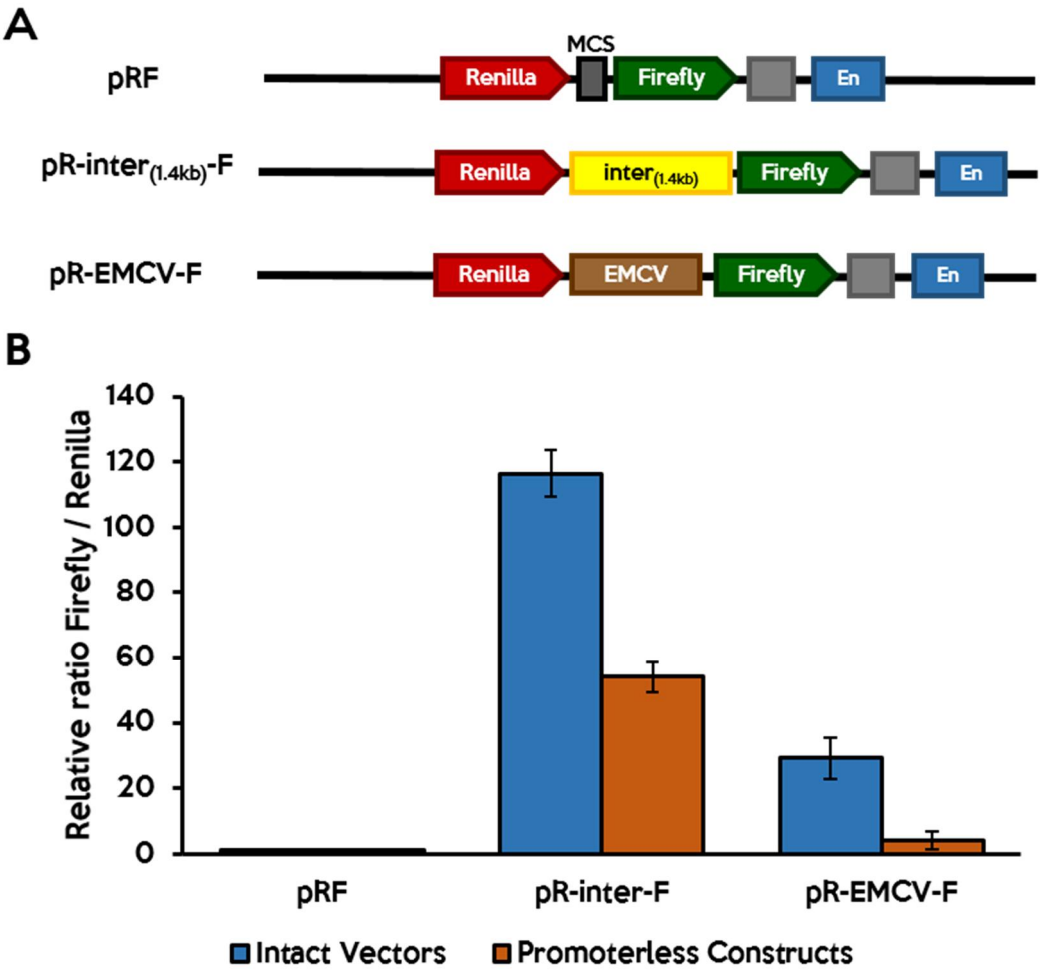

Figure 4.2. Examination of Intact Vectors and Promoterless Constructs. (A) Overview of the promoterless pRF, pR-inter$_{(1.4kb)}$-F and pR-EMCV-F constructs. (B) Fluc/Rluc ratios calculated for promoterless pRF, pR-inter-F and pR-EMCV-F transfected cells.

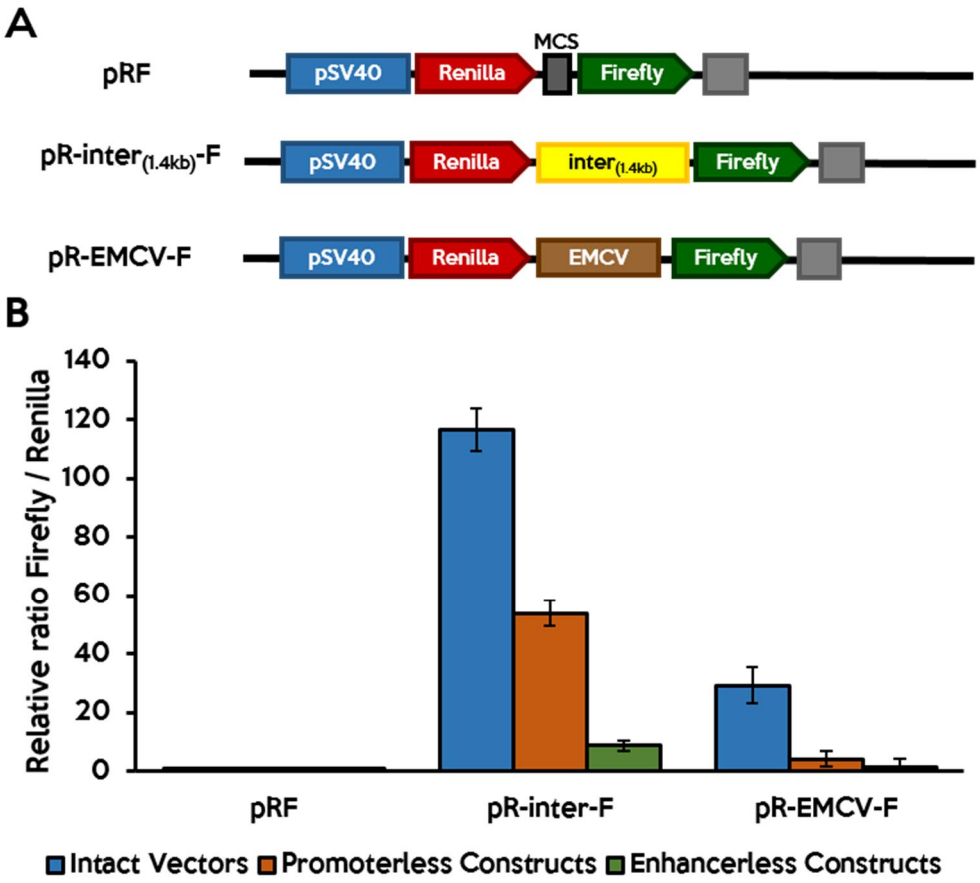

Figure 4.3. Examination of Intact Vectors, Promoterless Constructs and Enhancerless Constructs. (A) Overview of the enhancerless pRF, pR-inter$_{(1.4kb)}$-F and pR-EMCV-F constructs. (B) Fluc/Rluc ratios calculated for enhancerless pRF, pR-inter-F and pR-EMCV-F transfected cells.

The relative luciferase activity graph better represents the activity of each luciferase and a complete reduction of the renilla luciferase activity is evident for promoter- and enhancerless constructs or combinations thereof. However, there is still remaining basal firefly activity in control constructs. This firefly activity is decreased when the enhancer is excluded and completely disappears for the pRF and pR-EMCV-F constructs when both the promoter and the enhancer are excluded from the plasmids. A remaining 20% firefly activity is observed for the enhancer- and promoterless pR-inter$_{(1.4kb)}$-F construct, which may represent intrinsic promoter activity within the intergenic region.

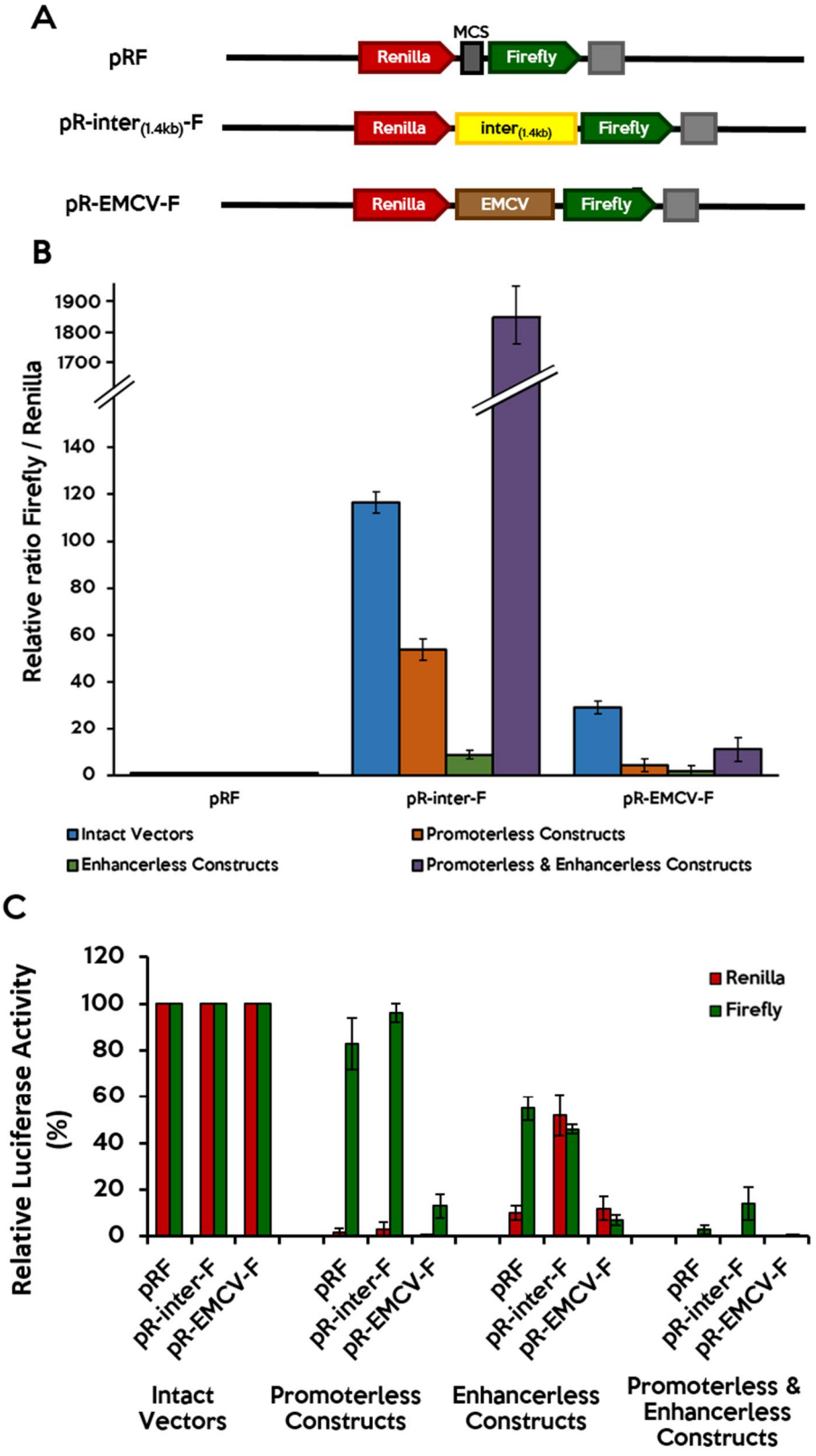

Figure 4.4. Examination of all *in vitro* constructs. (A) Overview of the promoterless- and enhancerless pRF, pR-inter$_{(1.4kb)}$-F and pR-EMCV-F constructs. (B) Fluc/Rluc ratios. (C) Relative Luciferase Activity for all pRF, pR-inter$_{(1.4kb)}$-F and pR-EMCV-F Constructs.

It was previously shown that an OR103-5 transcript initiates from a TSS located 189 bp upstream of OR103-5. In order to narrow down the sequence that regulates transcriptional activity within the intergenic region, a construct which only comprises the 189 bp downstream of the TSS was generated and referred to as pR-inter$_{(189bp)}$-F (Figure 4.5).

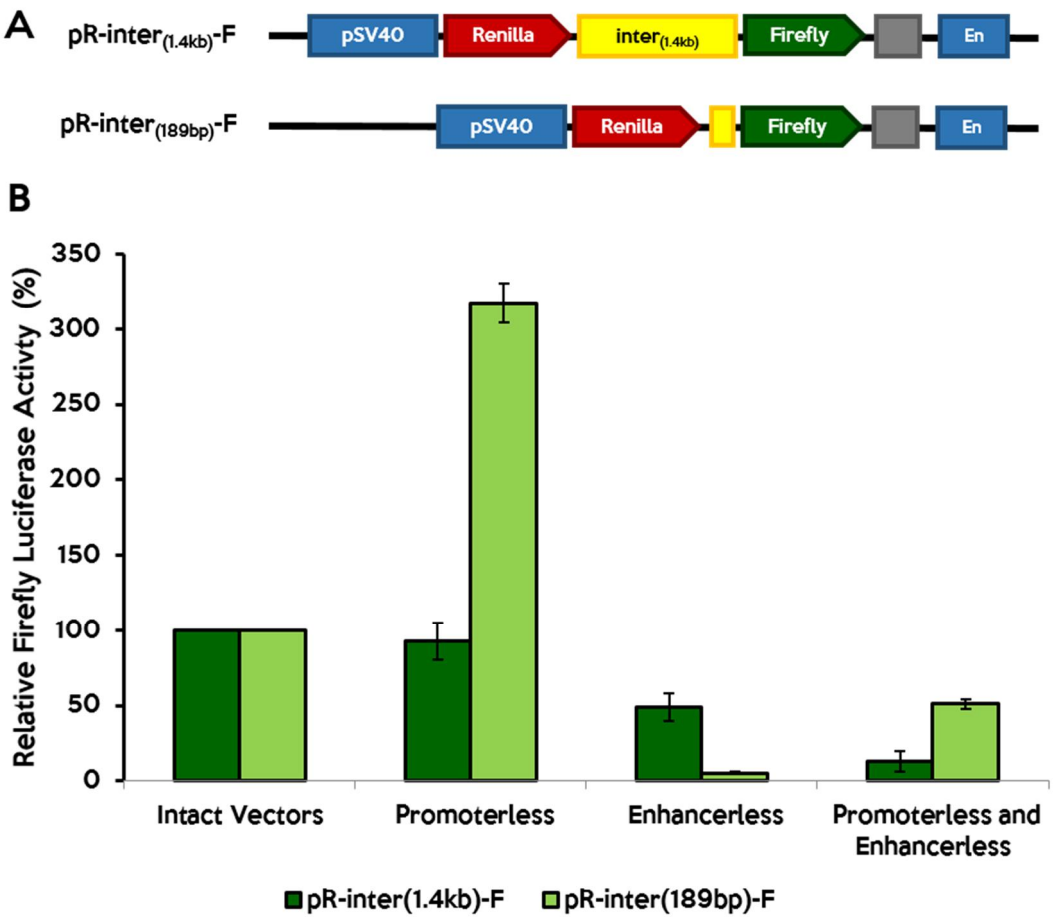

Figure 4.5. Examination of pR-inter$_{(1.4kb)}$-F and pR-inter$_{(189bp)}$-F Constructs. (A) Overview of the pR-inter$_{(1.4kb)}$-F and pR-inter$_{(189bp)}$-F constructs. (B) Relative Firefly Luciferase Activity of pR-inter$_{(1.4kb)}$-F and pR-inter$_{(189bp)}$-F Constructs.

Surprisingly, exclusion of the SV40 promoter from the pR-inter$_{(189bp)}$-F construct resulted in a 3-fold increase in firefly luciferase activity. A similar result is also observed by Bert *et al.*, (2006) 2-fold for pR-hif-F, 4-fold for pR-vegf-F and 6-fold for pR-myc-F. It is conceivable that upon exclusion of the SV40 promoter the SV40 enhancer was free to

interact with cryptic promoter sequence in pR-inter$_{(189bp)}$-F which resulted in increased firefly activity. Consequently, when the enhancer was excluded from the construct. Firefly activity was almost completely abolished, supporting the hypothesis that the enhancer interacted with the 189bp sequence to promote expression. However, in promoter- and enhancerless pR-inter$_{(189bp)}$-F constructs still a rather high relative luciferase activity of 51.1% could be observed, suggesting that the pR-inter(189bp)-F contains a cryptic promoter sequence.

4.1.2. *In Vivo* Characterization of Co-translation

4.1.2.1. Experimental considerations. Primary goal of this study is to investigate whether the OR103-1/5 intergenic region promotes bi-cistronic translation of two linked genes from a common mRNA transcript. The experiments presented above examined this function *in vitro* using a human HeLa cell line, showing that two luciferase reporter genes can be coexpressed when cells were transfected with various expression plasmids. Here, it will be investigated whether the intergenic region can also promote cotranslation of two linked genes *in vivo*, similar to its proposed function in the olfactory tissue. To assess IRES function of the intergenic region *in vivo* and similar to the considerations for *in vitro* tests presented above, it appears critical to first establish if, and to which extend, the intergenic region displays intrinsic promoter activity.

It was previously shown that an OR103-5 transcript initiates from a TSS located 189 bp upstream of OR103-5, thus within the intergenic region. Besides more distally located enhancer sequences, proximal promoter elements have been shown to critically regulate OR gene expression (refer to Section 1.3.4.2. for further details; Vassalli *et al.*, 2002; Rothman *et al.*, 2005; Vassalli *et al.*, 2011; Plessy *et al.*, 2012). In some cases, short sequences of 300-500 bp upstream of mouse OR coding sequence can replicate the expression pattern of endogenous OR gene expression in a transgenic context (Vassalli *et al.*, 2002; Vassalli *et al.*, 2011). Similar observations have been made for zebrafish OR genes, where equally short sequences upstream of an OR gene can drive reporter gene expression from transgenic constructs with high efficiency. For instance, 571bp upstream of the OR111-7 gene

constitute a minimal promoter, which drives reporter gene expression in olfactory tissue (Mori *et al.*, 2000), a finding that has been confirmed in our laboratory (Tastekin, 2012). Similarly, only 600 bp upstream of the OR101-1 gene are sufficient to drive reporter gene expression specifically in OSNs (Kazci, unpublished)

Because the intergenic region comprises the entire genomic sequence between OR103-1 and OR103-5 and because a TSS for OR103-5 transcripts has been experimentally identified within this sequence (Atasoy, 2011), it is conceivable that it contains regulatory elements that constitute a functional OR103-5 promoter. To be able to discriminate IRES-mediated co-translation from co-expression by independent initiation of transcription from the OR103-5 and a second upstream promoter, it is appears crucial to establish the extent to which the intergenic region contains intrinsic promoter activity. The quantification of this activity provides necessary background information on for the interpretation of further co-translation experiments. To experimentally investigate the activity of the intrinsic OR103-5 promoter, a transgenic construct which contains the intergenic region upstream of a sequence coding for Green Fluorescent Protein (GFP) and a SV40 polyadenylation sequence was generated and injected into fertilized zebrafish oocytes (Figure 4.6a).

An additional important aspect of the analysis is the exact developmental timepoint at which the intrinsic promoter activity of the intergenic region is assessed. In zebrafish embryos, OR gene expression starts as early as 18 hours post fertilization (hpf), however, significant numbers of OSNs expressing most OR genes is reached after 3 and 4 days post fertilization (dpf; Barth *et al.*, 1997; Argo *et al.*, 2003). At around the same time a stereotyped and functional glomerular map is established by axonal projections from OSNs to the OB (Dynes and Ngai, 1998; Li *et al.*, 2005). The expression of olfactory cell type-specific markers such as OMP and TRPC2 similarly reach robust levels around 3 dpf (Celik *et al.*, 2002; Sato *et al.*, 2005; Lakhina *et al.*, 2012; refer to Section 1.6. for further details). Most critically, OR gene-specific promoters appear to show their strongest activity between 3 and 7 dpf when used to drive transgene expression. For instance, when the OR 111-7 promoter was used in a transient transgenic study, reporter gene expression could be detected in OSNs as early as 24 hpf, yet, the number of transgene-positive cells increased steadily

until 3 dpf, remained at a peak until 5 dpf, and decreases afterwards (Tastekin, 2012). A similar effect was reported for a stable OR111-7 transgenic line where the number of OSNs increased to a maximum number by 3dpf but declined at around 9 dpf (Lakhina *et al.*, 2012). Thus, intrinsic promoter activity of the intergenic region is likely to follow a similar profile. In this study bi-cistronic expression constructs will be driven under the control of various promoters, such as the OMP, GAP-43 and OR101-1 promoters, for which robust expression at 3 & 4 dpf has previously been demonstrated and quantified (Celik *et al.*, 2002; Sogunmez, 2012). Thus, to allow for a quantitative comparison across different constructs and to compare the observed expression profiles with previously established reference data, all *in vivo* transgene expression assays throughout this study were performed at 3 and 4 dpf.

4.1.2.2. Intrinsic Promoter Activity of the Intergenic Region. To test the intrinsic activity of the OR103-5 promoter contained within the intergenic region a transgenic construct comprising the entire 1.4kb of the intergenic region, a sequence coding for GFP and a polyA signal were cloned into a basic vector. This inter$_{(1.4kb)}$-GFP-pA construct was injected into 92 fertilized zebrafish oocytes at the one-cell stage (three independent experiments: 21, 30 and 41 embryos, respectively) of which 37 embryos (10, 12 and 15 embryos, respectively) survived until the time of analysis at 3 and 4 dpf. Of those, 24% (9/37 embryos) expressed GFP in OSNs. A total of 26 GFP expressing OSNs, thus on average 2.9 ± 0.7 (average ± SEM) OSNs could be identified per embryo. The number of GFP-positive OSNs ranged between 1 to 6 OSNs per embryo. In some embryos, ectopic expression in muscle and notochord cells could also be detected.

The inter$_{(1.4kb)}$-GFP-pA was also co-injected with two other constructs in which mCherry reporter gene expression was driven by the 1.3 kb OMP (p$_{(1.3kb)}$OMP-mCherry-pA) and the 1.2 kb OR101-1 (p$_{(1.2kb)}$OR101-GFP-pA) gene promoters. When the inter$_{(1.4kb)}$-GFP-pA construct was coinjected with p$_{(1.3kb)}$OMP-mCherry-pA, 51 out of 124 injected embryos (2 independent injection experiments) survived until the time of analysis. Of those 31% (16/51 embryos) expressed GFP in OSNs. A total of 61 GFP-positive OSNs (average: 3.8 ± 0.6 cells per embryo) could be identified. When the inter$_{(1.4kb)}$-GFP-pA construct was coinjected with p$_{(1.2kb)}$OR101-GFP-pA 57 out of 119 injected embryos (2 independent

injection experiments) survived until the time of analysis. Of those, 15% (9/57 embryos) expressed GFP in OSNs with an average of of 3.4 ± 1.0 cells per embryo.

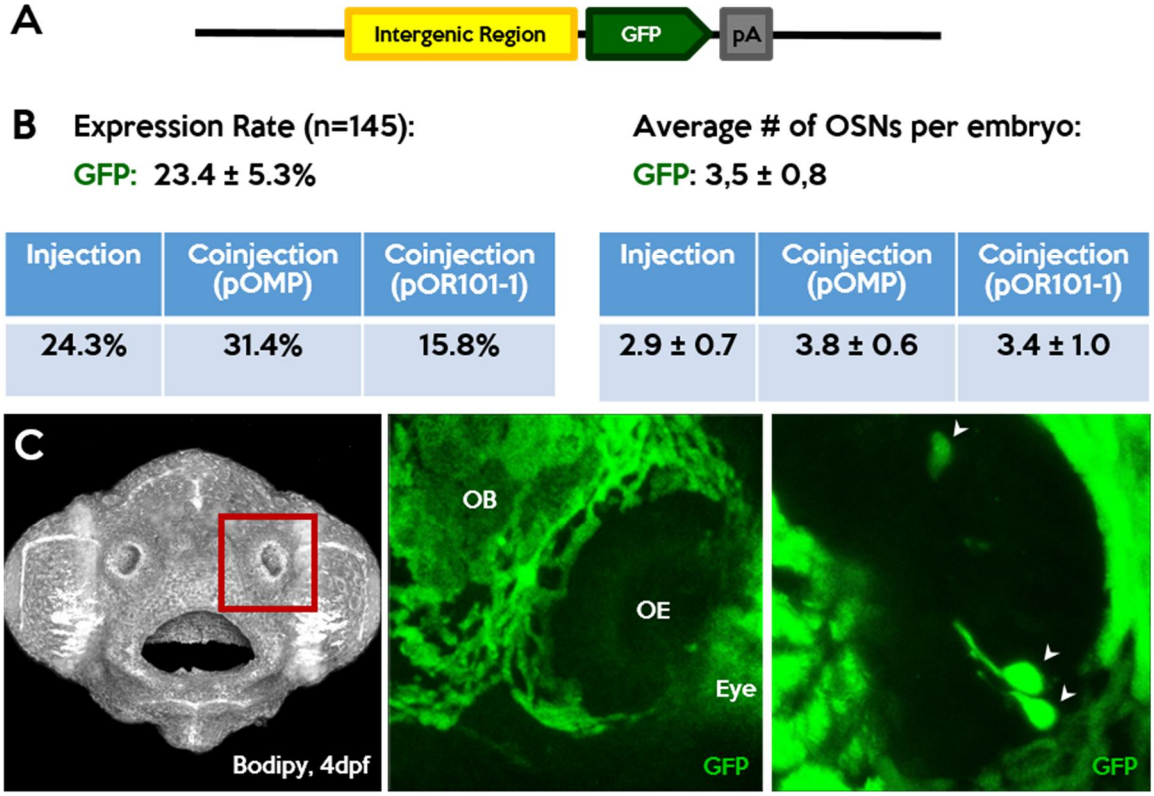

Figure 4.6. Transgene expression analysis of the inter$_{(1.4kb)}$-GFP-pA construct. (A) Overview of the construct. (B) Expression rate and average number of OSNs per embryo. (C) Left: Confocal z-stack of a bodipy stained zebrafish head at 4dpf.

In summary, the inter$_{(1.4kb)}$-GFP-pA construct drives transgene expression in 23.4±5.3% of injected embryos and on average in 3.5 ± 0.8 OSNs per embryo (Figure 4.6b). Thus, the intergenic sequence contains moderate promoter activity, most likely reflecting the transcriptional activity of the OR103-5 gene, which in the genome is located immediately downstream of the intergenic region. By comparison, an OR101-1 promoter construct typically drives reporter gene expression in up to 80% of injected embryos and on average in 6.8 ± 0.7 cells Therefore, the OR103-5 promoter is a relatively weak promoter and the observed transcriptional activity of the intergenic region is suitable for further characterization of bi-cistronic expression in *in vivo* experiments when compared to the

activity of a relatively strong promoter, such as $p_{(1.3kb)}$OMP-mCherry-pA or $p_{(1.2kb)}$OR101-GFP-pA.

4.1.2.3. The Intergenic Region Promotes Coexpression of Two Reporter Genes. To test whether the intergenic region promotes colabeling of individual cells with two different fluorescent reporters *in vivo*, it was cloned between sequences coding for mCherry and GFP reporter genes, thus, substituting the OR103-1 and OR103-5 genes which are normally located in these positions and the construct was expressed under the control of various strong promoters with different cell type specificity. This experimental paradigm can thus be used to examine if they recapitulate the apparent co-expression observed at the OR103-1 and OR103-5 gene locus by microinjection into zebrafish oocytes and analyzing the rate of co-expression of both reporter proteins.

Because expression of OR genes is largely restricted to the olfactory epithelium, we initially focused on olfactory tissue-wide expression of the candidate bi-cistronic construct. For this purpose, the OMP gene promoter, which drives reporter gene expression in a large number of ciliated OSNs, was employed (Celik *et al.*, 2002). The pOMP$_{(1.3kb)}$-mCherry-inter$_{(1.4kb)}$-GFP-pA construct was previously generated by cloning a 1.3 kb sequence containing the OMP promoter directly upstream of mCherry-inter$_{(1.4kb)}$-GFP followed by an SV40 polyadenylation signal at the 3' end (Atasoy, 2011). The OMP promoter is highly efficient and drives reporter gene expression in up to 90% of injected embryos and in a high number of OSNs. The underlying assumption is that if the intergenic region contains IRES activity, the majority of mCherry-positive OSNs should be double-positive for GFP, similar to the systematic co-expression of OR103-1 and OR103-5 /OR103-2 observed by Sato *et al.* (2007).

When the pOMP$_{(1.3kb)}$-mCherry-inter$_{(1.4kb)}$-GFP-pA construct was injected into 207 oocytes (three independent injection experiments: 11, 68, and 128 embryos, respectively) a total of 77 embryos (4, 21, and 52 embryos, respectively) survived until the time of analysis. Of those, 42% (32/77 embryos) expressed mCherry, while 40% (31/77 embryos) expressed GFP in OSNs.

Colabeling with mCherry and GFP was high at the individual cell level: a total of 364 OSNs expressed mCherry and 321 OSNs expressed GFP while 316 cells were double positive for both markers. A total of 86.8% (316/364 OSNs) of mCherry-expressing neurons were positive for GFP and 98.4% (316/321 OSNs) of GFP-positive cells colabeled for mCherry. On average 11.4 ± 1.5 mCherry and 10.4 ± 1.6 GFP expressing OSNs could be detected in the OE of transgenic embryos (Figure 4.7).

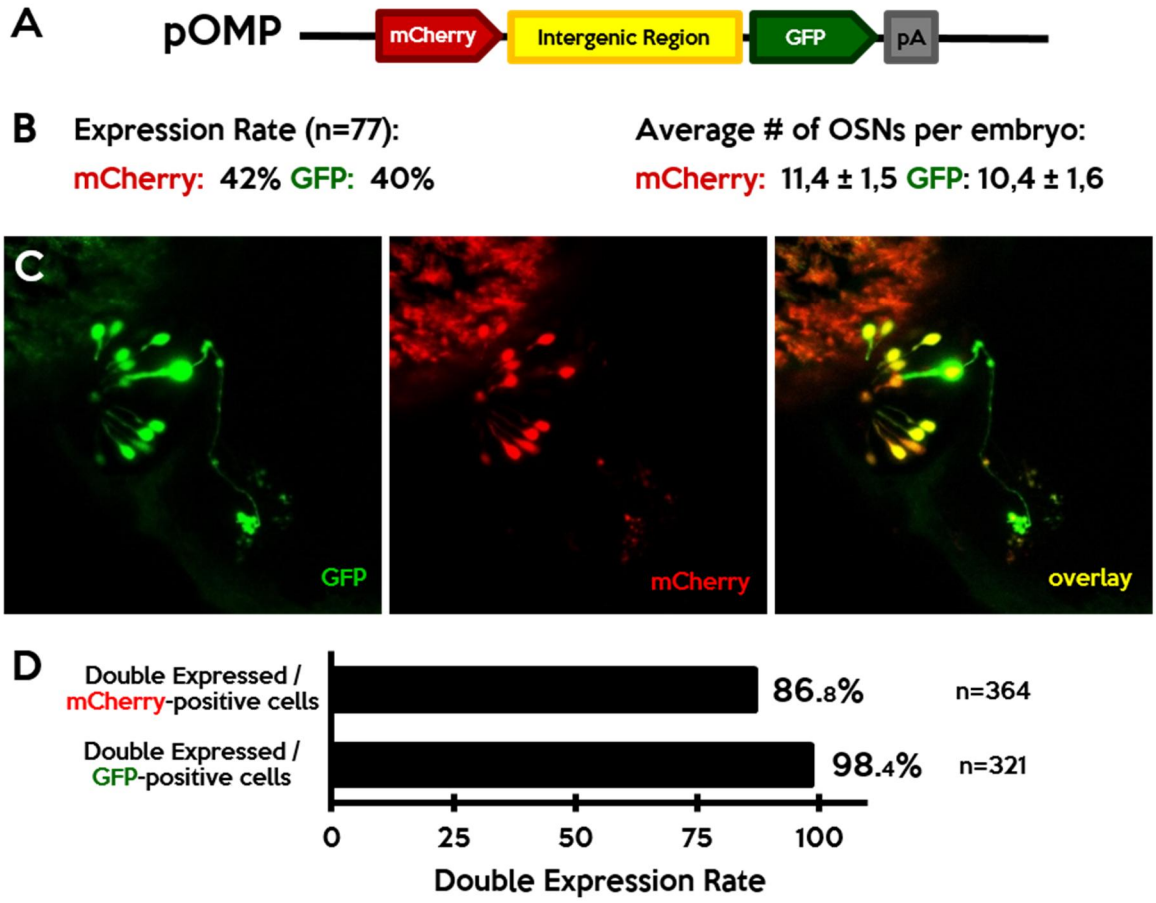

Figure 4.7. Transgene expression analysis of the pOMP$_{(1.3)}$-mCherry-inter$_{(1.4kb)}$-GFP-pA construct. (A) Overview of the construct. (B) Expression rates and average number of reporter gene-positive OSNs (C) Confocal z-stacks of 3dpf OE. (D) Double expression rates.

As described above, GFP expression from the intrinsic OR103-5 promoter of the intergenic region was as high as 23% when the basic inter$_{(1.4kb)}$-GFP-pA construct was

injected. However, in the context of the pOMP$_{(1.3)}$-mCherry-inter$_{(1.4kb)}$-GFP-pA construct expression of GFP, which in this construct is equally located downstream of the intergenic region, almost doubled and increased to 40%. A similar effect was observed for the average number of GFP-positive OSNs per embryo, which tripled and increased from 3.5 ± 0.8 to 10.4 ±1.6 when the strong OMP-promoter was included in the construct.

How could this increase in expression frequency be explained? One possibility, which is at the heart of this study, could be that the presence of the intergenic region downstream of a strong promoter promotes bi-cistronic translation from a long mRNA transcript. As a consequence, GFP expression from the second cistron would become coupled to the transcriptional activity of the OMP. Alternatively, as of yet unidentified regulatory elements contained within the OMP promoter could interact with and enhance transcriptional activity of the OR103-5 promoter within the intergenic region and thereby upregulate expression of the reporter gene in the second position downstream of the OR103-5 promoter. For the pOMP$_{(1.3)}$-mCherry-inter$_{(1.4kb)}$-GFP-pA construct, expression of GFP located in the second position approached the expression rate of the mCherry reporter gene that is located in the first position: 40% vs. 42%, respectively. Similarly, the average number of GFP-positive OSNs per embryo increased from 3.5 ± 0.8 to 10.4 ± 1.6, which is very close to the average number of mCherry-positive OSNs (11.4 ± 1.5). Importantly, 86.8% of mCherry-positive OSNs colabeled for GFP. Thus, under the experimental conditions employed here, expression of two reporter genes, mCherry and GFP, became highly correlate with a trend of the reporter gene in the second position to follow the behavior of the reporter that is located in the first position. However, all of these observations are equally compatible with both mechanisms and additional experiments were designed to discriminate between these possibilities (Section 4.1.2.4. and 4.1.2.5.).

The number of GFP-positive cells that colabeled for mCherry was even higher than double expression in mCherry-positive OSNs (98.4%). However, OMP is a general marker in the olfactory system that is generally expressed in all mature, ciliated OSNs. Thus a high correlation of mCherry expression in cells that express a reporter gene from an OR gene promoter would be expected to be high even if both reporters were expressed independently.

In summary, injection of the pOMP$_{(1.3)}$-mCherry-inter$_{(1.4kb)}$-GFP-pA construct promoted co-expression of GFP in 86.8% of mCherry-positive cells and within an average number of 10.4 ± 1.6 OSNs per embryo, which is a major increase in penetrance and expressivity when compared to the activity of the intrinsic OR103-5 promoter alone. However, the pan-olfactory OMP promoter that was utilized to drive expression of this construct bears some major experimental disadvantages, because of its broad expression in a high number of OSNs that precludes a clear interpretation of the results.

To circumvent the problem encountered with the broad expression of the OMP promoter and its potential contribution to the observed high double expression rate by independent transcription, the more specific OR101-1 promoter, which is active only in a restricted subset of OSNs, was used. Typically, OSNs only express one OR gene from the entire repertoire, thus by using a strong OR-specific promoter co-expression as a result of independent transcription from the OR101-1 and OR103-5 promoters is expected to be less likely.

The OR101-1 promoter appears to be the ideal substitute for the following reasons. First, the main promoter driving expression of the transgenic construct should be active in OSNs, yet, the subpopulations of OSNs that capable of expression from the main promoter and the intrinsic OR103-5 promoter should be different. The one neuron - one receptor rule, in principle, dictates that a specific OSN will choose only a single OR gene for expression from a much large and diverse repertoire (refer to Section 1.3.1. for further details). Hence, the promoters of two OR genes should not be active within the same OSN and drive expression in mutually exclusive OSN populations. This argument, however, is only valid if the transgenic construct promotes expression of an OR protein, which is not the case in the experiments described here. The OR101-1 gene promoter, to some extent, may recapitulate the expression of the endogenous OR 101-1 gene in embryos and leads to reporter gene expression in around 5 positive OSNs per OE in up to 75% of injected embryo (Kazci, unpublished).

The 1.2kb OR101-1 promoter was cloned directly upstream of mCherry-inter$_{(1.4kb)}$-GFP followed by a SV40 polyA transcription stop signal. The pOR101-1$_{(1.2kb)}$- mCherry-inter$_{(1.4kb)}$-GFP construct was injected into a total of 221 fertilized zebrafish oocytes (three independent injection experiments: 24, 68, and 129 embryos, respectively), 74 of which survived until the time of analysis at 3 and 4 dpf (10, 22, and 42 embryos, respectively). Of those, 59.5% (44/74 embryos) expressed mCherry and 59.5% (44/74 embryos) expressed GFP in OSNs. A total of 285 mCherry- and 252 GFP-expressing OSNs could be detected in transgenic embryos. Simultaneous expression of both reporter genes in the same OSN was observed in 234 cells. Thus, 82.1% (234/285 OSNs) of mCherry-positive OSNs colabeled for GFP while 92.9% (234/252 OSNs) of GFP-positive cells were simultaneously marked by mCherry. On average 6.5 ± 0.4 mCherry and 5.7 ± 0.4 GFP-expressing OSNs could be detected in the OE of transgenic embryos (Figure 4.8).

The observed expression pattern of mCherry with a penetrance of expression in 59% of injected embryos and an average of 6.5 ± 0.4 positive cells per embryo is in good compliance with the known activity of the OR101-1 gene promoter, which was previously shown to generate on average 61.3% transgene-expressing embryos and 5 positive OSNs per embryo (Sogunmez, 2012). Interestingly, GFP expression in injected embryos was also high and 59% of embryos expressed GFP, which represents a two-fold increase when compared to the activity of the intrinsic OR103-5 promoter (23%). The average number of GFP-positive OSN also increased from 3.5 ± 0.8 in the inter$_{(1.4kb)}$-GFP-pA construct to 5.7 ± 0.4 in pOR101-1$_{(1.2kb)}$-mCherry-inter$_{(1.4kb)}$-GFP-pA.

Similar to the results obtained for the pOMP$_{(1.3)}$-mCherry-inter$_{(1.4kb)}$-GFP-pA construct, expression of mCherry and GFP was highly correlated at the individual OSN level. 82.1% of mCherry cells expressed GFP while almost all (92.9%) GFP-positive OSNs colabeled for mCherry. This result is somewhat unexpected if GFP and mCherry were expressed independently from two different OR gene promoters and favors a model in which expression of GFP becomes coupled to the activity of the first promoter through IRES activity of the intergenic region. As presented below, independent expression from the OR101-1 and OR103-5 promoters results only in 54.8% of GFP cells that are colabeled by

mCherry. However, similar to the considerations for the pOMP$_{(1.3)}$-mCherry-inter$_{(1.4kb)}$-GFP-pA construct, it cannot be ruled out that regulatory sites within the OR101-1 gene promoter interact with the downstream OR103-5 promoter to increase its activity when those are linked on the same physical plasmid.

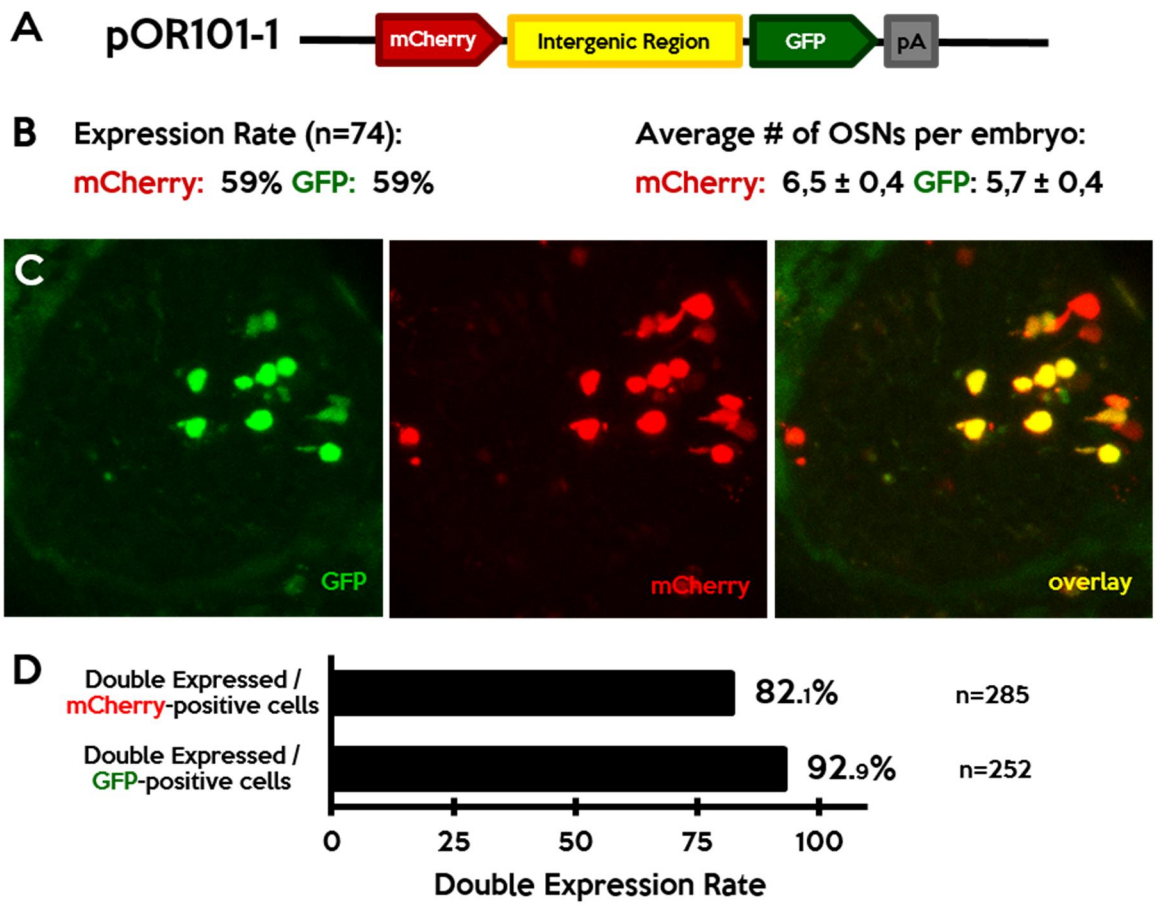

Figure 4.8. Transgene expression analysis of the pOR101-1$_{(1.2kb)}$-mCherry-inter$_{(1.4kb)}$-GFP-pA construct. (A) Overview of the construct. (B) Expression rates and average number of reporter gene-positive OSNs (C) Confocal z-stacks of 3dpf OE. (D) Double expression rates.

In summary, when olfactory epithelium-specific promoters, such as the OMP and OR101-1 gene promoters are used, the presence of the intergenic region tightly couples expression of two fluorescent reporter genes in a high number of OSNs. Both experiments demonstrate that expression of GFP, which is located in the second position downstream of the intergenic region, becomes highly correlated with mCherry expression which is driven

by an independent upstream promoter. Under these experimental conditions, the resulting pattern of GFP expression is clearly different from the pattern observed for the inter$_{(1.4kb)}$-GFP-pA construct. A major drawback of the experimental design is that both promoters contained within the same construct have activity within the OE. Thus, next we asked whether the observed effect is specific for olfactory tissue or if a similar effect can also be observed in different cell types of the zebrafish embryo.

By using two different promoters, p$_{(1.3kb)}$OMP and p$_{(1.2kb)}$OR101-1, to drive transgenic constructs that contain the intergenic region in olfactory tissue, high rates of mCherry and GFP colabeling been obtained in OSNs. However, both promoters, as well as the OR103-5 promoter located within the intergenic region are specifically active in the OE, precluding to some degree a clear distinction between bi-cistronic expression resulting from IRES activity of the intergenic region and independent expression from two promoters contained within the same construct. Therefore, the use of a different promoter that is active outside the OE could uncouple these effects and may provide useful information to distinguish between the two possibilities. Because the OR103-5 promoter did not result in expression in tissues outside the OE (refer to Section 4.1.2.2.), any observed colabeling of reporter genes could result from bi-cistronic translation. In addition, it will show, whether the observed colabeling is specific for the olfactory tissue or if it is a more general feature without any tissue specificity.

The GAP-43 (growth associated protein-43) gene is expressed in early neurons around the time of axon outgrowth (Udvadia *et al.*, 2001). A 1 kb sequence surrounding the transcriptional start site of rat GAP43 gene has been shown to drive expression in developing neurons and notochord cells when it is injected into fertilized zebrafish oocytes at the one-cell stage (Reinhard *et al.*, 1994; Udvadia *et al.*, 2001). The same 1 kb sequence has been cloned and used as a tool in our laboratory before and it mimics endogenous expression of the zebrafish GAP-43 gene (Tastekin, 2012). Expression from the GAP-43 promoter can be detected in 3 and 4 dpf transgenic embryos, the time window of expression analyses in experiments reported above.

The 1 kb rat GAP-43 promoter was previously cloned directly upstream of mCherry-inter$_{(1.4kb)}$-GFP followed by a SV40 polyadenylation signal (Atasoy, 2011) to drive expression of the construct outside the OE. When the pGAP43-mCherry- inter$_{(1.4kb)}$-GFP-pA construct was injected into 153 fertilized zebrafish oocytes (two independent injection experiments: 12 and 141 embryos, respectively), 46 embryos survived until the time of analysis (4 and 42, respectively). Of those, 63% (29/46 embryos) expressed mCherry and 63% (29/46 embryos) expressed GFP in various types of neurons outside the OE. A total of 298 mCherry-expressing and 220 GFP-expressing cells could be identified in transgenic embryos. Simultaneous expression of both reporter genes in the same cell was observed in 220 cells. A total of 73.8% (220/298 cells) of mCherry-expressing cells were double positive for GFP while 100% of GFP expressing neurons (220/220 cells) were positive for mCherry. On average 10.3 ± 1.4 mCherry- and 7.6 ± 1.1 GFP-expressing neurons could be observed in various tissues of each transgenic embryo (Figure 4.9). Tissues of expression included Rohon-Beard (RB) neurons, early spinal neurons, commissural neurons, notochord cells and muscle cells.

Without any exception, all mCherry-expressing transgenic embryos were also positive for GFP. More importantly, all (100%) GFP-positive cells were also mCherry positive, demonstrating a strong correlation between the expressions of both reporter genes in tissues outside the OE. However, only 73.8% of all mCherry-positive cells expressed GFP simultaneously in the same cell. A similar observation was made for the OMP and OR101-1 promoter-driven constructs in the OE where consistently a lower fraction of mCherry cells were double positive for GFP than vice versa. This imbalance is not easily understood. It is possible that sequences within the 3'-UTR of the OR103-1 gene, which forms the 5'-segment of the intergenic region contains a transcription stop signal that is read in some cells while not in others. However, this possibility is unlikely and failure of the RNA polymerase to read the transcription termination signal should not be cell-type specific, thus resulting in a mixture of short and long transcripts in the same cell and consequently report colabeling with both reporters in all cells. Another possibility may be the time individual cells had available to express the construct before analysis. The rat GAP43 promoter drives expression in immature neurons and ectopically in various other cell types in zebrafish. At the time point of analysis some cells may have expressed the construct for a longer time and produced

a higher amount of mCherry and GFP proteins, while in other cells transcription from the pGAP43 just started and sufficient amounts of protein for fluorescent analysis had not yet accumulated. Thus, inherent fluctuations in the timing of pGAP43 activity in different tissues or cells may be resulted in the decreased double expression rate of mCherry-positive cells.

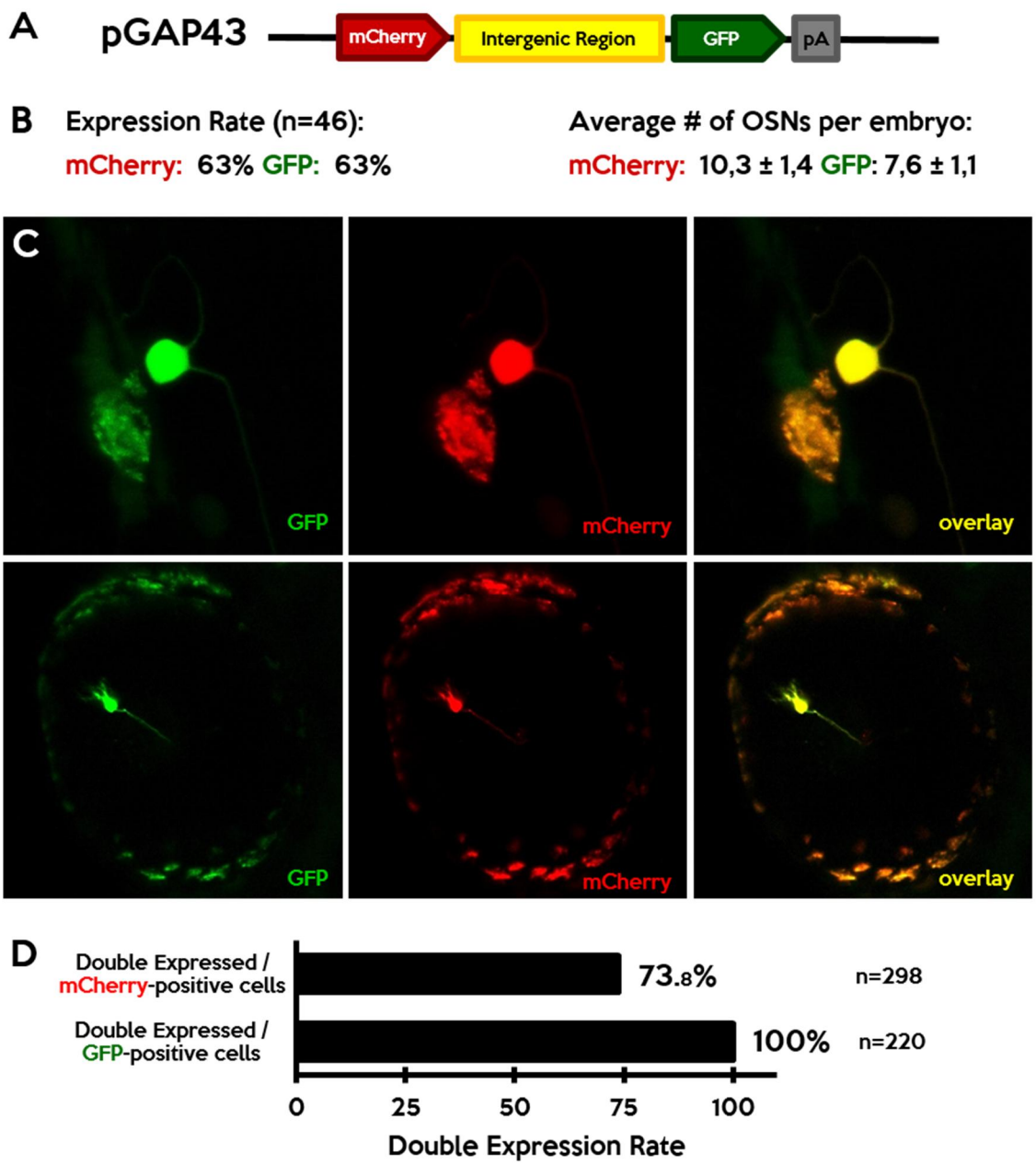

Figure 4.9. Transgene expression analysis of the pGAP43-mCherry- inter$_{(1.4kb)}$-GFP-pA construct. (A) Overview of the construct. (B) Expression rates and average number of reporter gene-positive neurons (C) Confocal z-stacks at 3dpf. (D) Double expression rates.

In order to further investigate the contribution of differences in transcript / protein levels caused by the differences in onset of pGAP43's activity to the colabeling rate the intensity of mCherry and GFP signals was scored as strong, intermediate and weak for each reporter gene-positive cell. In total, 75 mCherry-positive cells were scored to have weak signals, suggesting that in those neurons pGAP43 activity may have started only shortly before analysis or that the GAP-43 promoter only had weak activity at the time of analysis. Among those 75 cells, only one-third (24 cells) were GFP-positive, consistent with the idea that sufficient amounts of GFP protein has not been reached. Thus, when the 75 weak mCherry-positive neurons were excluded from the calculation of double expressions, colabeling increased from 73.8% to 87.8% which is very similar to the results obtained when the OMP and OR101-1 gene promoters were used.

In summary, a very high correlation of double expression of 87.8% (for strong expressing cells; 73.8% for all mCherry-positive cells) was observed even outside the olfactory tissue, indicating that the intergenic region may contribute to co-translation of reporter genes from the same promoter rather than co-expression from two independent promoters and two independent transcripts.

4.1.2.4. Colabeling with Two Reporter Genes is Dependent on the Intergenic Region. In the experiments presented above, high colabeling with mCherry and GFP could be detected after the injection of constructs that contained the OR103-1/5 intergenic region interspersed between the two different reporter genes. As briefly outlined above, at least two possible mechanisms could contribute to the observed colabeling: co-translation from a bi-cistronic transcript and independent expressions from two independent promoters. In the latter case, regulatory sites within the first, typically strong promoter, could spread to the second promoter and thereby increase its efficiency. Experimentally disabling either mechanism may reveal further insight into the true mechanism. There are in principle two different ways by which such an uncoupling could be achieved: by isolating the reporter genes on separate constructs and co-injection or by preventing the formation of a long transcript through a transcriptional stop signal downstream of the first reporter gene.

In order to uncouple the effects of the two different promoters and to ensure independent expression of the different reporter genes, pOMP$_{(1.3kb)}$-mCherry-pA and inter$_{(1.4kb)}$-GFP-pA constructs were coinjected into 124 embryos (two independent injection experiments: 56 and 68 embryos, respectively), 101 of which survived until the time of analysis (27 and 24 embryos, respectively). Of those, 47% (24/51) expressed mCherry and 31% (16/51) expressed GFP in OSNs. A total of 233 mCherry expressing and 61 GFP expressing OSNs could be detected in transgenic embryos. Simultaneous expression of both reporter genes in the same OSN was observed in 61 cells. In total, only 26.2% (61/233) of mCherry-expressing OSNs were positive for GFP, while 100% (61/61) of GFP-positive neurons expressed mCherry. On average 9.7±0.9 mCherry and 3.8±0.6 GFP expressing OSNs could be observed in the OE of each transgenic embryo (Figure 4.10).

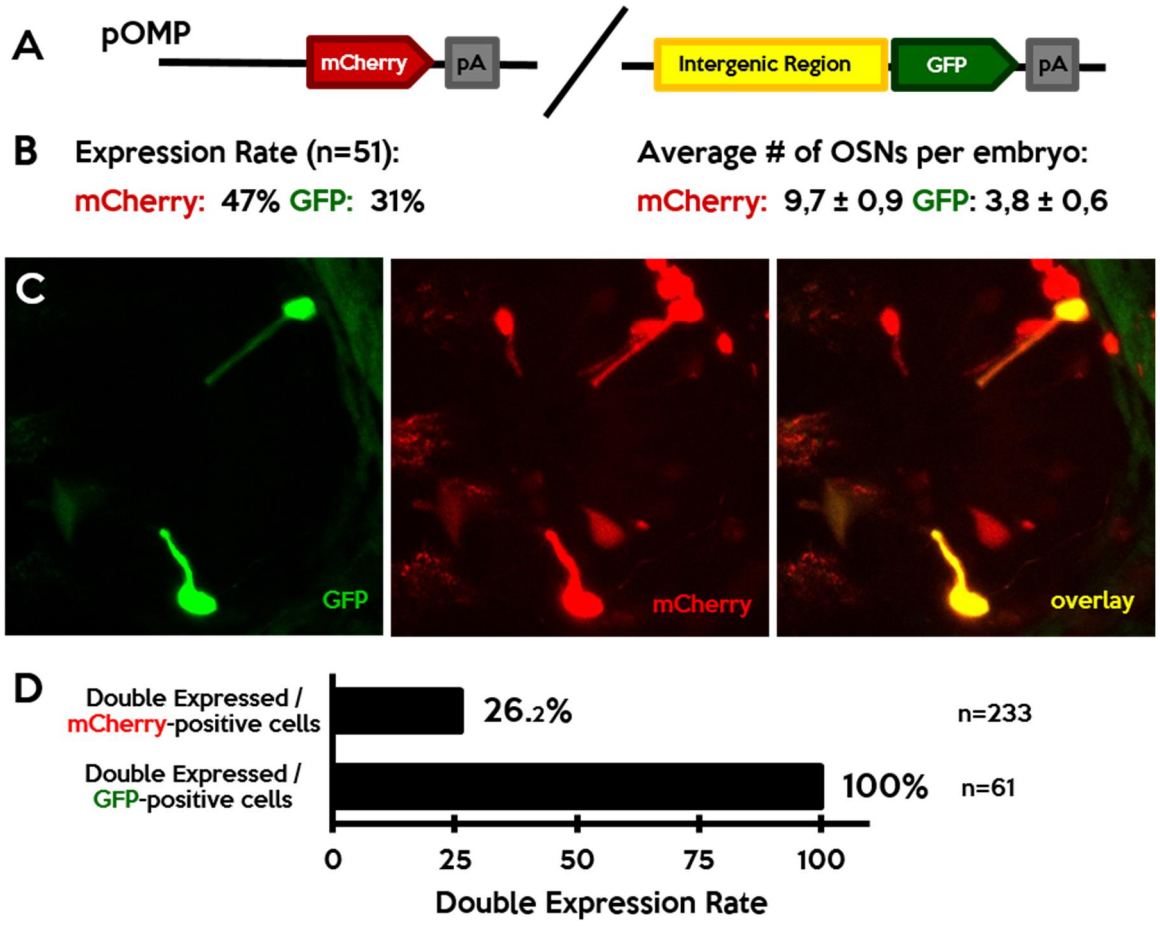

Figure 4.10. Transgene expression analysis of pOMP-mCherry-pA and inter$_{(1.4kb)}$-GFP-pA co-injection. (A) Overview of the constructs. (B) Expression rates and average number of reporter gene-positive OSNs (C) Confocal z-stacks at 3dpf. (D) Double expression rates.

The penetrance of expression from the OMP promoter and the number of transgene-positive OSNs is consistent with previous experiments (Section 4.1.2.3.), 42% transgene-positive embryos for the pOMP-mCherry- inter$_{(1.4kb)}$-GFP-pA construct compared to 47%for the pOMP-mCherry-pA construct that was used here. Importantly, when the two promoter-reporter constructs were coninjected as separate plasmids GFP expression became largely independent of mCherry expression at the whole embryo level and decreased from 40% in the context of the pOMP-mCherry- inter$_{(1.4kb)}$-GFP-pA construct to 31%, which is consistent with previous results for the inter$_{(1.4kb)}$-GFP-pA construct (Section 4.1.2.2.) where 23% transgene expression was observed.

The comparison of average number of positive OSNs per embryo between injection of the long construct and co-injection of two short constructs shows a similar trend. The OMP promoter activity resulted in mCherry expression in 9.7 ± 0.9 OSNs when coinjected with inter$_{(1.4kb)}$-GFP-pA, which is similar to the pOMP-mCherry-inter$_{(1.4kb)}$-GFP-pA injection results with 11.4 ± 1.5 OSNs per embryo. On the other hand, the average number of GFP expressing OSNs drastically decreased from 10.4 ± 1.6 obtained from the long construct to 3.8 ± 0.6 when separate constructs were injected. This low number is similar to the results obtained from injection of the inter$_{(1.4kb)}$-GFP-pA construct with 3.5 ± 0.8 positive OSNs per embryo. The most important outcome of the coinjection experiment, however, is the significant decrease in fraction of double positive OSNs per mCherry-positive neurons from 86.8% to 26.2%, which is similar to the promoter activity of the intergenic region. Thus, the activity of the OMP and OR103-5 promoters became largely uncoupled when injected as separate constructs.

Nonetheless, a large fraction of GFP-positive OSNs still colabel for mCherry: 98.4% and 100%. The promoter of OMP gene, in principle, drives expression in all mature ciliated OSNs. The intrinsic OR103-5 promoter of the intergenic region targets a subpopulation of those cells. Thus, GFP-positive OSNs form a subset of mCherry expressing neurons, even if the transgenes are expressed from independent promoters and thus produce the apparent high colabeling rate, which reached 100% in this case. The prediction is that another promoter which targets a narrower subset of OSNs such as the promoter of another OR gene should

prevent this high double expression rate (refer to Section 3.3.2. for further details). For this reason, the co-injection approach was extended to coinjection of $p_{(1.2kb)}$OR101-1-mCherry and inter $_{(1.4kb)}$-GFP-pA constructs.

A significant decrease of double-positive embryos and OSNs was observed when the pOMP-mCherry and inter $_{(1.4kb)}$-GFP were injected as separate constructs. However, under these experimental conditions, most GFP-positive cells were still double-positive for mCherry. A possible explanation is that the OMP gene promoter is active in the same cell type as the intrinsic OR103-5 promoter and with high efficiency leading to independent expression of both constructs in the same cell. In order to employ the same strategy with a promoter that is active in a more restricted and largely non-overlapping OSN population, the pOR101-1-mCherry-pA and inter $_{(1.4kb)}$-GFP-pA constructs were co-injected and compared to the results obtained with the pOR101-1-mCherry-inter $_{(1.4kb)}$-GFP-pA construct.

The pOR101-1-mCherry-pA and inter $_{(1.4kb)}$-GFP-pA constructs were co-injected into 119 embryos (two independent injection experiments: 57 and 62 embryos, respectively) of which 49 survived until analysis (15 and 34 embryos, respectively). Of those, 25% (12/49 embryos) expressed mCherry and 18% (9/49 embryos) expressed GFP in OSNs. A total of 48 mCherry-expressing and 31 GFP-expressing OSNs could be observed. Simultaneous expression of both reporter genes in the same OSN was observed in 17 cells. The fraction of mCherry-positive OSNs that express GFP was 35.4% (17/48) and the percentage of GFP-expressing neurons that were positive for mCherry was 54.8% (17/31). On average 5.3 ± 1.1 mCherry and 3.4 ± 1.0 GFP expressing OSNs could be identified in the OE of each transgenic embryo (Figure 4.11).

The coinjection of pOR101-1-mCherry-pA and inter $_{(1.4kb)}$-GFP-pA resulted in a dramatic decrease in the number of reporter gene-positive embryos and a decrease in the rate of double-positive cells when compared to the linked pOR101-1-mCherry-inter $_{(1.4kb)}$-GFP-pA construct. For the long construct, mCherry and GFP were expressed in 59% of embryos, but after co-injection of reporter genes these rates decreased into 25% and 18%, respectively. When the pOR101-1-mCherry-inter $_{(1.4kb)}$-GFP-pA construct was injected all mCherry-

expressing transgenic embryos also expressed GFP. Yet, when coinjected as separate plasmids only half of the mCherry-positive embryos expressed GFP in OSNs, implying that expression of both reporter genes has been successfully uncoupled.

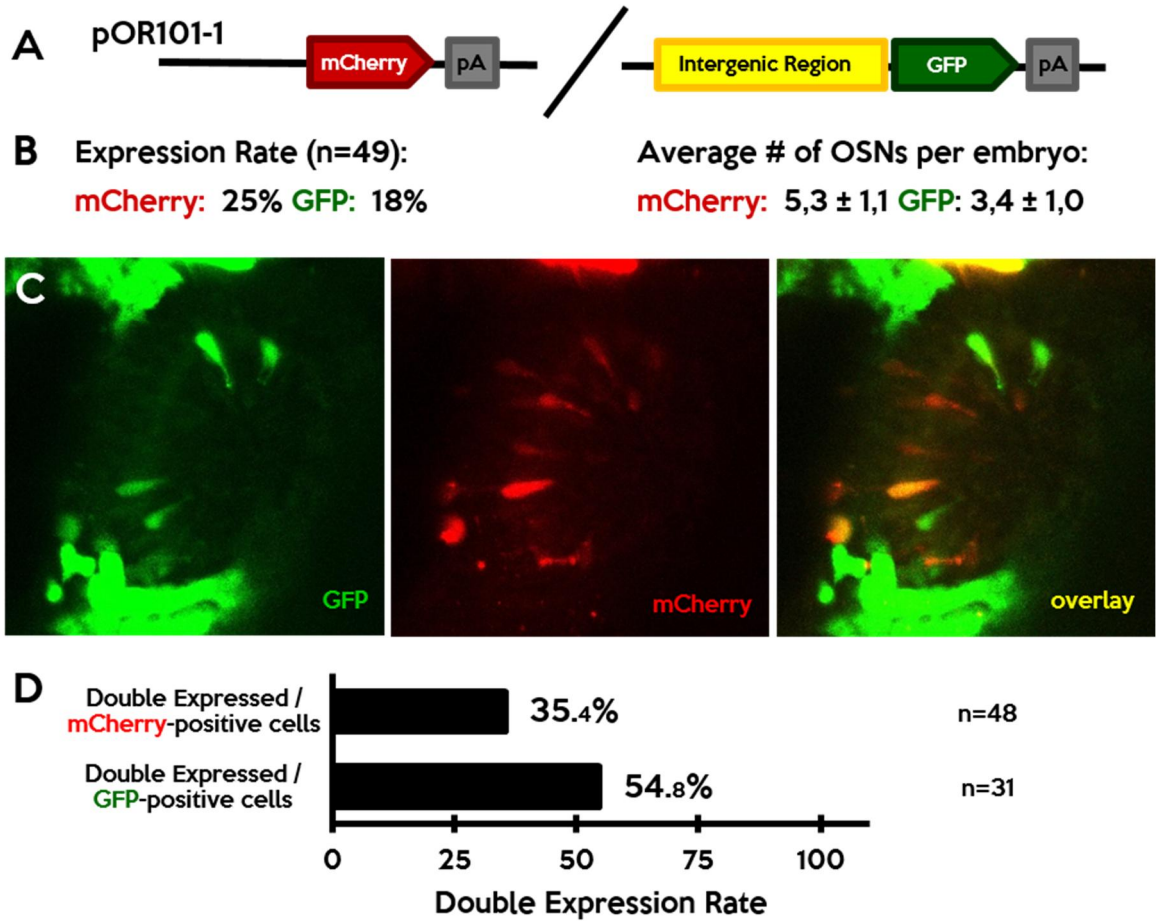

Figure 4.11. Transgene expression analysis of $p_{(1.2kb)}$OR101-1-mCherry-pA & inter $_{(1.4kb)}$-GFP-pA co-injection. (A) Overview of the constructs. (B) Expression rates and average number of reporter gene-positive OSNs (C) Confocal z-stacks at 3dpf. (D) Double expression rates.

A similar decrease was observed for the number of GFP-positive OSNs, while the number of mCherry-positive cells remained largely unchanged with 6.5 ± 0.4 and 5.3 ± 1.1 for injection of the long and coinjection of the independent plasmids, respectively. On the other hand, the average number of GFP-positive OSNs per transgenic embryo diminished from 5.7 ± 0.4 to 3.4 ± 1.0 similar to the 3.5 ± 0.8 OSNs that were observed when the inter

$_{(1.4kb)}$-GFP-pA was injected. This similarity suggests that the promoters within the different plasmids act independently when coinjected.

The most significant difference is observed among mCherry-positive cells that colabel for GFP. Only 35.4% of mCherry-positive OSNs expressed GFP as compared to the 82.1% seen for pOR101-1-mCherry-inter $_{(1.4kb)}$-GFP-pA. The double expression rate in GFP-positive OSNs also diminished from 92.9% to 54.8%, again pointing out the autonomous actions of pOR101-1 and OR103-1/5 intergenic region when isolated into different plasmids.

In conclusion, similar to the results obtained with the OMP promoter, an uncoupling of reporter gene expression was observed for the OR101-1 and OR103-5 promoters when the reporter genes were not linked physically by the intergenic region. These results strongly suggest that the intergenic region has the capacity to promote bi-cistronic translation. However, a pitfall of the experimental approach that is presented here is that the two different reporter genes and promoters reside on physically distinct plasmid molecules. Even though both plasmids are present in the same cell and might co-integrate into the same genomic locus after injection, this experimental condition creates some uncertainty as to how these plasmids could interact with each other. To better control this issue the promoters for OR101-1 and OR103-5 were uncoupled on the same plasmid through the insertion of a polyadenylation signal.

Because in the co-injection experiments the two promoters and reporter genes were on physically isolated plasmids which may lead to a loss of interaction between regulatory sites contained within the two different promoters, another control experiment was performed where the promoters and reporter genes were uncoupled on the same plasmid through the insertion of a polyadenylation signal. In this experiment, the reporter genes are located on the same DNA, however, they are forced to be transcribed separately from different promoters by the usage of a polyadenylation signal which triggers the termination of pol2 transcription (Kim and Martinson, 2003).

A 260 bp SV40 polyA sequence was cloned between mCherry and the intergenic region to terminate transcription from the first promoter after the mCherry sequence. Thus,

RNA polymerase will not be able to continue its elongation through the intergenic region, which would be a strict requirement for bi-cistronic translation. As a result, the pOR101-1-mCherry-pA-inter $_{(1.4kb)}$-GFP-pA construct will produce two different transcripts where the reporter genes are isolated, while still allowing for possible interactions between the promoters.

The new pOR101-1-mCherry-pA-inter $_{(1.4kb)}$-GFP-pA construct was injected into 149 zebrafish oocytes of which 76 embryos survived until the time of analysis. Of those, 58% (44/76 embryos) expressed mCherry and 46% (35/76 embryos) expressed GFP in OSNs. A total of 307 mCherry-expressing and 97 GFP-expressing OSNs were detected in the transgenic embryos. Simultaneous expression of both reporter genes in the same OSN was observed in 96 cells. Thus, 31.3% (96/307 OSNs) of mCherry-expressing neurons colabeled for GFP and 98.9% (96/97) of GFP-expressing neurons were found to be positive for mCherry. On average 7 ± 0.6 mCherry and 2.8 ± 0.3 GFP expressing OSNs could be detected in the OE of transgenic embryos (Figure 4.12).

The changed experimental conditions did not affect the activity of the OR101-1 promoter. Expression of mCherry was observed in 58% of embryos and in 7.0 ± 0.6 OSN per transgenic embryo, similar to the results obtained when the pOR101-1-mCherry-inter $_{(1.4kb)}$-GFP-pA was injected where 59% positive embryos and on average 6,5 ± 0.4 OSNs per embryo were obtained. Strikingly, however, the expression of GFP in the second position was dramatically reduced from 59% to 46% positive embryos and an average number of GFP-positive OSNs from 5,0 ± 0.4 to 2,8 ± 0.3. These results are similar to the efficiencies observed when the inter $_{(1.4kb)}$-GFP-pA was injected alone or in combination with pOR101-1-mCherry-pA, which were 2.9 ± 0.7 and 3.4 ± 1.0 GFP-positive OSNs, respectively. In those cases GFP was driven by the intrinsic OR103-5 promoter that resides in the intergenic region. Thus, the inserted pA appears to successfully uncouple reporter gene expression, most likely by initiating transcription of each reporter from a different promoter. The most sensitive indicator of co-expression, the number of mCherry-positive cells that colabel for GFP, decreased dramatically from 82.1% to 31.3% similar to the results observed when both promoter-reporter pairs were injected as separate constructs, which was as high as 35%.

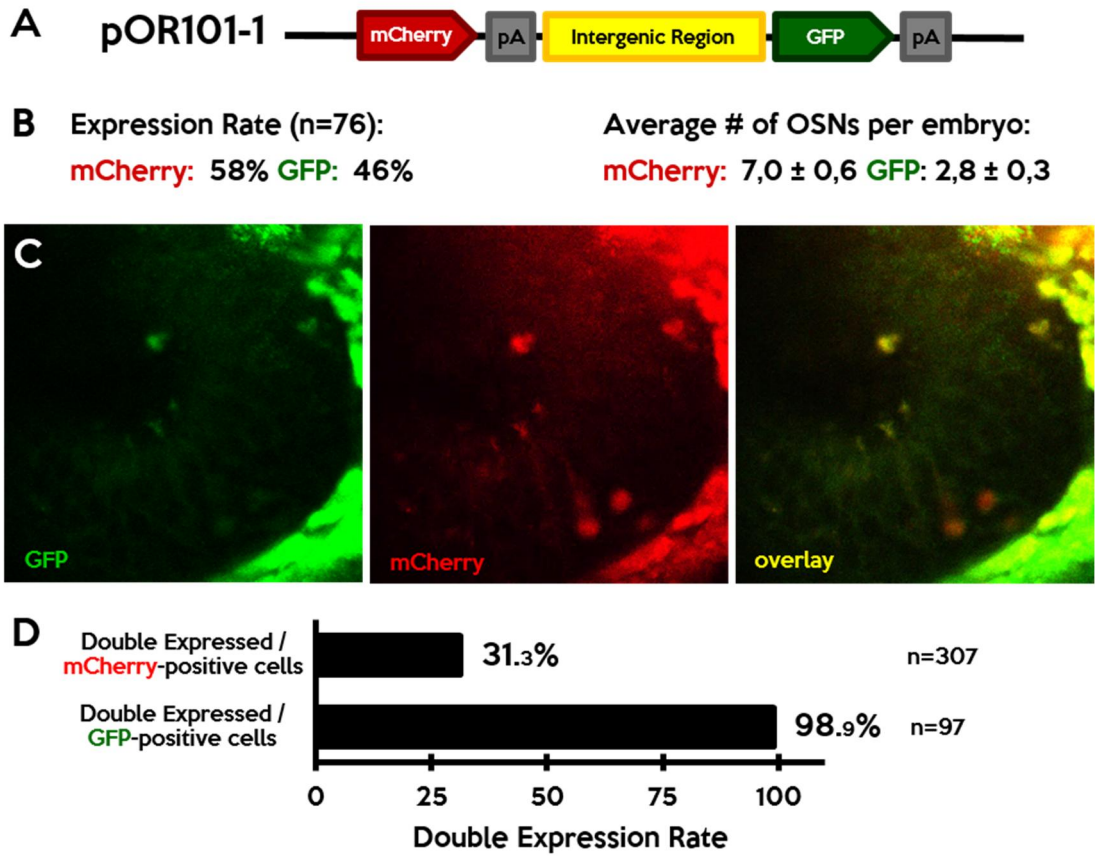

Figure 4.12. Transgene expression analysis of the pOR101-1-mCherry-pA- inter $_{(1.4kb)}$-GFP-pA construct. (A) Overview of the construct. (B) Expression rates and average number of reporter gene-positive OSNs (C) Confocal z-stacks at 3dpf. (D) Double expression rates.

In summary, when pOR101-1-mCherry and inter $_{(1.4kb)}$-GFP were separated by a transcription stop signal the pattern of expression and coexpression resembled the results obtained when both parts were injected as separate constructs. Therefore, the polyA sequence acts as expected and may successfully terminated transcription after mCherry sequence and in the absence of a single transcript suitable for bi-cistronic expression the double expression rate of mCherry-positive OSNs diminished severely. Thus, the high colabeling rates achieved in previous experiments may originate from intergenic region's ability to promote bi-cistronic expression from a long RNA transcript.

4.1.2.5. Substitution of the Intergenic Region with Different Promoters. Another contribution to high colabeling rates detected in previous injection experiments may be the possible upregulation of the intrinsic promoter within OR103-1/5 intergenic region, caused by the strong promoter situated in the first position of the construct. Both, the pOMP and pOR101-1 are fairly strong promoters, which are shown to have high penetrance of expression and expressivity in transgenic embryos (Celik *et al.*, 2002; Sogunmez, 2012). For instance, nucleosome dynamics at promoters and surrounding DNA regions (Mellor, 2005), or the spread of unknown enhancer elements could boost the activity of sequences adjacent to these promoters. Chromatin remodeling or recruitment of transcription factors by the main promoter in the long constructs may thus promote transcription from adjacent loci, in this case the intrinsic OR103-5 promoter. One way to investigate the possible impact of a strong upstream promoters on the downstream OR103-5 promoter the intergenic region was replaced with the promoter of the OR111-7 gene. The underlying idea is that any modulatory influence of the strong upstream promoter should be similar on a different downstream promoter.

There are several criteria that should be met by the substitute OR gene promoter in order to provide sufficient experimental information. First of all, the OR gene promoter that replaces the intergenic region should have previously been characterized, i.e it's penetrance and expressivity should be known. As a second criterion, considering the difficulty encountered for the discrimination of intrinsic promoter and IRES activity in previous experiments, the substitute OR gene promoter should have a relatively weak expression profile. In this case, a high correlation of mCherry and GFP reporter gene expression will indicate an increase in co-transcription. In addition, the length of the substitute promoter appears to be important. If it exceeds the size of the intergenic region of 1.4 kb, any possible enhancing impact may be diminished or lost (Lomvardas *et al.*, 2006).

The previously characterized promoter of the OR111-7 gene seems to be a suitable tool with respect to the criteria listed above. A 571 bp long sequence comprising the transcriptional start site of the gene has been identified as the minimal promoter that drives reporter gene expression in OSNs (Mori *et al.*, 2000). A pOR111-7$_{(0.6kb)}$-eYFP-pA construct

has previously been generated in the laboratory and shown to be expressed in 3% of injected embryos with an average number of 3 positive OSNs per transgenic embryo (Tastekin, 2012). The size of the 571bp OR111-7 promoter sequence does not exceed the length of OR103-1/5 intergenic region.

In order to substitute the intergenic region with the OR111-7 gene promoter, the 571bp pOR111-7 sequence was cloned between mCherry and GFP, which was subsequently cloned downstream of pOR101-1 and upstream of a SV40 polyadenylation signal. The pOR101-$1_{(1.2kb)}$-mCherry-pOR111-$7_{(0.6kb)}$-GFP-pA construct was injected into 181 (two independent injection experiments: 87 and 94 embryos, respectively) embryos, 68 of which (36 and 32 embryos, respectively) survived until the time of analysis. Of those, 46% (31/68 embryos) expressed mCherry while only 13% (9/68 embryos) expressed GFP in OSNs. A total of 128 mCherry expressing and 16 GFP expressing OSNs were detected in transgenic embryos. Simultaneous expression of both reporter genes in the same OSN was observed in 11 cells. The number of mCherry-positive neurons that were double positive for GFP was 8.6% (11/128) while 68.8% (11/16 cells) of GFP-expressing OSNs were also positive for mCherry. On average 4.1 ± 0.5 mCherry and 1.8 ± 0.2 GFP expressing OSNs could be detected in the OE of transgenic embryo (Figure 4.13).

With an average of 4.1 ± 0.5 positive OSNs detected in 46% of the injected embryos; the pattern of mCherry expression appears similar for the pOR101-1-mCherry-pOR111-7-GFP-pA construct as in other constructs that utilize the same promoter throughout this study. However, expression of GFP which typically was high and strongly correlated with mCherry expression when located downstream of the intergenic region decreased in the pOR101-$1_{(1.2kb)}$-mCherry-pOR111-$7_{(0.6kb)}$-GFP-pA construct. Only 13% of the embryos expressed GFP in OSNs, and the average number of GFP-positive cells per transgenic embryo was as low as 1.8 ± 0.2. More importantly, colabeling decreased tenfold from 82.1% into 8.6%. This finding strongly argues against a possible augmentation of a second downstream promoter by regulatory sequences contained within a strong upstream promoter in dual promoter constructs.

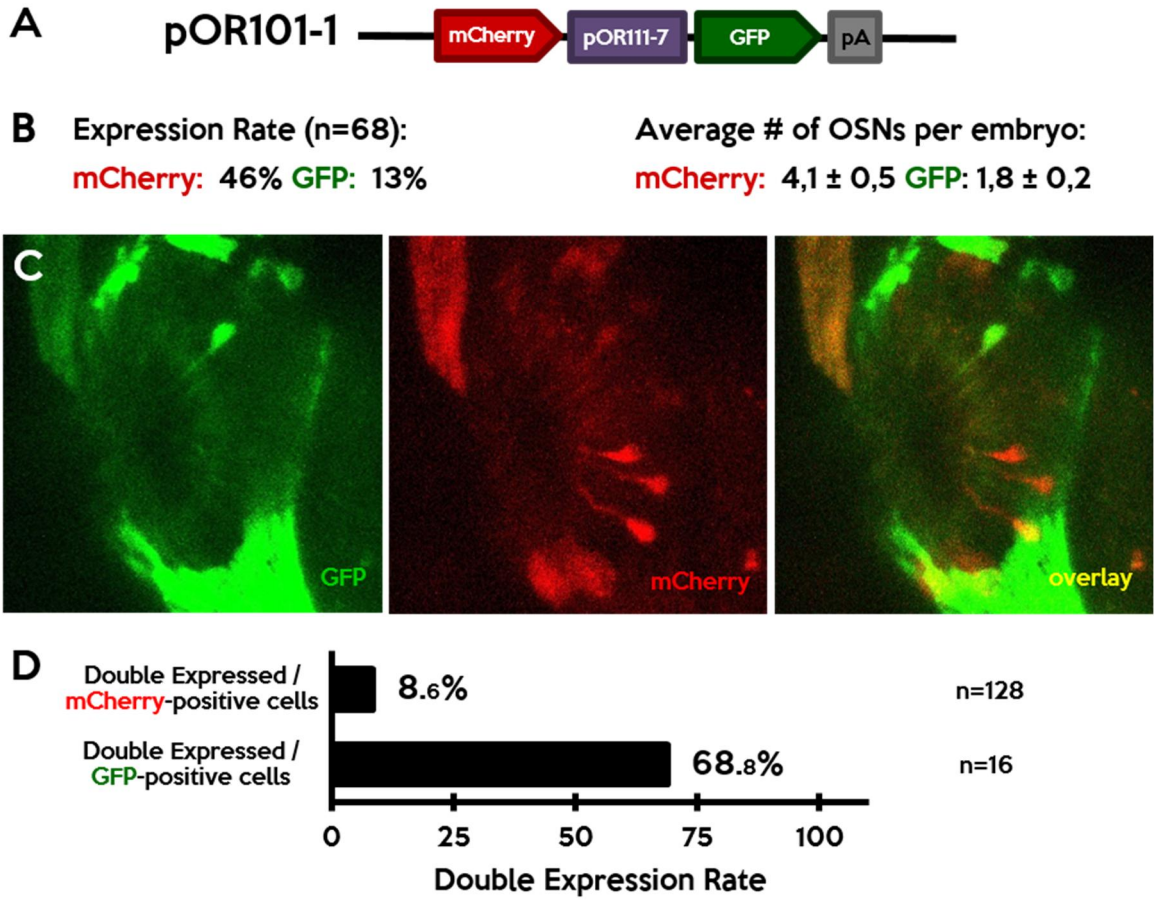

Figure 4.13. Transgene expression analysis of the $p_{(1.2kb)}$OR101-1-mCherry-$p_{(0.6kb)}$OR111-7-GFP-pA construct. (A) Overview of the construct. (B) Expression rates and average number of reporter gene-positive OSNs (C) Confocal z-stacks at 3dpf. (D) Double expression rates.

In order to provide the necessary reference data on independent expression and co-expression from the pOR101-$1_{(1.2kb)}$-mCherry and pOR111-$7_{(0.6kb)}$-GFP-pA constructs, pOR111-$7_{(0.6kb)}$-GFP-pA and pOR101-$1_{(1.2kb)}$-mCherry were coinjected as independent plasmids, similar to the experiments described above. A total of 239 embryos (four independent injection experiments: 34, 113, 48 and 98 embryos, respectively) were injected, 73 of which survived until the time of analysis (2, 8, 17 and 46 embryos, respectively). Of those, 49% (36/73 embryos) expressed mCherry while 32% (23/73 embryos) expressed GFP in OSNs. A total of 119 mCherry-expressing and 38 GFP-positive OSNs were observed in the transgenic embryos. Simultaneous expression of both reporter genes in the same OSN could be observed in 33 cells. Thus, a total of 27.7% (33/119) of mCherry-positive cells expressed GFP and 86.8% (33/38) of GFP-expressing neurons were double positive for

mCherry. On average 3.3 ± 0.4 mCherry and 1.7 ± 0.2 GFP-expressing OSNs could be observed in the OE of transgenic embryos (Figure 4.14).

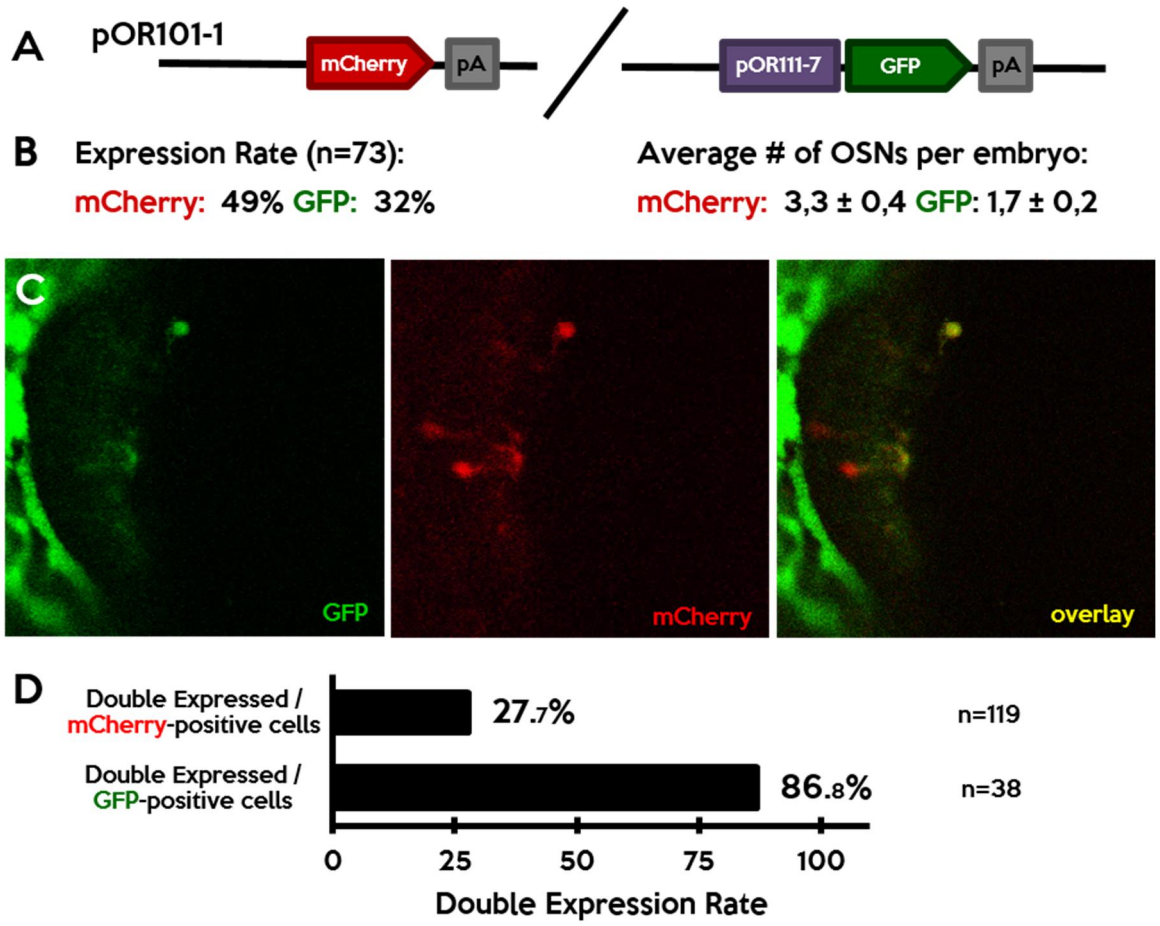

Figure 4.14. Transgene expression analysis of $p_{(1.2kb)}$OR101-1-mCherry-pA & $p_{0.6kb)}$OR111-7-GFP-pA co-injection. (A) Overview of the construct. (B) Expression rates and average number of reporter gene-positive OSNs (C) Confocal z-stacks at 3dpf. (D) Double expression rates.

Similar to previous coinjection results for pOR101-1 and pOMP, the mCherry expression pattern remained unchanged, regardless whether it was injected as an independent plasmid or as part of long construct. For the long construct, mCherry was expressed in 46% of injected embryo in 4.1 ± 0.5 cells. When coinjected the OR101-1 promoter drove mCherry expression in 49% of injected embryos and in 3.3 ± 0.4 OSNs. Similarly, the behavior of the OR111-7 promoter did not change regardless whether it was part of the long construct (13% in 1.8 ± 0.2 OSNs) or injected as a simple promoter construct

(32% in 1.7 ± 0.2 OSNs). Coexpression was uncorrelated under either condition, only 8.6% or 27.7% of mCherry cells colabeled for GFP. Surprisingly, however, the fraction of GFP-positive cells that colabeled for mCherry was high in both cases (68.8% and 86.8%).

4.1.2.6. Summary of *in vivo* Studies. In summary, correlated expression of two fluorescent reporters can be achieved in transgenic constructs in which the two reporter genes are connected by the intergenic region. This effect appears to be largely independent of the promoter used or the tissue specificity of the promoter. Similar results were obtained for olfactory tissue-specific promoters, such as pOMP and pOR101-1, and for the GAP-43 promoter that is active in neurons including neurons outside the OE. The correlation of dual reporter gene expression is maintained whenever the two reporter genes are located on the same physical DNA and as long as expression of a long transcript encompassing both reporter sequences is permitted by the intergenic region. Interruption of transcription after the first reporter gene by insertion of a polyadenylation signal largely abolishes dual reporter gene expression by the same cell. The effect is most likely due to co-translation of both reporters from a single mRNA transcript and consistent with the definition of an IRES. Several experimental observations favor bi-cistronic translation over correlated expression from two linked promoters and spread of regulatory influences from one promoter to the other. The colabeling is abolished when both promoters reside on different plasmids. Although located on different plasmid DNAs, typically both DNAs would cointegrate into the genome thereby creating a situation similar to the long expression constructs. Colabeling is sequence-specific and substitution of the intergenic region with a different promoter does not lead to similar colabeling of OSNs. Interruption of a long transcript by a polyadenylation signal abolishes the effect. It is expected that the rather short 260 bp polyA sequence should not perturb the spread of regulatory influences from one promoter to another, be it chromatin based, based on the recruitment of transcription factors, or physical interactions between those sequences. Correlation was typically higher and less sensitive to the effect for the weaker promoter in the second position. This is somewhat surprising, but could be explained by the fact that all transgenic constructs used here utilize OR gene promoters but do not express an OR coding sequence. Expression from these promoters might be disregulated in the sense that they show a broader than usual expression profile because formation of OR

protein from these promoters would normally prevent expression of other OR genes. (Figure 4.15).

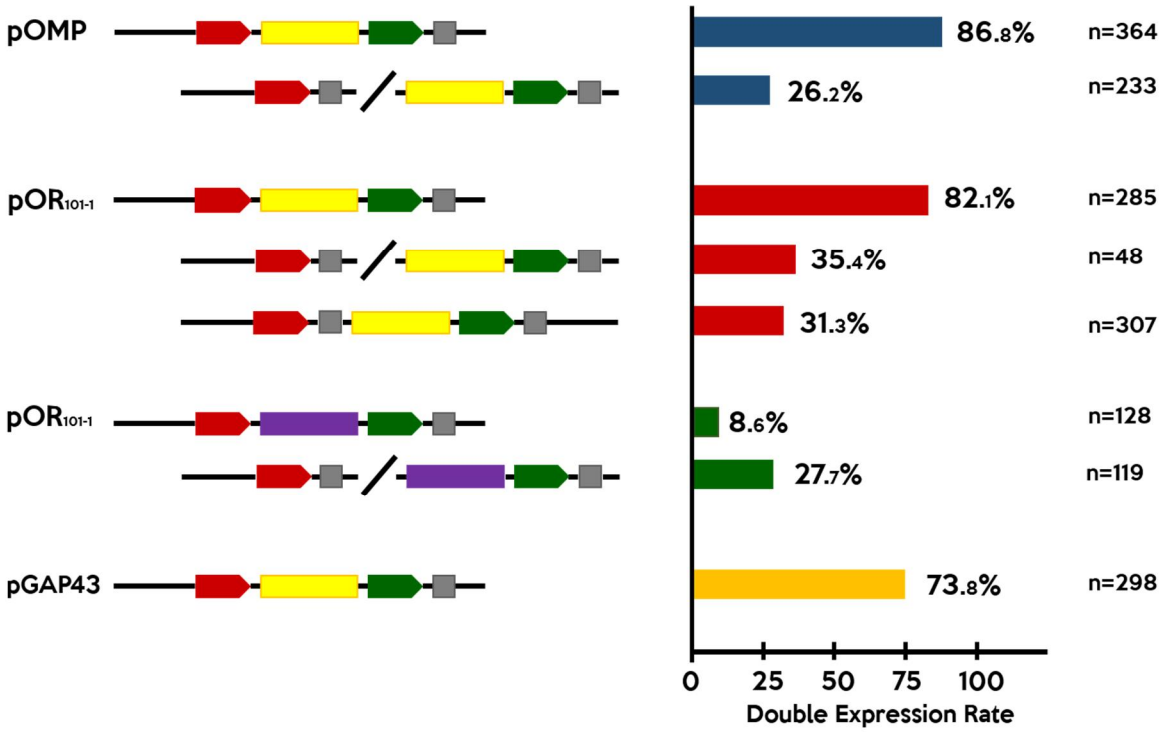

Figure 4.15. Double expression rates generated by transgenic constructs throughout Section 4.1.2.

4.2. Use of the Intergenic Region as a Molecular Tool

The previous experiments suggest that the intergenic sequence promotes cotranslation of two proteins from a single long transcript. This property could be used as a molecular tool to direct gene and reporter gene expression to specific cell types under the control of selected promoters. In the following experiments it was sought to use the intergenic region to force coexpression (cotranslation) of an OR gene and a fluorescent marker in specific OSN subpopulations. OR proteins appear to have multiple roles in the olfactory system, including axonal wiring of OSNs to the olfactory bulb. Thus, OSNs expressing a specific OR can often be identified by their axonal trajectories and target glomeruli in the olfactory bulb (Mombaerts *et al.*, 1996). The position of these targets or the axonal trajectories towards glomeruli may change for OSNs that express transgenic ORs. For instance, the position of

specific glomeruli appears to depend both on the identity of the expressed OR as well as the expression level of the OR protein (Wang et al., 1998; Feinstein *et al.*, 2004). Because glomerular targeting is a sensitive indicator of OR gene expression it was essential to better understand the properties and emergence of the embryonic glomerular map before investigating OR-transgenic OSNs and their axonal projections in detail.

In the literature, a stereotyped glomerular pattern in the embryonic OB has been described (refer to Section 1.6. for further details). An initially fuzzy pattern of axonal projections can be detected as early as 2 dpf, which transforms into a more elaborate map containing distinct and recognizable protoglomeruli by 3.5 dpf (Dynes and Ngai, 1998). In transient transgenic and some stable transgenic studies, labeled OSNs also reach a maximum number by 3.5 dpf to 5 dpf before the number declines in at later developmental times (Tastekin, 2012; Lakhina *et al.*, 2012). Thus, an ideal experimental timepoint to analyze transgene-expressing OSNs in transient transgenic zebrafish embryos lies around 4 dpf. Here, experiments were performed to describe the embryonic glomerular map during early development and more specifically at 4 dpf according to the nomenclature established by Dynes and Ngai (1998).

4.2.1. Embryonic Glomerular Map

To demonstrate the embryonic glomerular array during the first 13 days of zebrafish development the vital dye bodipy (boron-dipyrromethene) was used. Bodipy preferentially stains cell membranes leaving nucleoplasm and interstitial space devoid of the fluorophore. It allows individual cell boundaries and cell nuclei to be imaged clearly. Glomeruli are spherical neuropil structures in the OB where OSN axons form synapses with dendrites of projection neurons and interneurons and are devoid of cell bodies. Because glomeruli are essentially composed only of membrane they can be visualized easily upon bodipy staining. Zebrafish of various age (1, 2, 3, 4, 7 and 13 dpf) were stained by simple incubation in bodipy solution and subsequently analyzed by confocal microscopy (Figure 4.16).

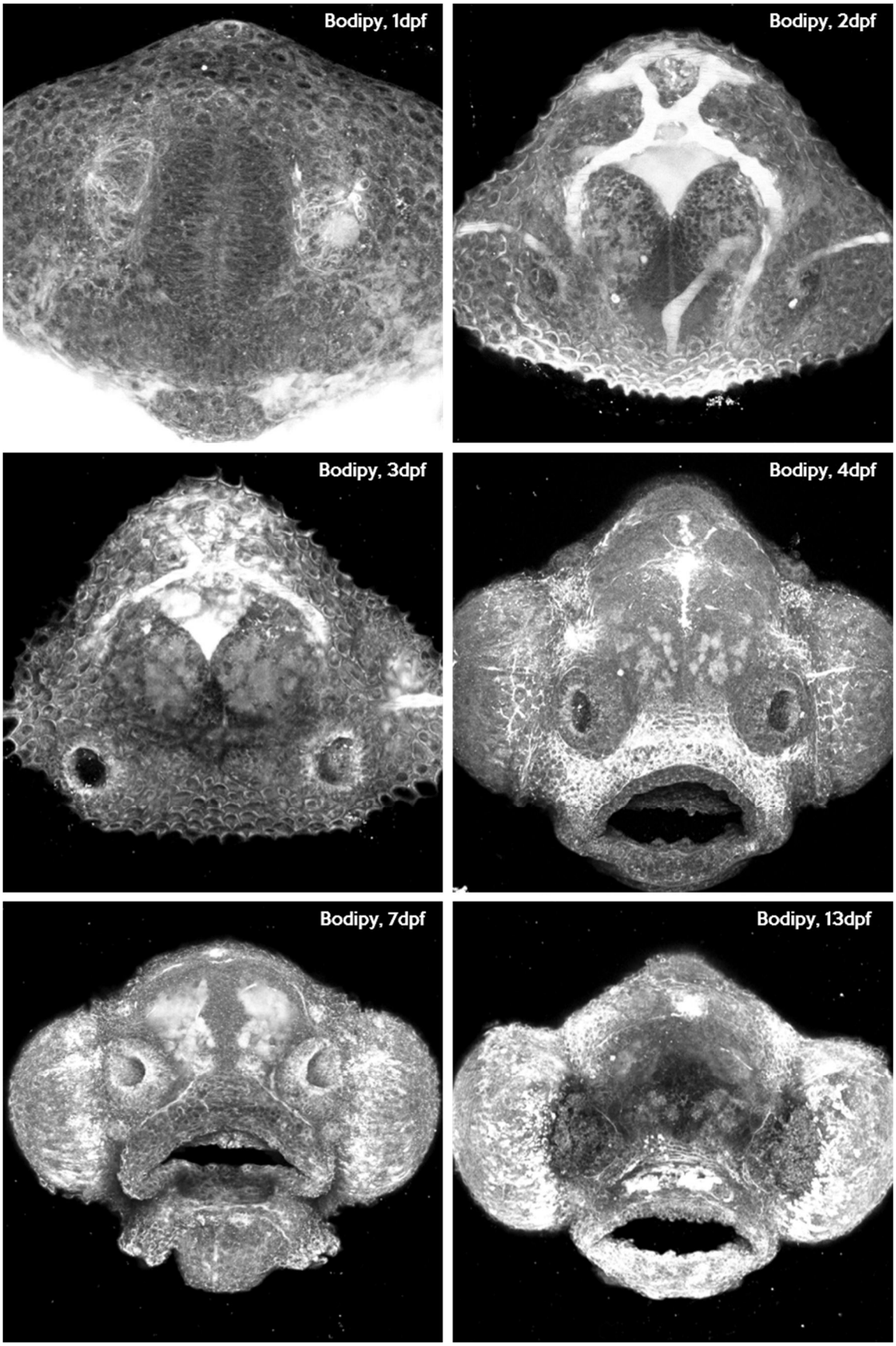

Figure 4.16. Visualization of glomerular development pattern using bodipy staining

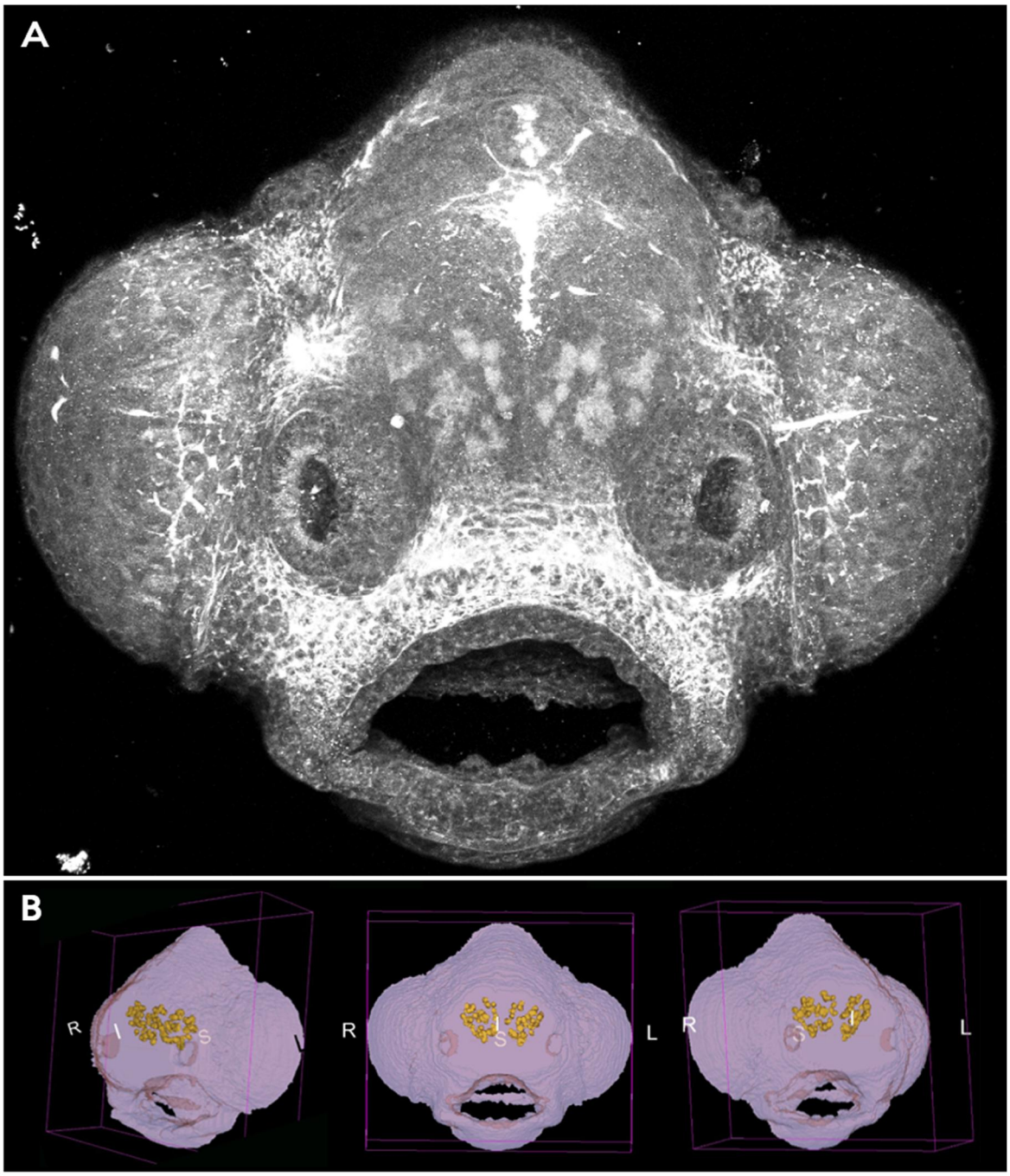

Figure 4.17. Visualization of olfactory glomeruli using bodipy staining. (A) Confocal z-stack of a zebrafish embryo head at 4dpf, stained with bodipy. (B) 3D model of the embryonic glomerular map at 4dpf.

In these embryos, bodipy-stained territories start to form in the OB between 1 and 2 dpf. Yet, clear glomerular structures are not readily apparent at these early timepoints. By 3dpf, bodipy-stained territories expand in the OB, which are still densely packed acellular in

which individual spherical structures are not clearly discernible. The pattern changes around 4 dpf, when protoglomerular structures first become evident and can be recognized in the central, dorsal, lateral and medial parts of the OB. The gross pattern of glomerular clusters remains similar up until 13 dpf, the latest timepoint of this analysis, yet, the number of individual spherical structures forming larger glomerular clusters increases.

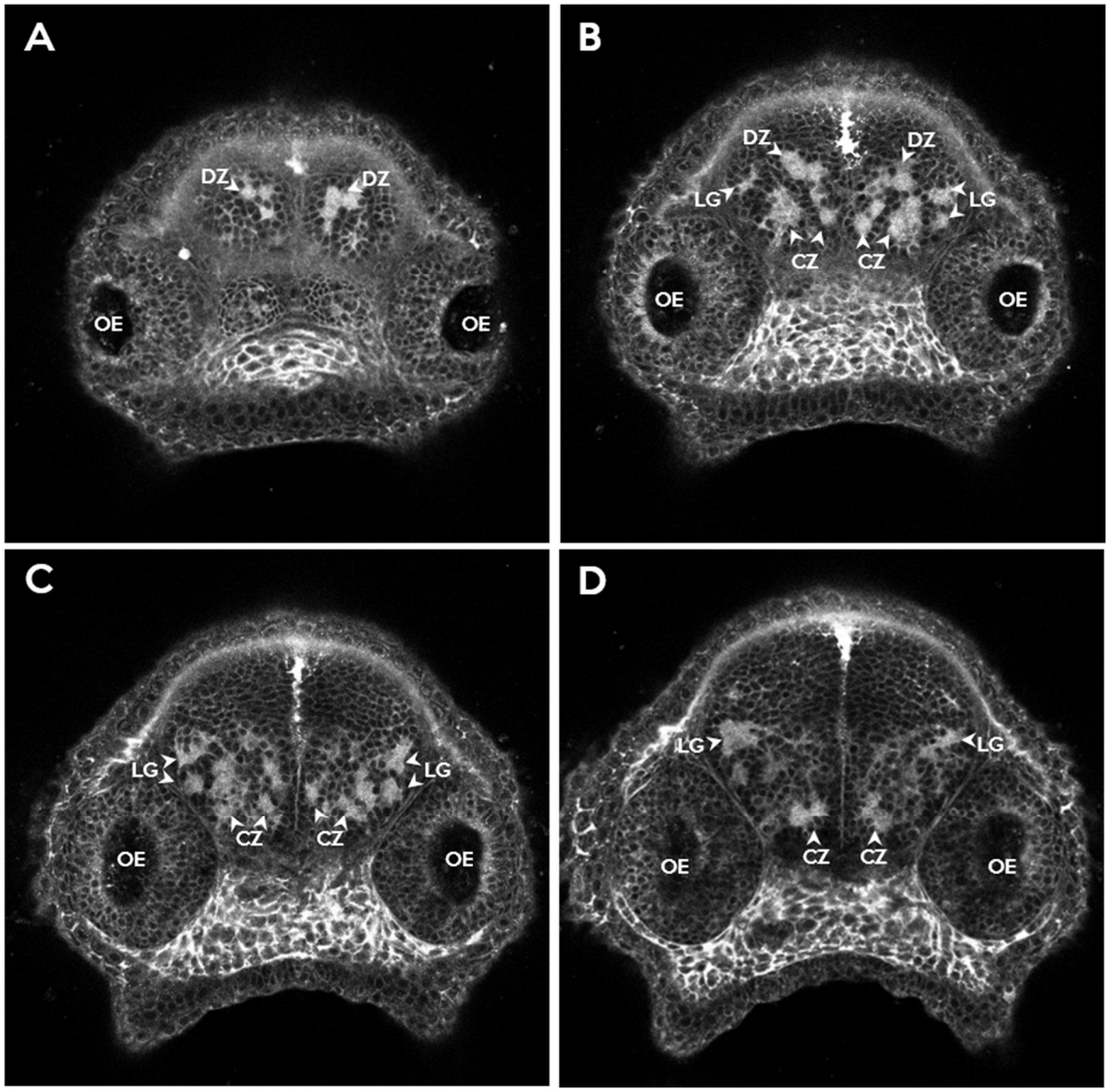

Figure 4.18. Visualization of the glomerular map in OB by bodipy staining. (A-D) Single confocal sections ordered anterior to posterior. Arrowheads indicate identified protoglomeruli and glomeruli according to their positions (Dorsal Zone, DZ; Lateral Glomeruli, LG; Central Zone, CZ).

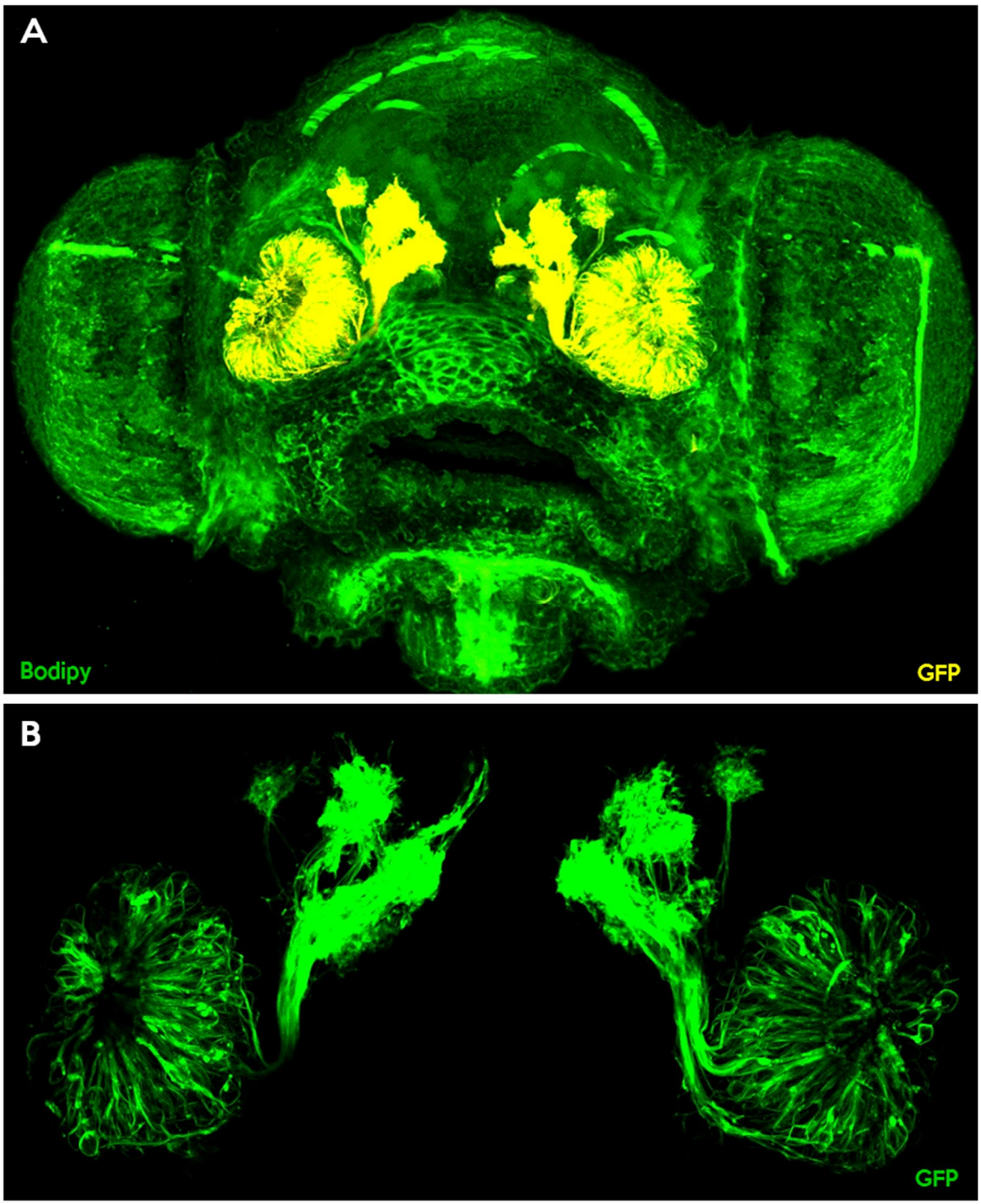

Figure 4.19. Axonal segregation of ciliated OSNs in Tg(OMP:tauGFP) embryos. (A) Confocal z-stack of a 4 days old zebrafish embryo head, costained with bodipy. GFP expression: yellow, bodipy: green. (B) Confocal z-stack of Tg(OMP:tauGFP) embryonic OE and OB at 4dpf.

Because transgene analysis will be carried out at 3 and 4 dpf the 4 dpf glomerular pattern was investigated in more detail. Using confocal imaging of high-resolution optical

sections through the first 50 µm of the entire embryonic head the entire glomerular pattern could be revealed. Individual glomeruli are recognizable as 15 µm spherical structures, which are densely packed in some regions of the OB, whereas they are more loosely packed in other regions (Figure 4.17a). Using the 3D-Slicer program, a three dimensional reconstruction of the embryonic glomerular map was generated (Figure 4.17b). Individual spheres were traced and a three-dimensional rendering was generated. The combined analysis of 3D reconstruction and bodipy staining revealed two larger clusters of glomeruli, which were denoted as central zone (CZ) and dorsal zone (DZ), according to the nomenclature of Dynes and Ngai (1998, Figure 4.18). These two clusters comprise 4 and 6 protoglomeruli, respectively. In addition, 3-4 lateral glomeruli could be consistently identified in each OB (Figure 4.18).

In an alternative approach a stable transgenic fish line Tg(OMP:tauGFP) was used to visualize the glomerular map during early zebrafish development. In this transgenic line, all ciliated OSNs express the fluorescent marker GFP fused to the microtubule-associated protein tau under the control of the OMP promoter (Sato *et al.*, 2005). Ciliated OSNs constitute a major subpopulation of OSNs and expression of tauGFP allows a clear visualization of their axonal projections to the OB. For this purpose, 4 dpf embryos of the Tg(OMP:tauGFP) line were analyzed in detail using whole-mount confocal microscopy (Figure 4.19). In the OB of 4 dpf Tg(OMP:tauGFP) embryos four different projection fields that are invariant across individual embryos can be identified. Two of them form larger glomerular clusters that contain densely packed individual protoglomeruli and which correspond to the central and dorsal zones (CZ, DZ) already described in the bodipy stainings. In addition, only one lateral glomerulus can be identified by GFP expression. As described above, the full embryonic glomerular map comprises four lateral glomeruli (Dynes and Ngai, 1998), but only one of them, LG3, is Tg(OMP:tauGFP)-positive (Lakhina *et al.*, 2012). Thus, LG1, 2 and 4 most likely receive innervation from non-cilitated OSNs. An additional glomerulus can be detected in the medial OB in half of the analyzed embryos (n=10) and is referred to as medial glomerulus (MG) in maps subsequently used (Figure 4.20a).

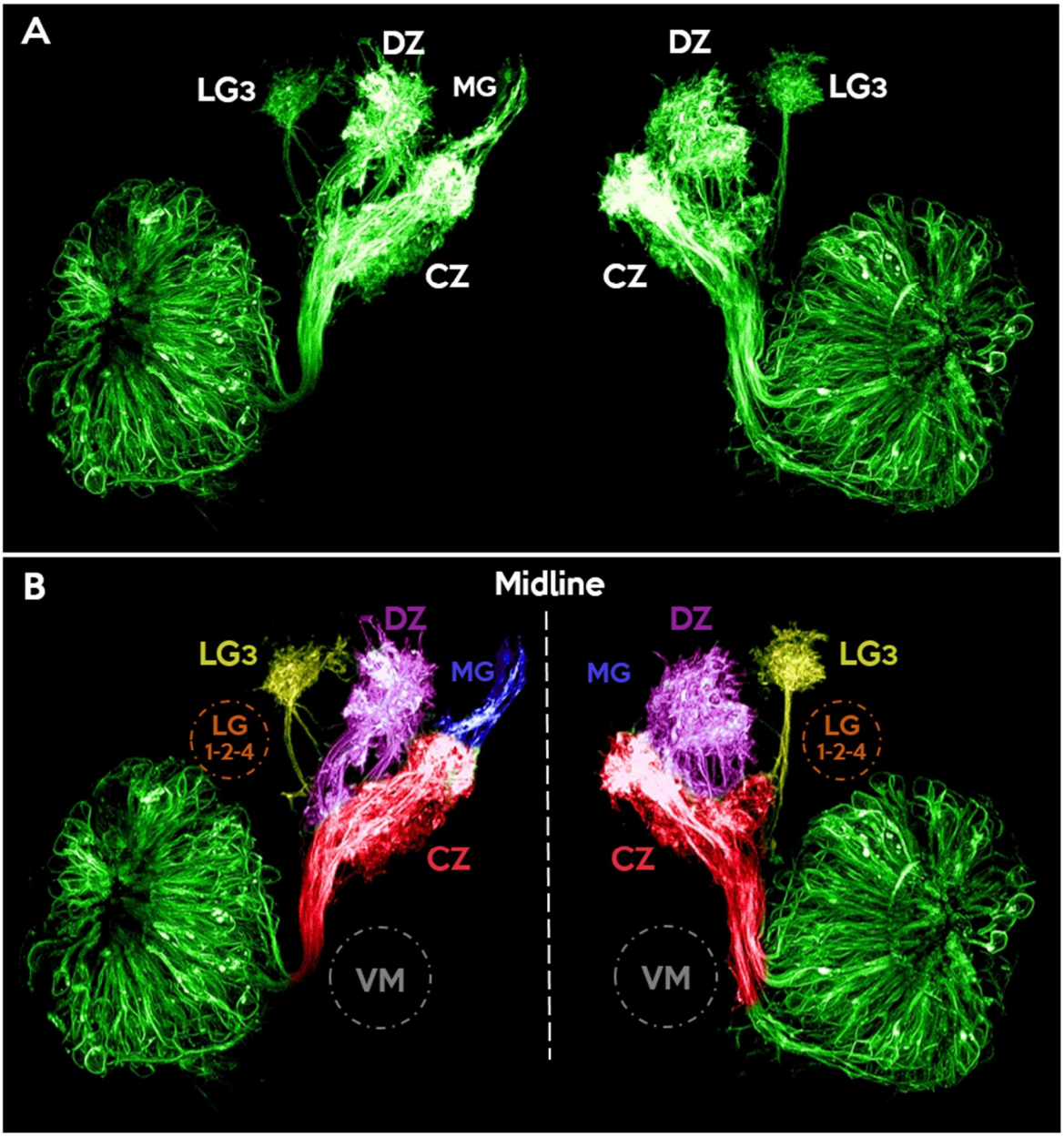

Figure 4.20. Embryonic glomerular map. (A) Identified glomeruli in Tg(OMP:tauGFP) embryo. (B) Finalized version of the embryonic glomerular map.

The combined analysis of bodipy staining and Tg(OMP:tauGFP) expression allowed for a clear overview of major structures within the 4dpf embryonic glomerular pattern. In subsequent experiments, both techniques were used in combination with injection of transgenic constructs to understand where transgene-expressing axons make connections in the OB. An idealized map of the glomerular pattern was generated (Figure 4.20b) to serve

as a reference map for those experiments. This reference map includes LG1, 2, and 4 in addition to a medial glomerulus MG and a ventromedial cluster (VM).

4.2.2. Use of the Intergenic Region to Express OR Coding Sequences

IRESs have been valuable tools to study gene and reporter gene expression without perturbing expression of the gene of interest. The IRES approach was successfully and repeatedly used in the mouse olfactory system to direct coexpression of an OR and marker genes (Mombaerts *et al.,* 1996).. Many times, gene expression can be studied with simple promoter transgenes that recapitulate the expression of the gene of interest or in heterozygous animals where one allele has been replaced with a reporter gene while maintaining gene function from the second allele. In the olfactory system, however, a simple substitution of the OR gene with the marker would severely affect OR gene expression. Because OR genes are monoallelically expressed, the second allele cannot be used for marker expression. Monogenic expression of OR genes extends to transgenically expressed ORs. Thus, IRES sequences ensure cotranslation of the OR and the marker by the same OSN without perturbing OR expression. However, attempts to adopt the OR-IRES-marker strategy to visualize specific subpopulations of OSNs in the zebrafish olfactory system have failed (Sato *et al*., 2007; Tastekin, 2012). An possible explanation for this failure may be a difference in the efficiency of viral IRES sequences to initiate translation in non-mammalian hosts. Alternatively IRES sequences may be temperature sensitive. Fish, different from mammals are kept at 28ºC and proper thermodynamic folding of the IRES might be compromised at low temperatures. This caveat in zebrafish studies could eventually be bypassed by the utilization of sequences that show IRES-like activity and which are derived from the zebrafish genome itself. In the previous sections evidence was presented that the OR103-1/5 intergenic region may contain IRES activity and has the ability to promote colabeling of the same cell with two different reporter proteins (refer to Sections 4.1. and 4.2. for further details). Here, we asked whether this ability can be used to tag specific OSN subpopulations that express a transgenic OR gene with a fluorescent marker *in vivo*.

In a first attempt addressing this a $p_{(1.2kb)}$OR101-1-mCherry-inter$_{(1.4kb)}$-OR101-1-pA construct was used. The construct was generated by replacing the GFP sequence of the $p_{(1.2kb)}$OR101-1-mCherry-inter$_{(1.4kb)}$-GFP-pA construct with the 948 bp coding sequence of the OR101-1 gene. The construct will be driven under the control of the 1.2 kb OR101-1 promoter and, as expected from previous results, a subset of mCherry-positive OSNs should coexpress the OR101-1 protein. The $p_{(1.2kb)}$OR101-1-mCherry-inter$_{(1.4kb)}$-OR101-1-pA construct was injected into 123 fertilized zebrafish oocytes at the one-cell stage of which 29 embryos survived until the time of analysis. First, we wanted to understand if injection of this constructs results in OSNs that label positive for both genes by in situ hybridization, similar to the observed coexpression of OR103-1 and OR103-5. Therefore, embryos were fixed in 4% PFA at 3 dpf and subjected to double *in situ* hybridization using haptene-labeled antisense riboprobes against mCherry and the OR101-1 coding sequence. Of the injected embryos 52% (15/29 embryos) stained positive for mCherry and 55% (16/29) stained positive for OR101-1. This was surprising because OR101-1 is also expressed from its endogenous alleles and a 100% OR101-1-positive embryos were expected. It is likely, that the sensitivity threshold used in this experiment was set to high levels of OR101-1 expression and that expression levels from the transgenic construct were higher than endogenous OR101-1 expression. The observed 55% of OR101-1-positive embryos are in the same range as the efficiency of OR101-1 promoter-driven constructs used throughout this study, supporting this interpretation.

Using in situ hybridization, a total of 45 mCherry- and 121 OR101-1-positive OSNs could be detected in transgenic embryos. Co-labeling of both signals in the same OSN was observed in 45 cells. Thus, only 37% (45/121 OSNs) were double positive for the mCherry marker. On 7.6±1.7 OR101-1-positive OSNs could be detected in the OE of transgenic embryos. Again, this is lower than the expected number of 15 OR101-1-positive OSNs which can be consistently found at this developmental age per OSN (Tinaztepe, 2010), further supporting the idea that only transgenic OSNs with elevated expression levels were successfully labeled under the conditions applied. Importantly, all 45 mCherry-positive OSNs colabeled for OR101-1 and on average 3 ± 0.6 mCherry OSNs could be detected in the OE each transgenic embryo (Figure 4.21).

Although the overall expression rate of mCherry (52% of mCherry-positive embryos) was comparable to previous experiments using the same promoter, the average number of mCherry-positive OSNs decreased to 3 ± 0.6 cells as compared to 7, 6.5 and 4.1 cells for comparable constructs that did not contain an OR coding sequence. This reduction may be due to the inclusion of an OR coding sequence in the construct. Previously we have shown that the presence of an OR coding sequence can inhibit expression of transgenic constructs (Tastekin, 2012; Nguyen *et al.*, 2007).

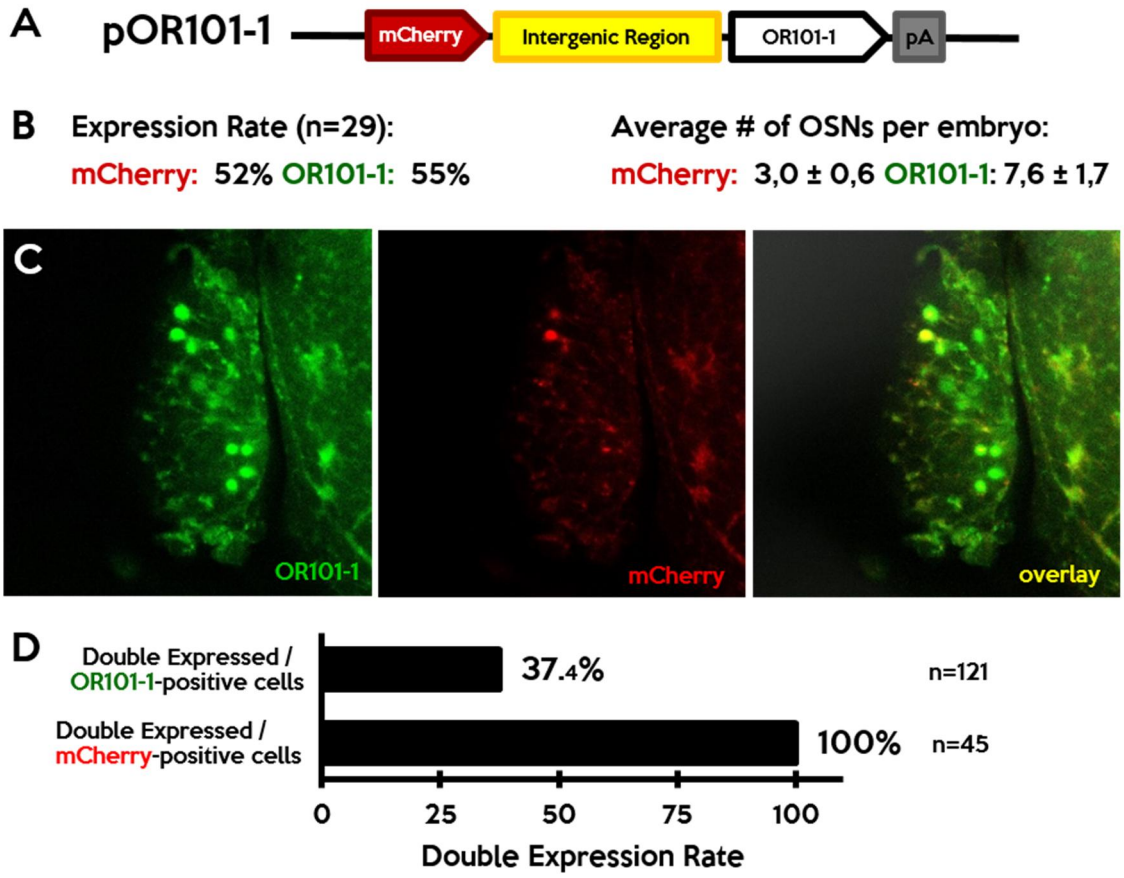

Figure 4.21. Transgene expression analysis of $p_{(1.2kb)}$OR101-1-mCherry-$inter_{(1.4kb)}$-OR101-1-pA injection. (A) Overview of the construct. (B) Expression rates and average number of reporter gene-positive OSNs (C) Confocal z-stacks at 3dpf. (D) Double expression rates.

A coexpression rate at the mRNA level of 100%, however, is very promising. Because the overall number of OR101-1-positive cells was much lower than endogenous expression

of the gene, it is conceivable that the results presented here originate entirely from expression of the transgenic construct.

To be able to confirm possible colocalization of reporter and OR gene expression at the protein level, a new construct, $p_{(1.2kb)}$OR101-1-mCherry-inter$_{(1.4kb)}$- OR111-7^{myc}-pA was generated, which contains the coding sequence of the OR111-7 gene fused to a myc epitope tag at its 3' end. The construct was injected into 32 fertilized zebrafish oocytes at the one-cell stage of which 11 embryos survived until the time of analysis. Of those, 45.5% (5/12 embryos) expressed mCherry. On average 3.6 ± 0.7 mCherry expressing OSNs could be detected in the OE of transgenic embryos (Figure 4.22).

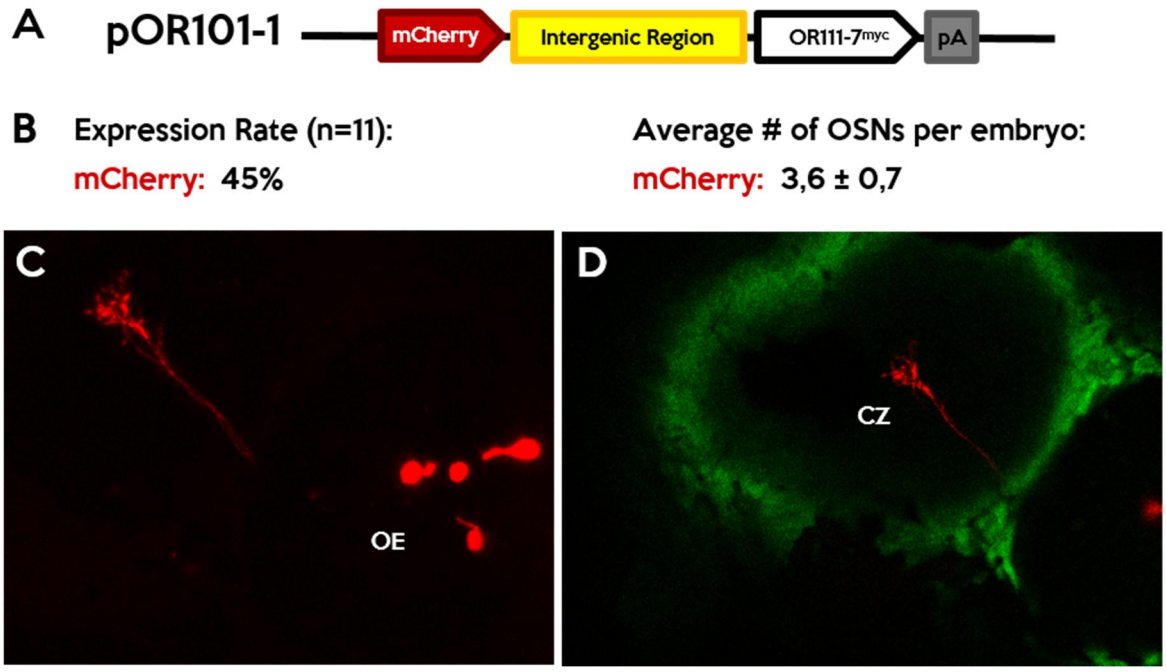

Figure 4.22. Transgene expression analysis of $p_{(1.2kb)}$OR101-1-mCherry-inter$_{(1.4kb)}$-OR101-1-pA injection. (A) Overview of the construct. (B) Expression rate and average number of reporter gene-positive OSNs (C) Confocal z-stack at 3dpf. (D) Single optical section of embryonic OB at 3dpf.

Again, a low average number of mCherry-positive OSNs could be observed, which is very similar to the OR101-1-containing construct. Interestingly, axons of mCherry positive OSNs had a tendency to coalesce and to form a narrow projection domain. In the OB, mCherry-positive axons converged onto a single protoglomerulus that was located in the CZ (Figure 4.22). This is a significant finding, as it implies that transgene-expressing OSNs can be transformed with the identity of the expressed OR and that ORs are instructive in guiding OSN axons to specific glomeruli in the OB. From in situ hybridization against expressed mCherry and OR sequences a 100% colabeling of mCherry neurons with OR101-1 transcripts has been found. Thus, the observed coalescence of axons for $p_{(1.2kb)}$OR101-1-mCherry-$inter_{(1.4kb)}$- OR111-7^{myc}-pA might indicate the position of the endogenous OR111-7 glomerulus and mCherry-positive axons that also express OR111-7 coconverge onto this glomerulus.

Unfortunately, for both constructs, the average number of mCherry-positive cells per embryo was very low. Driving the OR expression constructs in a larger subset of cells might obtain more clearcut results. Broader expression could be achieved by using an appropriate enhancer that will increase the activity of pOR101-1 into a larger OSN population. Previously, fusion of the 1.4 kb mouse H-region with proximal OR promoters in transgenic constructs was shown to significantly increase the number of transgene-expressing OSNs in zebrafish (Nishzumi *et al.*, 2007; Tastekin, 2012; refer to Section 1.3.4.1. for further details). Thus, to increase the number of OSNs that could potentially express the transgene, the H region was cloned upstream of the OR101-1 gene promoter in the OR expression constructs.

4.2.3. Overexpression of an OR Gene Coding Sequence Results in Novel Glomeruli

In order to drive expression of an OR sequence within a large set of OSNs, the 1.4 kb H-region was cloned directly upstream of the pOR101-1 promoter. The H-region is a powerful enhancer in the mouse olfactory system that shows cross-species activity in zebrafish (Nishizumi *et al.*, 2007). Two new constructs were generated this way, one in which the OR101-1 coding sequence was inserted downstream of the intergenic region and a second construct in which the OR111-7^{myc} was used (Figure 4.23a & 4.24a).

The H-$p_{(1.2kb)}$OR101-1-mCherry-$inter_{(1.4kb)}$-OR111-7^{myc}-pA construct eventually allows OR111-7-expressing transgenic cells to be detected by immunohistochemistry using an anti-myc antibody. Introduction of the H-enhancer upstream of the OR101-1 promoter resulted in a ten-fold increase in the average number of mCherry-positive OSNs per embryo for both constructs, similar to previous observations for H-enhancer-containing constructs (Sogunmez, 2012; Tastekin 2012).

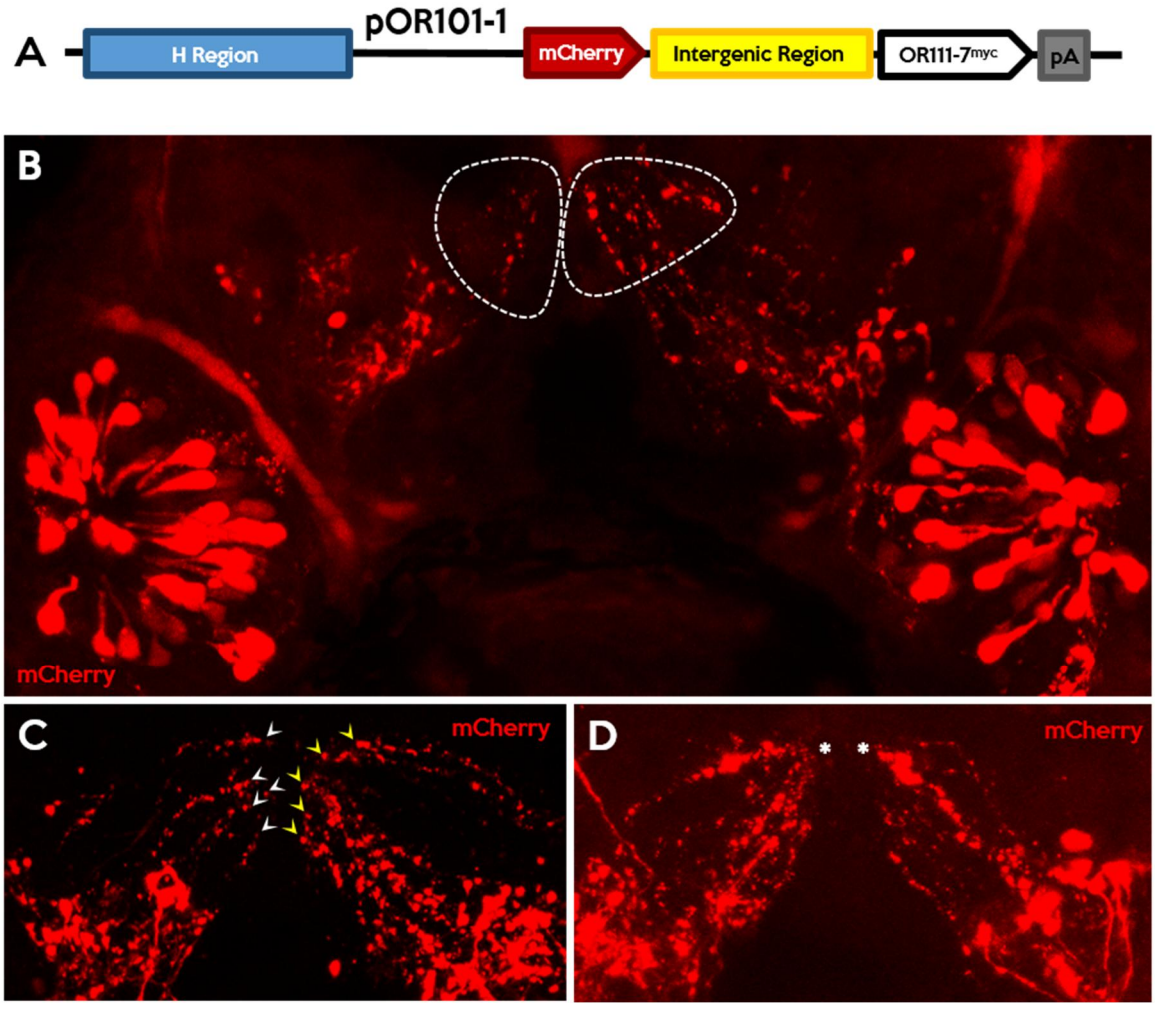

Figure 4.23. Transgene expression analysis of a H-$p_{(1.2kb)}$OR101-1-mCherry-$inter_{(1.4kb)}$-OR111-7^{myc}-pA. (A) Overview of the construct. (B) Axonal projection pattern detected in injected embryos at 4dpf. The midline glomeruli are outlined with dashed lines. (C-D) Close-up images of axons.

When the Hregion-pOR101-1-mCherry-IntergenicRegion-OR101-1-pA was injected into zebrafish oocytes on average 38.75 ± 5.8 mCherry-positive OSNs could be detected per OE in 58.3% of injected embryos (14/24 embryos) at 4 dpf. A similar high number of transgene-expressing OSNs were obtained for the H-pOR101-1-mCherry-IntergenicRegion-OR111-7^{myc}-pA construct: expression of the mCherry reporter could be detected in 55% (55 embryos analyzed out of 77 injected) of the embryos with an average number of 35.75 ± 2.1 mCherry-positive OSNs per OE. In both cases, a large number of mCherry-positive axons (between 17 and 39 per embryo) could be identified that project to the OB. For a large number of axons it was possible to trace their individual trajectories and target regions in the OB. Axons predominantly targeted glomeruli of the central zone but also projected to lateral glomeruli and to glomeruli in the dorsal zone.

Interestingly, a new pair of glomerulus-like structures became apparent for each construct, which is not present in the wild-type pattern as revealed by bodipy staining or analysis of the Tg(OMP:tauGFP) line. These novel glomerular structures were located near the midline in the mediodorsal OB and were innervated by a fraction of mCherry-positive axons (Figure 4.23c; Figure 4.23d; Figure 4.24c; Figure 4.24d). On average 10.1 ± 0.9 axons innervated the bilaterally symmetric structure on either side of the OB.

These novel projections may arise from to the overexpression of the transgenic OR included in either construct. This finding was surprising and it remains unclear at this point why overexpression of the OR under these conditions would lead to the formation of a novel glomerulus, rather than axons targeting the endogenous glomerulus that is appropriate for the expressed OR, as observed for the p$_{(1.2kb)}$OR101-1-mCherry-inter$_{(1.4kb)}$- OR111-7^{myc}-pA construct. A major difference between these constructs, however, is the presence of the H-enhancer in constructs that resulted in the formation of a novel glomerulus. Thus, the H-enhancer may somehow change the expression profile of the transgenic constructs in a way that is different from the basic activity of the OR101-1 promoter alone. To understand this phenomenon better, the midline glomeruli were analyzed in detail.

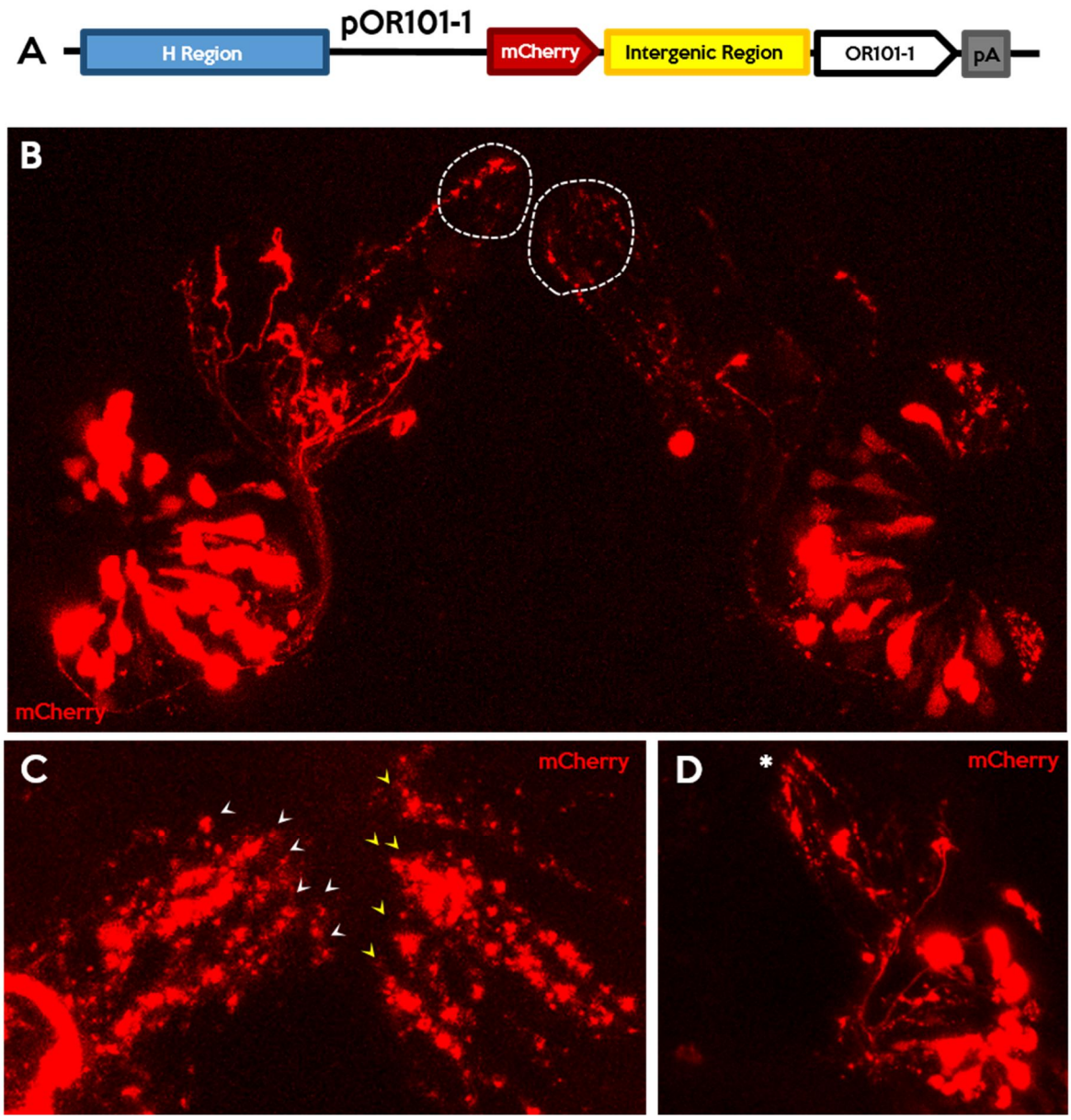

Figure 4.24. Transgene expression analysis of the H-$p_{(1.2kb)}$OR101-1-mCherry-$inter_{(1.4kb)}$-OR101-1-pA construct. (A) Overview of the construct. (B) Axonal projection pattern in injected embryos at 4dpf. The midline glomeruli are outlined with dashed lines. (C-D) Close-up images of axons.

4.2.4. Analysis of Novel Midline Glomeruli

For both constructs that were driven by the H-enhancer, H-$p_{(1.2kb)}$OR101-1-mCherry-inter$_{(1.4kb)}$-OR111-7^{myc}-pA and H-$p_{(1.2kb)}$OR101-1-mCherry-inter$_{(1.4kb)}$-OR101-1-pA, a large subset of axons converged onto novel midline glomeruli, which were not detected in previous injection experiments or in the basic glomerular pattern at 4 dpf. It is likely that these axons have the identity of the expressed OR and that the expressed OR guides the axons to form novel structures. However, the novel glomerular structures only appeared in constructs that included the H-enhancer.

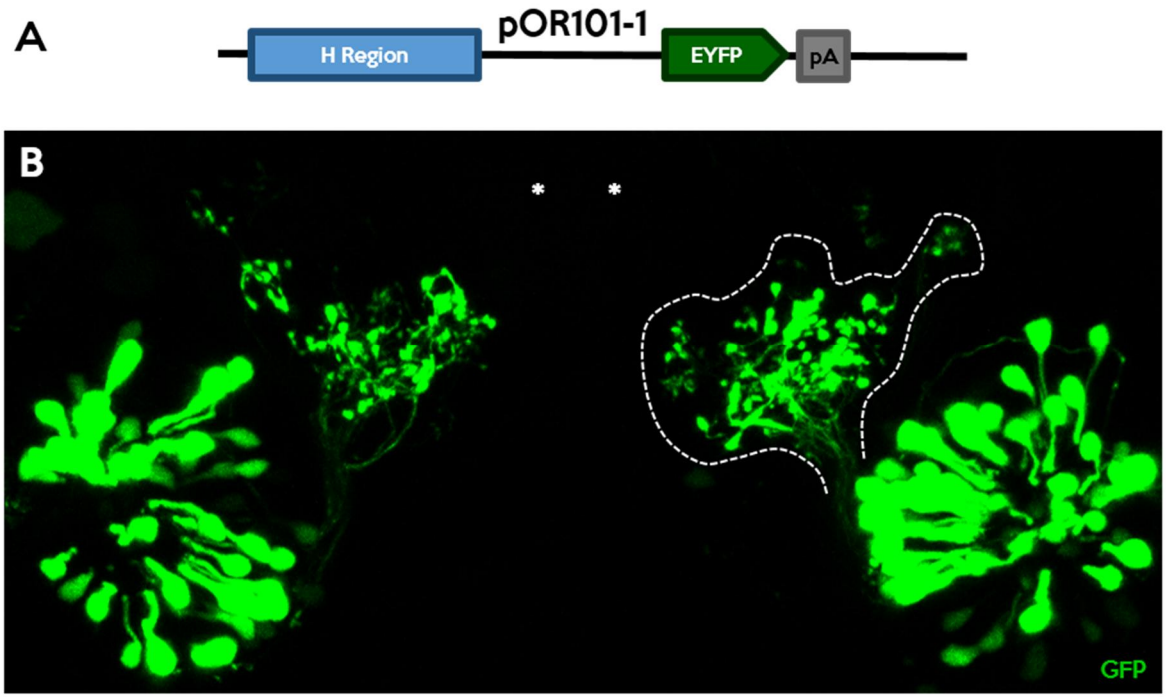

Figure 4.25. Transgene expression analysis of a H-$p_{(1.2kb)}$OR101-1-EYFP-pA construct. (A) Overview of the construct. (B) Axonal projection pattern detected in injected embryos at 4dpf.

The H-enhancer was previously shown to expand expression of pOR101-1 into different types of OSNs. To better describe the population of OSNs that express transgenic constructs driven by H-$p_{(1.2kb)}$OR101-1 and their axonal projections to the OB a basic H-$p_{(1.2kb)}$OR101-1 construct that drives expression of the EYFP reporter was injected (generated by Xalid Bayramlı). The axonal projection pattern observed in the H-

$p_{(1.2kb)}$OR101-1-EYFP-pA construct and its comparison to the OR-expressing constructs may provide additional information about the origin of axons that converge onto the novel midline glomeruli.

In order to establish this reference pattern the H-$p_{(1.2kb)}$OR101-1-EYFP-pA construct was injected into 39 embryos and analyzed under the confocal microscope. On average 52.75 + 7.0 EYFP-positive cells could be detected in the OE of transgenic embryos. Reporter gene-positive axons project axons to various regions of the OB, including CZ, DZ, LG3, LG1-2-4, MG and VM (Figure 4.25b). Thus, H-$p_{(1.2kb)}$OR101-1-EYFP-pA axons also innervate glomeruli that are not innervated from OMP-expressing OSNs as revealed by analysis of the Tg(OMP-tauGFP) transgenic line. The additional regions that were innervated by H-$p_{(1.2kb)}$OR101-1-EYFP-pA included the LG1, LG2, and LG4 glomeruli, as well as glomeruli in MG and VM. Interestingly, no axons extending axons to positions in the dorsomedial OB were observed.

Thus, it is conceivable that the activity of H-$p_{(1.2kb)}$OR101-1-driven expression constructs have a broader expression profile that constructs driven only from $p_{(1.2kb)}$OR101-1 and that H-$p_{(1.2kb)}$OR101-1-EYFP-pA is expressed in non-ciliated OSNs in addition to OMP-positive ciliated OSNs. Thus, the possibility exists that the novel midline glomeruli may be formed by non-ciliated OSNs under the influence of the the H-region on pOR101-1, which are now guided by the transgenic OR111-7 or OR101-1 proteins that were expressed in these constructs.

To further explore this possibility the differences in axonal projections between the two transgenic constructs that do or do not contain an OR coding sequence, the H-$p_{(1.2kb)}$OR101-1-mCherry-inter$_{(1.4kb)}$-OR111-7^{myc}-pA construct was coinjected with H-$p_{(1.2kb)}$OR101-1-EYFP-pA.

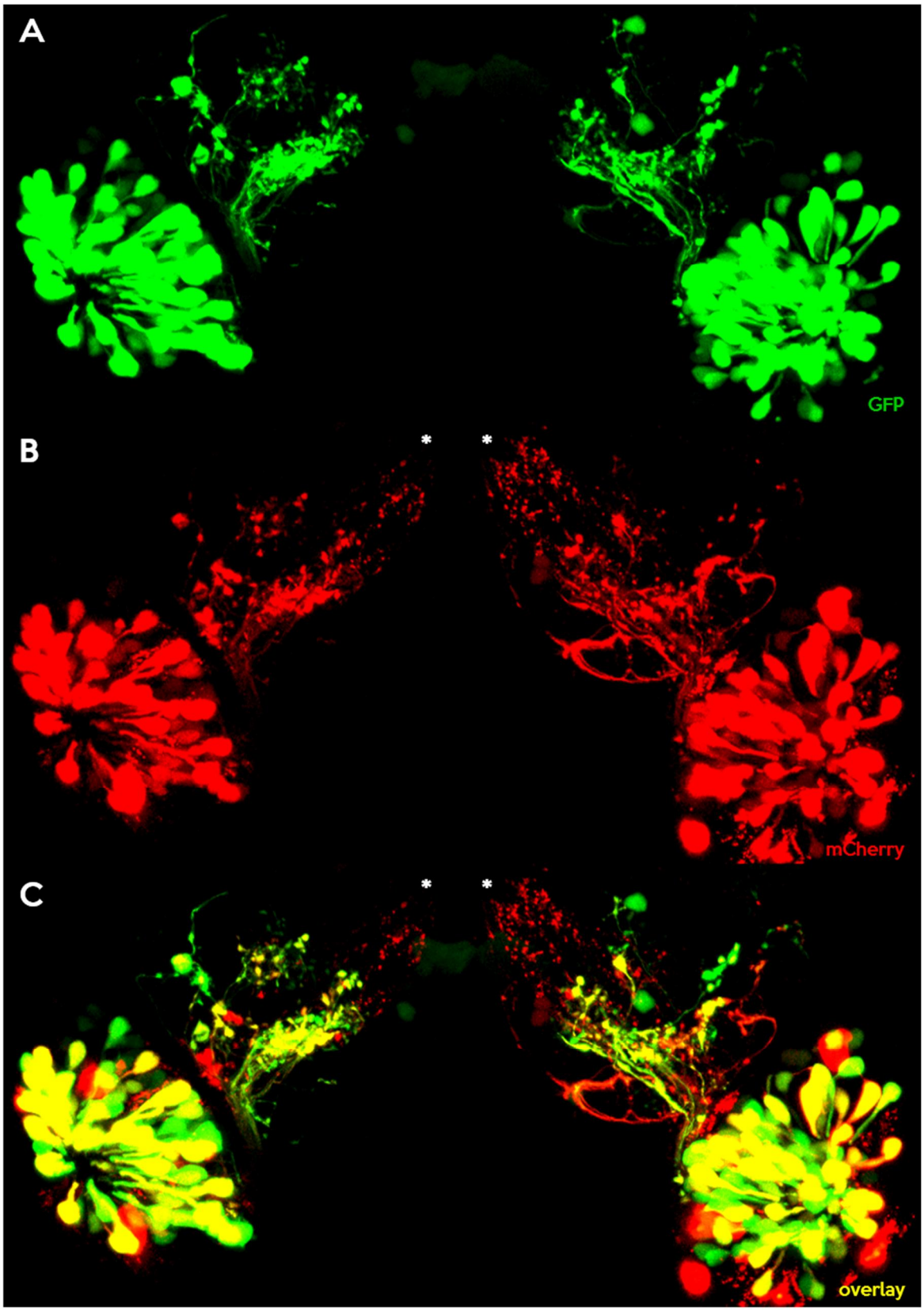

Figure 4.26. Confocal z-stacks of embryonic olfactory epithelia coinjected with H-$p_{(1.2kb)}$OR101-1-mCherry-$inter_{(1.4kb)}$-OR111-7^{myc}-pA and H-$p_{(1.2kb)}$OR101-1-EYFP-pA constructs. (A) EYFP expression. (B) mCherry expression. (C) Overlay of both images.

Under these conditions, EYFP-positive axons project to the OB in a pattern that is indistinguishable from the pattern that was obtained when H-$p_{(1.2kb)}$OR101-1-EYFP-pA was injected alone (Figure 4.26a). In the coinjection experiment the EYFP-positive glomeruli were innervated by a subset of mCherry-labeled axons (Figure 4.26b). Thus, the projections of mCherry and EYFP axons largely overlap in the cental zone, dorsal zone and in the lateral glomeruli. Different from the behavior of EYFP axons, a subset of mCherry-positive axon projected to the novel glomerular structures in the dorsal midline. Interestingly, those axons were never positive for EYFP (n=97; Figure 4.26b, Figure 4.26c).

Identical results were obtained when the H-$p_{(1.2kb)}$OR101-1-mCherry-$inter_{(1.4kb)}$-OR101-1-pA construct was coinjected with H-$p_{(1.2kb)}$OR101-1-EYFP-pA. EYFP-positive axons projected to CZ, DZ, LG1, 2, 3, and 4, MG and VM glomeruli similar to H-$p_{(1.2kb)}$OR101-1-EYFP-pA (Figure 4.27a) while a significant subset of mCherry-positive axons (Figure 4.25b) projected to the dorsal midline (Figure 4.27b, Figure 4.27c). Thus, constructs that contain an OR coding sequences guide a subset of transgene positive axons to new glomerular targets in the OB when expressed under the influence of the H-enhancer.

The observed effect is a direct consequence of the expressed OR gene, because the midline glomeruli were not present in H-$p_{(1.2kb)}$OR101-1-EYFP-pA-injected embryos. Because midline glomeruli are only detected after injection of OR-containing constructs the most parsimonious explanation is that a subset of OSNs has been transformed to adopt the identity of the expressed OR and that the expression of this OR guides axons to new target positions in the OB. The observed effect is also dependent on the H-enhancer because similar midline structures were not observed in $p_{(1.2kb)}$OR101-1-OR101-1-pA or $p_{(1.2kb)}$OR101-1-EOR111-7-pA constructs. It is possible that the broader expression profile of H-$p_{(1.2kb)}$OR101-1-driven constructs allows for expression of OR101-1 or OR111-7 in non-ciliated OSNs and that these non-ciliated OSNs form novel glomerular targets in the dorsal midline.

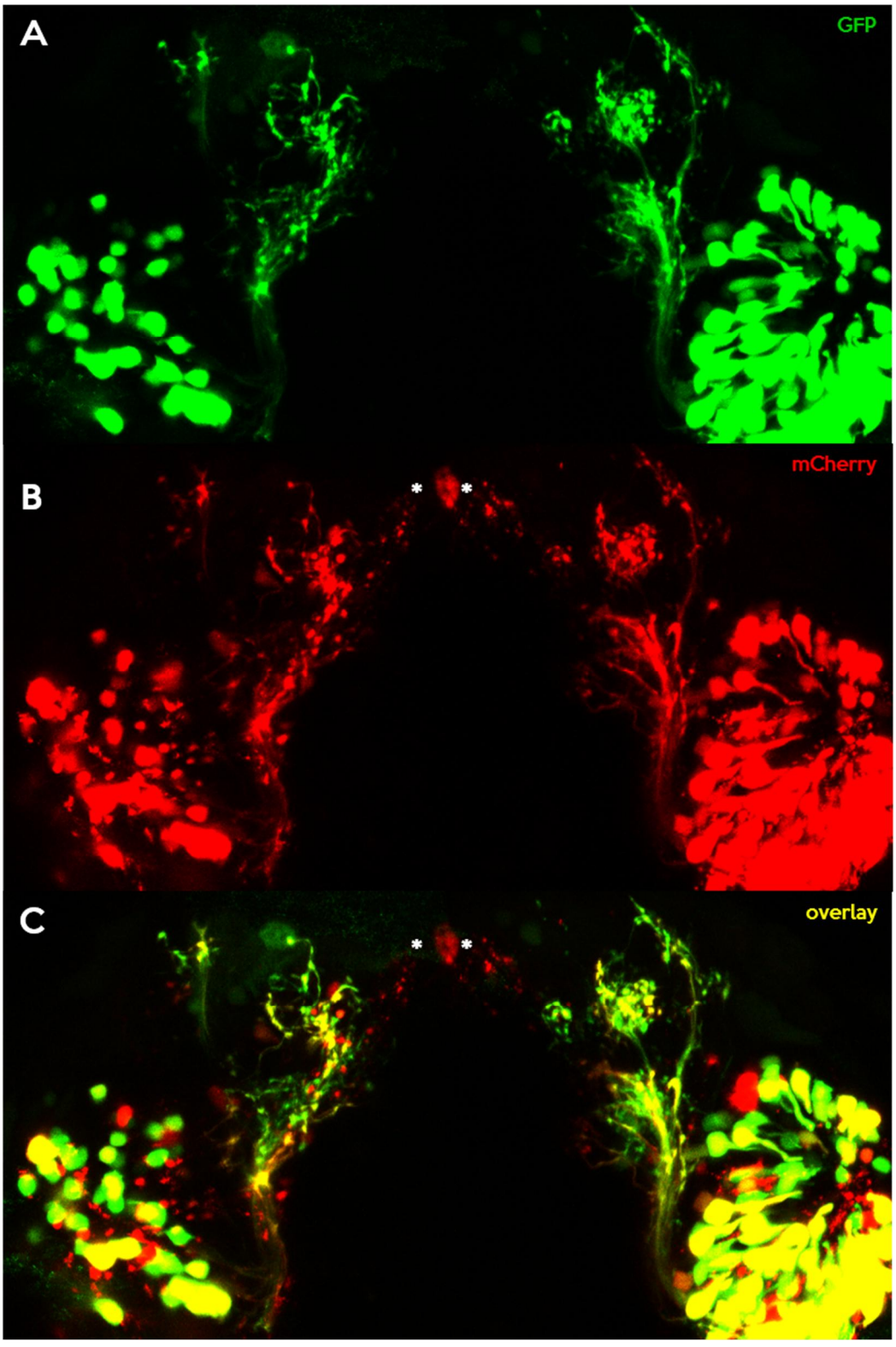

Figure 4.27. Confocal z-stack of a H-$p_{(1.2kb)}$OR101-1-mCherry-$inter_{(1.4kb)}$-OR101-1-pA and H-$p_{(1.2kb)}$OR101-1-EYFP-pA co-injected embryo. (A) EYFP expression. (B) mCherry expression. (C) Overlay of both images.

4.2.4.1. Comparison to Tg(OMP:tauGFP). The axonal projection pattern observed in H-$p_{(1.2kb)}$OR101-1-mCherry-inter$_{(1.4kb)}$-OR111-7^{myc}-pA and H-$p_{(1.2kb)}$OR101-1-mCherry-inter$_{(1.4kb)}$-OR101-1-pA included novel glomerular structures in the dorsal midline that might be formed by OR-expressing non-ciliated OSNs. To test this possibility directly, the OR-expressing constructs were cinjected into the Tg(OMP:tauGFP) stable transgenic line in which axons of ciliated OSNs con be identified by their GFP expression.

When H-$p_{(1.2kb)}$OR101-1-mCherry-inter$_{(1.4kb)}$-OR111-7^{myc}-pA or H-$p_{(1.2kb)}$OR101-1-mCherry-inter$_{(1.4kb)}$-OR101-1-pA were injected into Tg(OMP:tauGFP) embryos colabeling mCherry- and GFP-positive axons were detected in multiple glomeruli in the OB, such as CZ, DZ and LG3 (Figure 4.28). In addition, mCherry-expressing axons also projected to the OMP-negative lateral glomeruli, LG1, 2, and 4, and to the novel glomerular structures in the dorsal midline, which did not receive any innervation from GFP-positive axons.

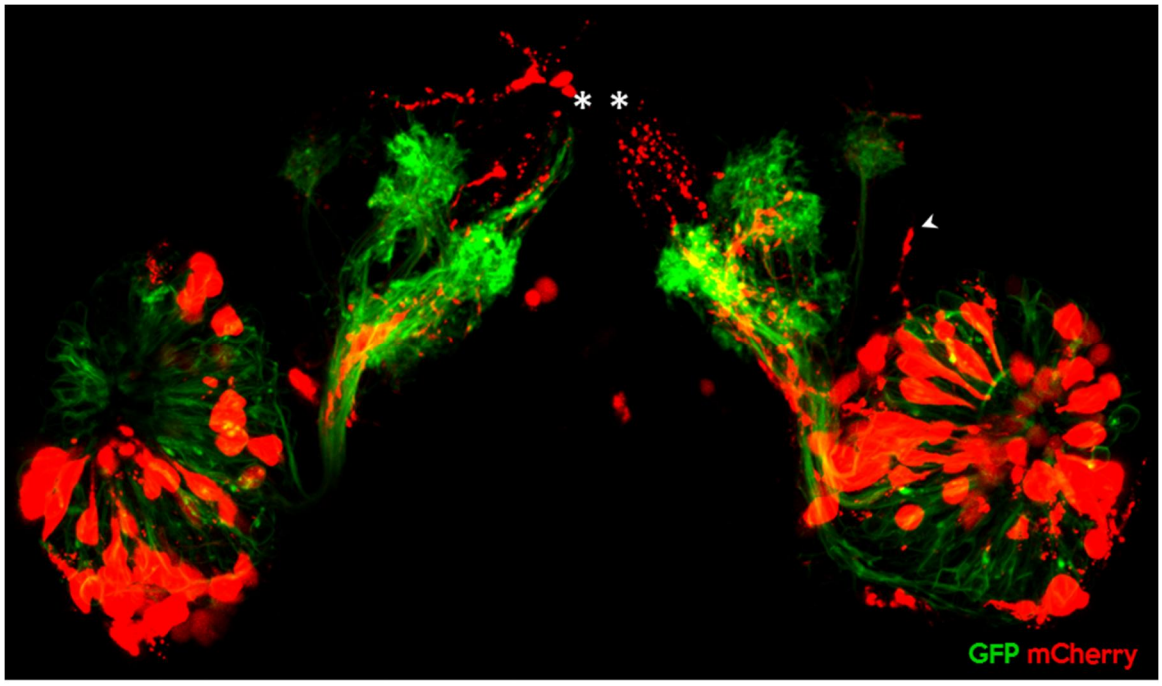

Figure 4.28. Confocal z-stack from a Hregion-pOR101-1-mCherry-IntergenicRegion-OR111-7^{myc}-pA injected Tg(OMP:tauGFP) embryo at 4dpf. Arrowhead indicate axons projecting LG1-2-4; Asterisks indicate the midline glomeruli.

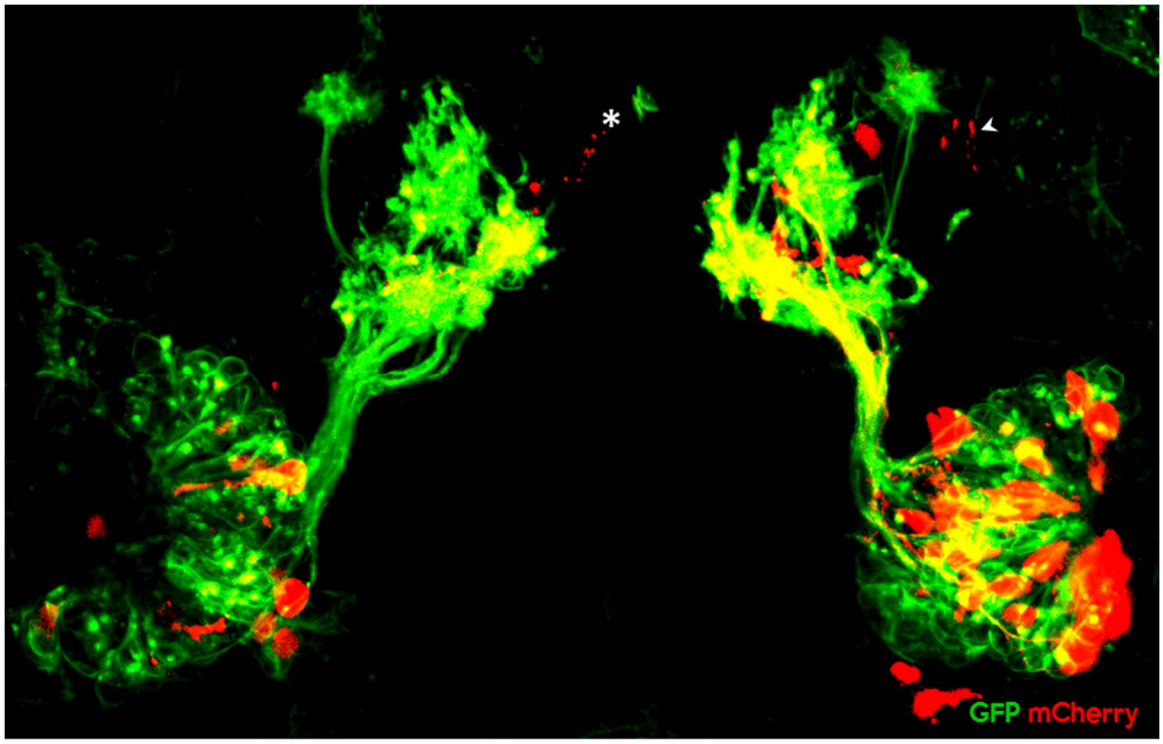

Figure 4.29. Confocal z-stack from a Hregion-pOR101-1-mCherry-IntergenicRegion-OR101-1-pA injected Tg(OMP:tauGFP) embryo at 4dpf. Arrowhead indicate axons projecting LG1-2-4; Asterisk indicate the midline glomeruli.

Thus, injections of H-$p_{(1.2kb)}$OR101-1-driven OR-expressing constructs into the Tg(OMP:tauGFP) line revealed that the midline glomeruli are a novel axonal target, which is not innervated by OMP-positive axons but only by a fraction of mCherry-positive neurons. This observation is consistent with the interpretation that these axons are guided by the expressed OR but cannot project to the endogenous glomerulus that is appropriate for the OR because it is now expressed in a different cell type.

4.2.4.2. Comparison to Bodipy Staining. In previous experiments a high correlation between mCherry-expressing and OR-expressing OSNs has been demonstrated. However, more OR expressing OSNs that did not express the mCherry reporter have been identified. To understand whether additional axons contribute to the novel midline structures that are not mCherry-positive, H-$p_{(1.2kb)}$OR101-1-mCherry-$inter_{(1.4kb)}$-OR111-7^{myc}-pA injected embryos were stained with bodipy at 4 dpf and analyzed using confocal microscopy (Figure 4.30a).

In previous experiments two populations of mCherry-positive axons were identified: those that colocalize with EYFP-positive (Section 4.3.3.1.) or tauGFP-positive axons (Section 4.3.3.2.) and those that converge onto novel midline glomeruli. The former subset of mCherry-positive neurons innervates regions that densely stained for bodipy, similar to the wild-type bodipy pattern (Figure 4.30b). The axon terminals that project to the dorsal midline also colocalize with bodipy, however, different from axons that project to CZ, MZ and LG1, 2, 3, and 4, bodipy staining was restricted to mCherry-positive axons and no additional structures resembling glomeruli were obvious surrounding these axons (Figure 4.30c). This indicates that the position of the midline glomeruli is a novel glomerular target and that few, if any, non-labeled axons contribute to the new projection field.

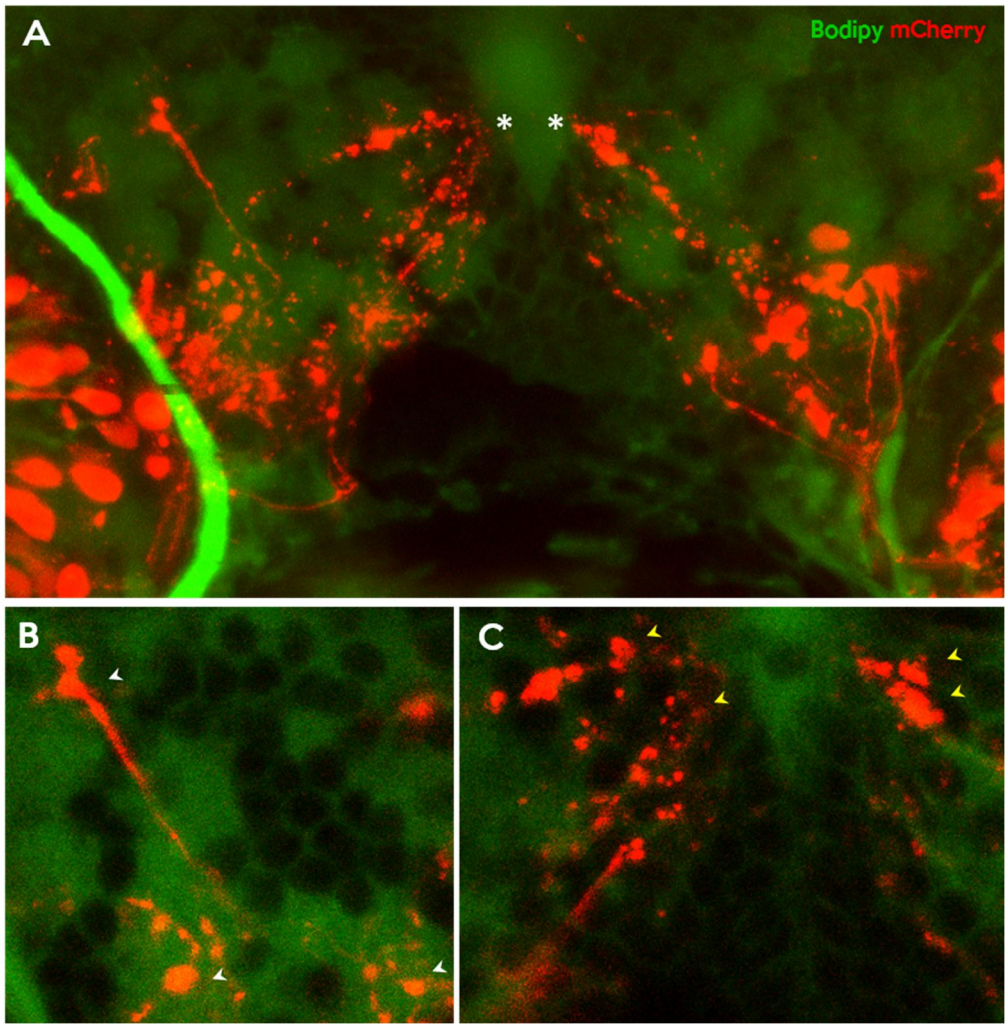

Figure 4.30. Hregion-pOR101-1-mCherry-IntergenicRegion-OR111-7^{myc}-pA injection combined with bodipy staining. (A) Axonal projection pattern. (B-C) Single confocal sections of OB.

Identical results were obtained for H-$p_{(1.2kb)}$OR101-1-mCherry-$inter_{(1.4kb)}$-OR101-1-pA (Figure 4.31). Most of the bodipy stained glomeruli were innervated by mCherry-positive neurons (Figure 4.31b), however, axons that converged onto the midline glomeruli seems to penetrate a region that is devoid of bodipy, except for the mCherry axons themselves (Figure 4.31c). In conclusion, the axons that are guided by transgenic OR proteins target an area that is distinct from the usual pattern of embryonic glomerular map and no mCherry-negative axons contribute to the novel structures.

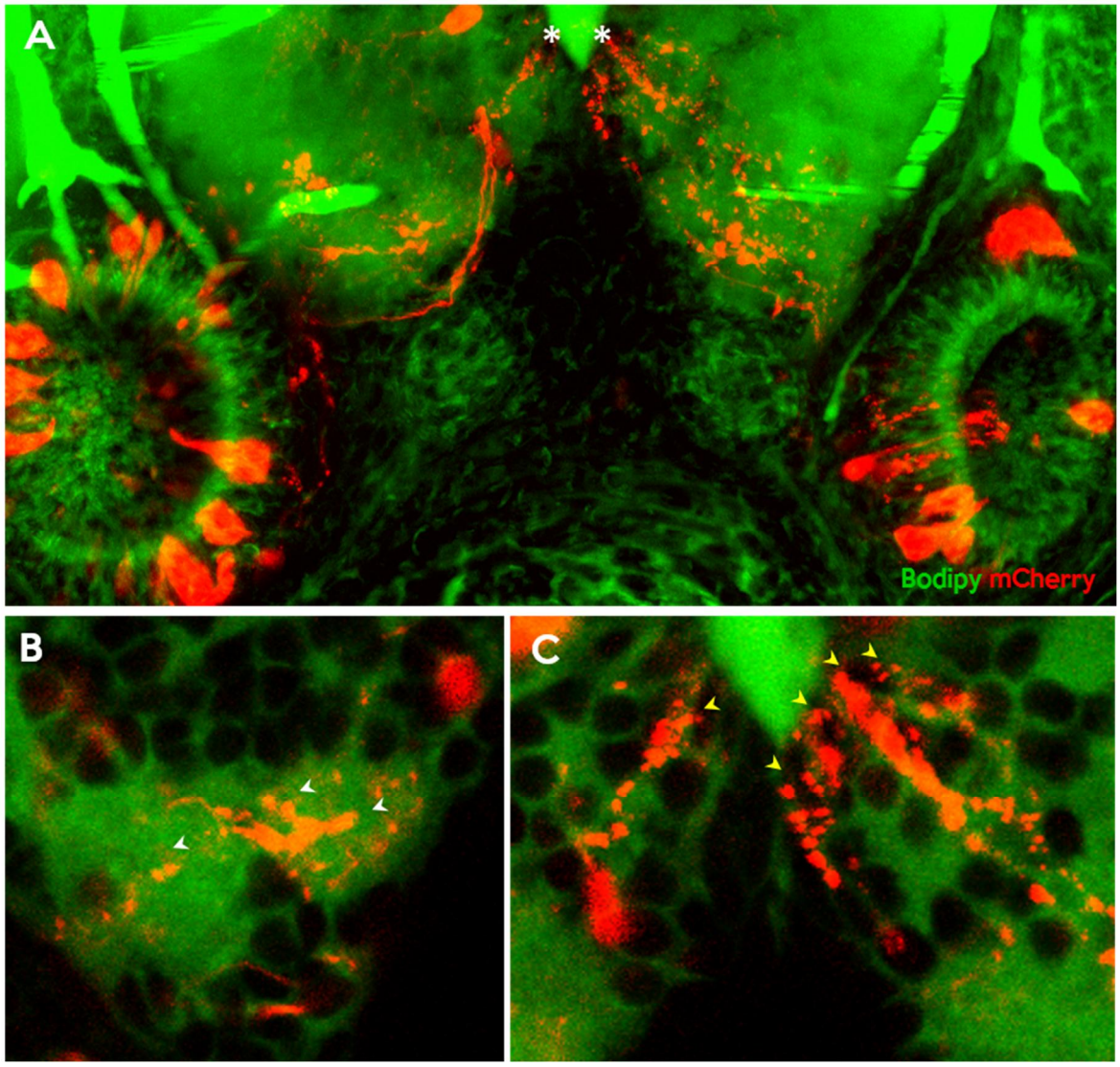

Figure 4.31. Hregion-pOR101-1-mCherry-IntergenicRegion-OR101-1-pA injection combined with bodipy staining. (A) Axonal projection pattern. Asterisks indicate the midline glomeruli. (B-C) Single confocal sections of OB.

4.2.4.3. Comparison to Tg(pOR101-1:EYFP). The axonal projection pattern of Hregion-pOR101-1-mCherry-IntergenicRegion-OR111-7^{myc}-pA and Hregion-pOR101-1-mCherry-IntergenicRegion-OR101-1-pA was also compared to a Tg(pOR101-1:EYFP) line. The Tg(pOR101-1:EYFP) line expresses the EYFP reporter gene from the 1.2 kb OR101-1 promoter. The transgenic line was generated by Xalid Bayramlı through integration of pOR101-1-EYFP-pA construct into the zebrafish genome. In the Tg(pOR101-1:EYFP) line a subset of OSNs expresses EYFP instead of an OR gene. Thus, these cells may undergo second OR gene choice (refer to Section 1.3.5. for further details). Second OR gene choice has previously been shown to be class restricted in the mouse (Bozza *et al.*, 2009) and OR cluster-restricted in zebrafish (Sato *et al.*, 2007). Because the OR101-1 gene is the only class II OR in the zebrafish OR gene repertoire (Tınaztepe, 2009) it should (theoretically) select the endogenous OR101-1 gene for second choice. Hence, in the Tg(pOR101-1:EYFP) line, reporter gene-positive axons may converge onto the endogenous OR101-1 glomerulus. Indeed, in the Tg(pOR101-1:EYFP) line a a single glomerulus with a pattern that is invariant across individuals can be observed (Bayramlı, unpublished data).

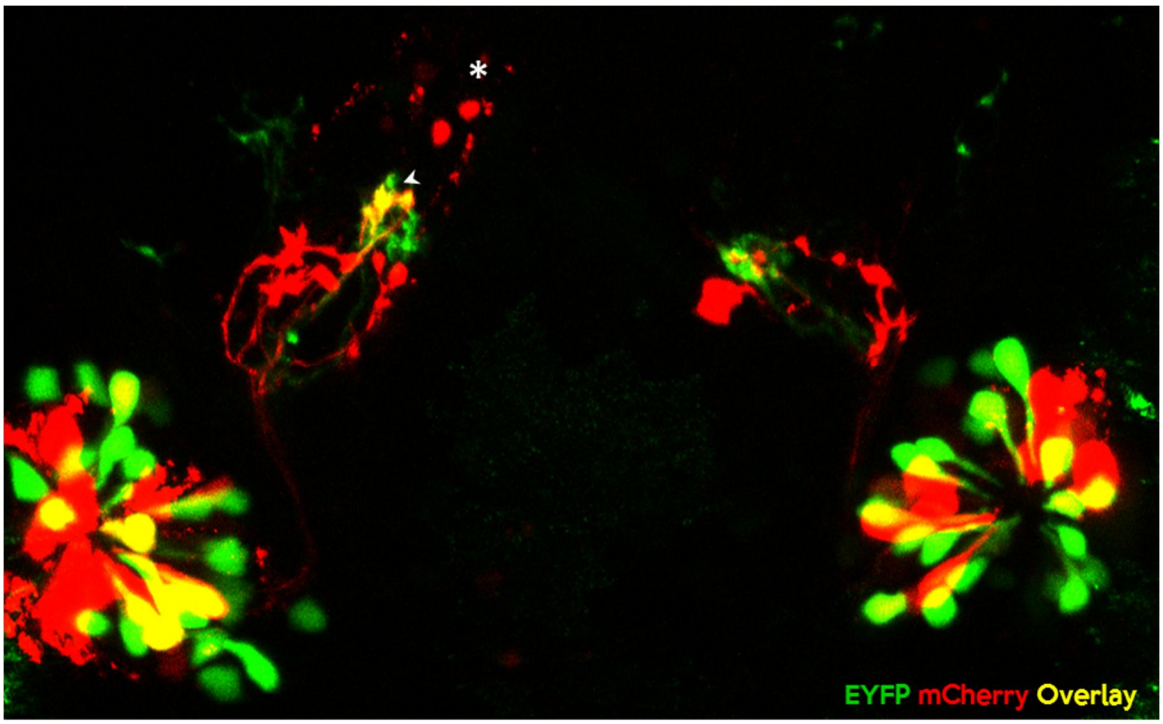

Figure 4.32. Confocal z-stack from a Hregion-pOR101-1-mCherry-IntergenicRegion-OR111-7^{myc}-pA injected Tg(pOR101-1:EYFP) embryo at 4dpf. Arrowhead indicates double labeled axons; Asterisk indicates the midline glomeruli.

When the H-p$_{(1.2kb)}$OR101-1-mCherry-inter$_{(1.4kb)}$-OR111-7^{myc}-pA construct was injected into Tg(pOR101-1:EYFP) embryos at one-cell stage, a single EYFP-positive glomerulus was visible in CZ (Figure 4.32). In some cases the same glomeruli were also innervated by mCherry-labeled axons. As previously seen, mCherry-positive glomeruli are also observed in other glomeruli in CZ and DZ, in addition to midline glomeruli.

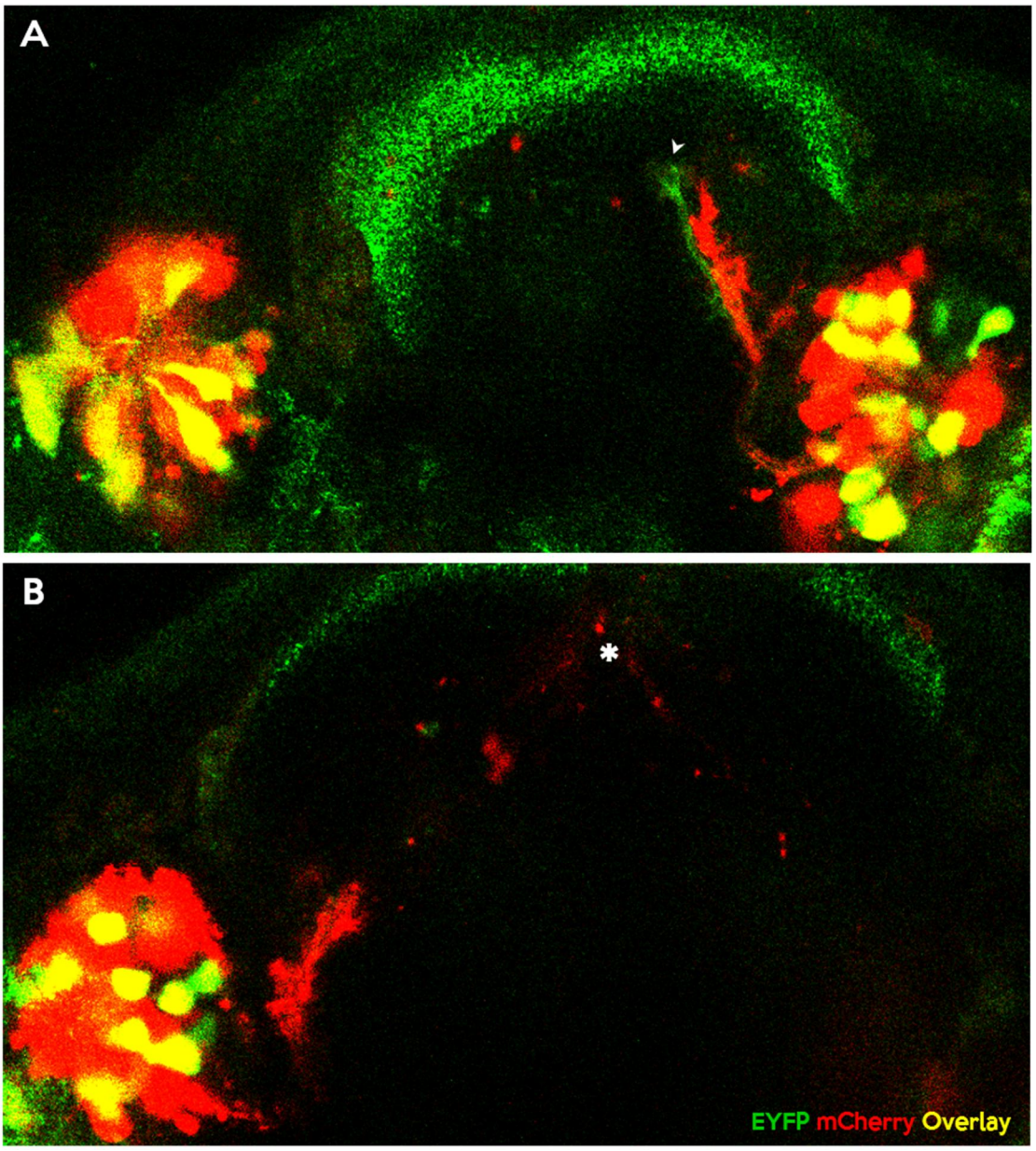

Figure 4.33. Confocal z-stack from a H-p$_{(1.2kb)}$OR101-1-mCherry-inter$_{(1.4kb)}$-OR101-1-pA injected Tg(pOR101-1:EYFP) embryo at 4dpf. Arrowhead indicates EYFP-positive glomeruli; Asterisk indicates the midline glomeruli.

The H-$p_{(1.2kb)}$OR101-1-mCherry-$inter_{(1.4kb)}$-OR101-1-pA construct was also injected into fertilized oocytes of the Tg(pOR101-1:EYFP) transgenic line. OBs of injected embryos were analyzed at 4dpf using confocal microscopy. Surprisingly, EYFP-positive glomeruli were not innervated by mCherry-positive axons, and the axons that converged onto the midline glomeruli were found to be only mCherry-positive (Figure 4.33).

As a result, the difference of EYFP-positive glomeruli of the Tg(pOR101-1:EYFP) transgenic line and mCherry-positive midline glomeruli may suggest that the midline glomeruli are specific to transgenic OR111-7 and OR101-1 protein expression. However, the detection of the same glomeruli in H-$p_{(1.2kb)}$OR101-1-mCherry-$inter_{(1.4kb)}$-OR101-1-pA injections and their divergence from the EYFP-positive glomeruli in the Tg(pOR101-1:EYFP) line proves that transgenic OR proteins develop a novel axonal identity which results in formation of distinct glomeruli.

4.2.5. Axons Innervating the Midline Glomeruli Are Stable Until 8dpf

The efficiency and stability of axonal wiring in the olfactory system is not well understood (Mombaerts *et al.*, 2006). Because a functional OR is required for stable OR gene expression (Shykind, 2004), it is possible that innervation of an appropriate glomerulus and establishment of functional synaptic connections within OB may be important for an axon survival. Axons that are miswired may be pruned over time. To understand whether axons that converge onto midline glomeruli form stable synaptic connections they were followed over the first week of development.

For that purpose, H-$p_{(1.2kb)}$OR101-1-mCherry-$inter_{(1.4kb)}$-OR111-7^{myc}-pA injected embryos were kept in separate containers after confocal imaging at 4dpf to be able to reidentify them later. Emrbyos were reanalyzed at 7dpf to examine changes in axonal trajectories within the OB (Figure 4.34). Similar experiments were also conducted for H-$p_{(1.2kb)}$OR101-1-mCherry-$inter_{(1.4kb)}$-OR101-1-pA injected embryos at 4, 6, and 8dpf (Figure 4.35).

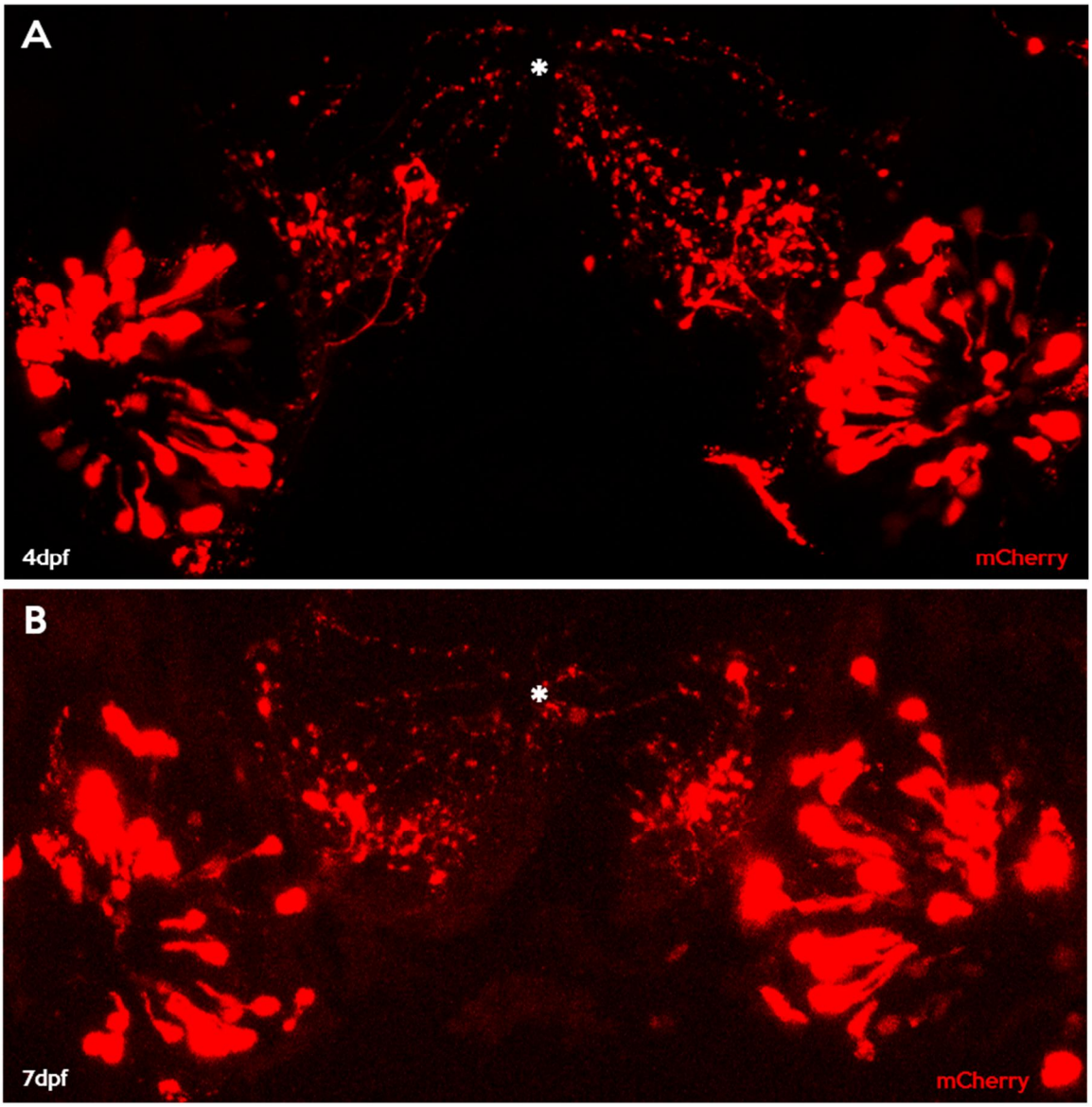

Figure 4.34. Analysis of axons that converge onto the midline glomeruli within the first week of development. (A-B) Confocal z-stacks of H-$p_{(1.2kb)}$OR101-1-mCherry-$inter_{(1.4kb)}$-OR111-7^{myc}-pA at 4dpf and 7dpf. Asterisks indicate the midline glomeruli.

In both cases, mCherry-positive axons that converge onto midline glomeruli remain stable until 7 or 8 dpf. The stability of these axons throughout the first week of development implies that they are not misrouted axons but are functional and establish synaptic connections within the OB.

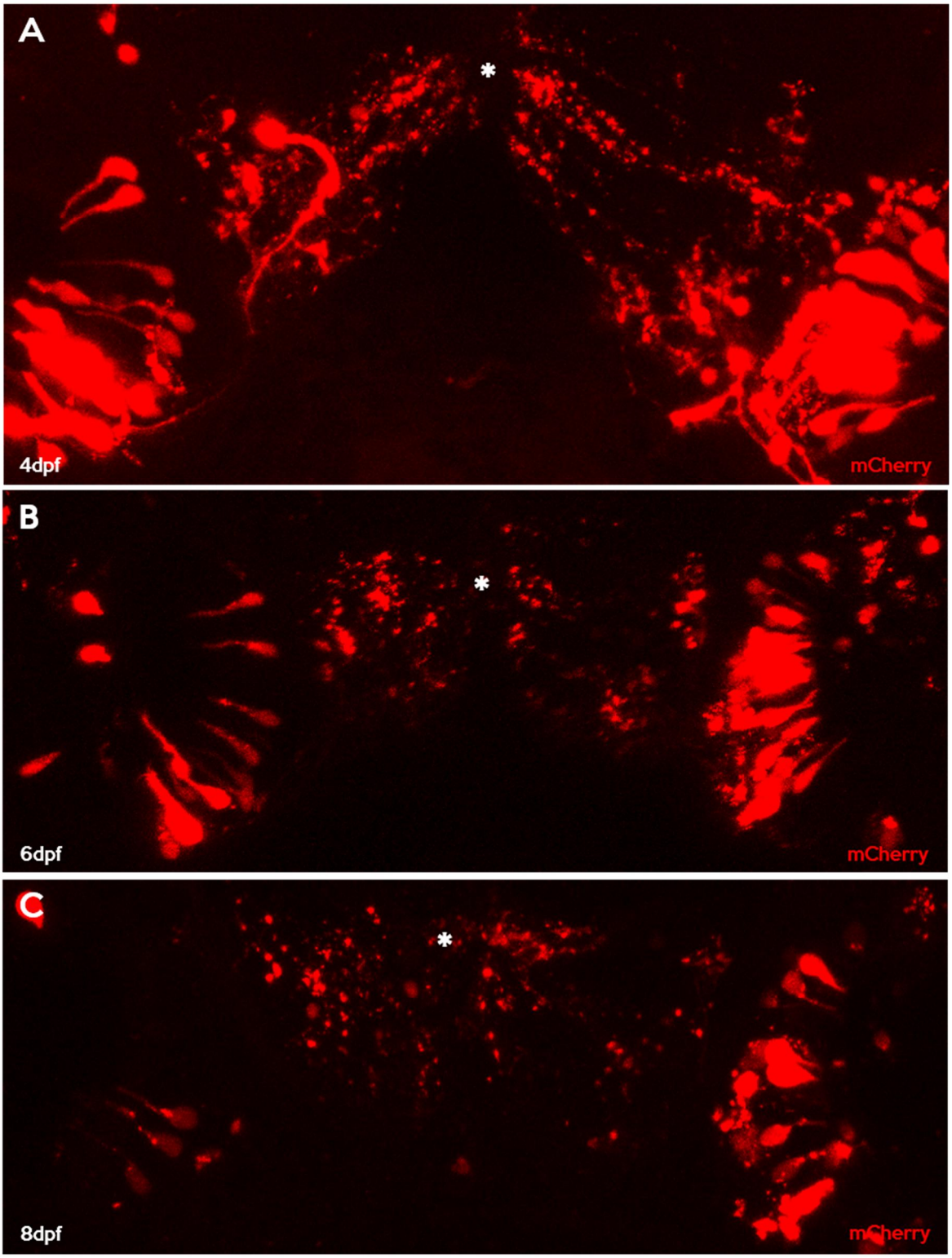

Figure 4.35. Analysis of axons that converge onto the midline glomeruli within the first week of development. (A-C) Confocal z-stacks of H-p$_{(1.2kb)}$OR101-1-mCherry-inter$_{(1.4kb)}$-OR101-1-pA at 4dpf, 6dpf and 8 dpf. Asterisks indicate the midline glomeruli.

4.2.6. Quantification of Axons

A novel glomerular phenotype where mCherry-labeled axons converge onto midline structures was observed for the H-$p_{(1.2kb)}$OR101-1-mCherry-inter$_{(1.4kb)}$-OR111-7^{myc}-pA and H-$p_{(1.2kb)}$OR101-1-mCherry-inter$_{(1.4kb)}$-OR101-1-pA transgenic constructs. These midline glomeruli are novel OB structures as confirmed by bodipy staining, injections into transgenic Tg(OMP:tauGFP) and Tg(pOR101-1:EYFP) lines and co-injections with a H-$p_{(1.2kb)}$OR101-1-EYFP-pA construct.

To better understand to origin and extend of these structures, mCherry transgene expressing axons were quantified according to their target glomeruli in the embryonic OB (refer to Section 4.2.1. for further details). The quantification of axons of H-$p_{(1.2kb)}$OR101-1-mCherry-inter$_{(1.4kb)}$-OR111-7^{myc}-pA injected transgenic embryos can reveal the subset of axons that converge onto midline glomeruli over the entire axonal population. Furthermore, a comparison of innervated glomerul between H-$p_{(1.2kb)}$OR101-1-EYFP-pA and H-$p_{(1.2kb)}$OR101-1-mCherry-inter$_{(1.4kb)}$-OR111-7^{myc}-pA injected embryos provides quantitative information about the phenotypic changes observed in the axonal projection pattern when an OR coding sequence was expressed from the bi-cistronic construct.

Confocal z-stacks from all H-$p_{(1.2kb)}$OR101-1-mCherry-inter$_{(1.4kb)}$-OR111-7^{myc}-pA injections, including injection of the construct into wild type embryos and the OMP-tauGFP and Tg(pOR101-1:EYFP) lines, or co-injection with H-$p_{(1.2kb)}$OR101-1-EYFP-pA, were re-analyzed for axons quantification. In 28 transgenic embryos a total of 583 mCherry-labeled axons could be detected in the OB, thus on average of 20.8 ± 1.9 mCherry-positive axons per embryo. Of those, 283 axons or 48.5% of the axonal population targeted midline glomeruli. The second largest group, 29.3% (171/583 axons) of axons projected to the central zone. An additional 51 axons converged onto the dorsal zone and LG3, which together form 8.7% of the entire population and18 axons targeted LG1, 2, and 4 (3.1%), while 3 (0.5%) and 6 (1.0%) axons terminated in MG and VM, respectively (Figure 4.36b).

The fraction of axons that converged onto midline glomeruli the largest population with 48.5%. As outlined previously, there is experimental support that those axons may express OR111-7. Typically a 73.8% - 86.8% correlation of reporter gene colabeling was observed for mChery and GFP in Section 4.1.2, a ratio that is almost twice as large as the 48.5% of axons that targeted midline glomeruli. Possible explanations might be that additional OSNs that project to glomeruli different from the midline glomeruli also express OR111-7 or that the correlation between translation of the two cistrons was reduced in OR expression constructs. Because midline-projecting axons were OMP-negative, it is likely that an additional subpopulation of ciliated OSNs also express OR111-7.

To quantify axons that expressed the H-$p_{(1.2kb)}$OR101-1-EYFP-pA construct, confocal z-stacks from all previous experiments, including injection into wild type AB/AB embryos, co-injection with H-$p_{(1.2kb)}$OR101-1-mCherry-inter$_{(1.4kb)}$-OR111-7^{myc}-pA and H-$p_{(1.2kb)}$OR101-1-mCherry-inter$_{(1.4kb)}$-OR101-1-pA, were re-analyzed and EYFP-positive axons were counted and scored for their projection to the OB. In 22 transgenic embryos a total of 436 EYFP-labeled axons could be detected, thus, on average 19.8 ± 1.9 EYFP-positive axons per embryo. None of the 436 labeled axons projected to the dorsal midline. The largest group, 56.2% (245/436 axons) of axons project to the central zone, 77 (17.7%) to the dorsal zone, 76 (17.4%) to LG3, while 27 axons targeted LG1, 2, and 4 (6.1%), 7 (1.6%) projected to MG, and 4 (0.9%) axons terminated in VM (Figure 4.36b).

In order to compare the axonal projection patterns, the quantification of H-$p_{(1.2kb)}$OR101-1-mCherry-inter$_{(1.4kb)}$-OR111-7^{myc}-pA was normalized by excluding axons that converged onto midline glomeruli. The normalized data comprise 300 mCherry-labeled axons of which 57%, 17%, 17% and 6% converged onto CZ, DZ, LG3 and LG1, 2, and 4, respectively (Figure 4.36b).

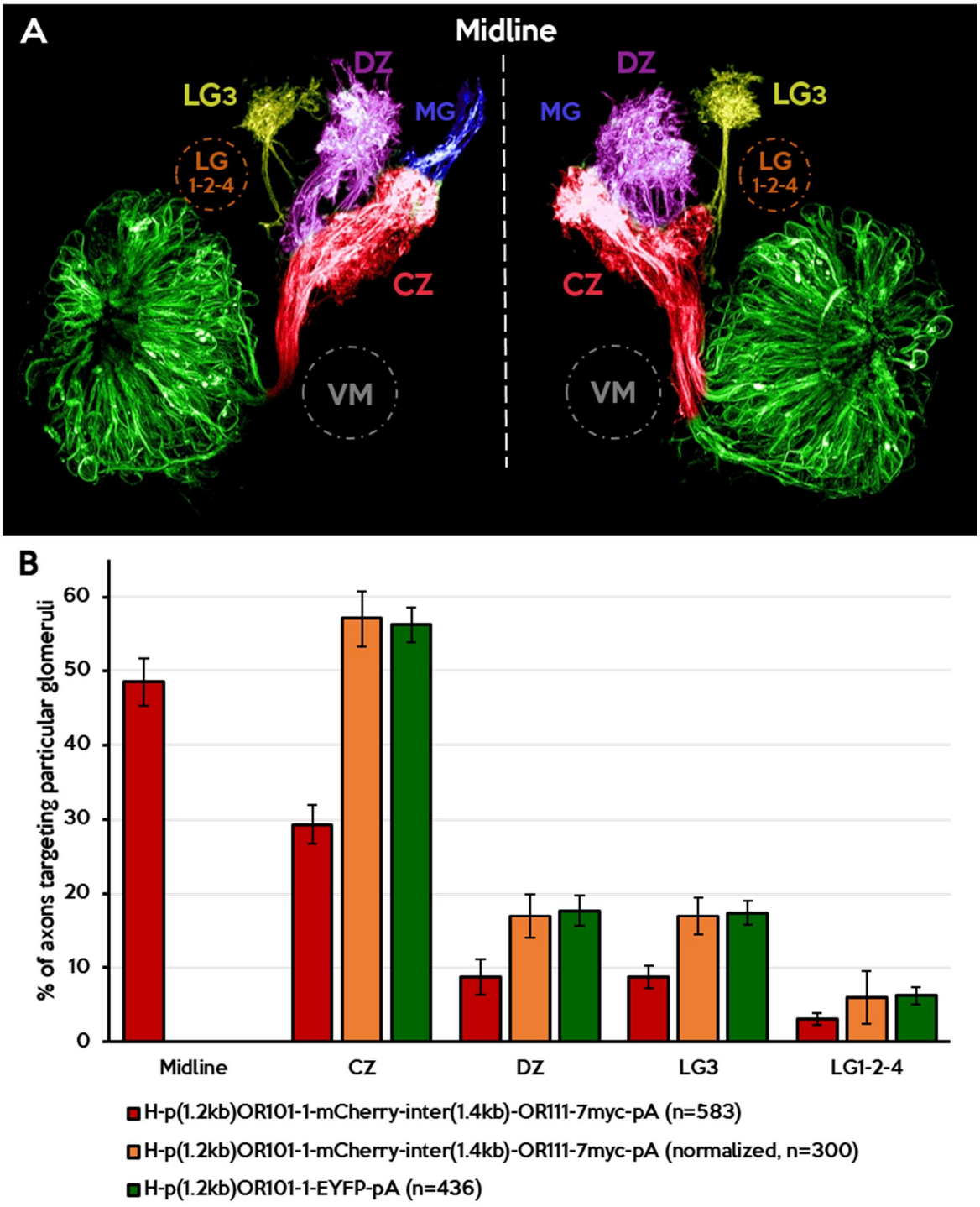

Figure 4.36. Quantification of axons after H-$p_{(1.2kb)}$OR101-1-mCherry-$inter_{(1.4kb)}$-OR111-7^{myc}-pA injections according to their target glomeruli. (A) Embryonic glomerular map. (B) Percentage of axons targeting specified glomeruli.

Interestingly, the normalized distribution of axons was identical for constructs that did or did not include an OR coding sequence: 57% vs. 56.2% of axons converged onto CZ; 17% vs. 17.7% of axons converged onto DZ; 17% vs. 17.4% of axons converged onto LG3; 6% vs. 6,2% of axons converged onto LG1, 2, and 4; 1% vs. 1.6% of axons converged onto MG, and 2% vs. 0.9% of axons converged onto VM (Figure 4.34b). The similarity of the EYFP and mCherry projection patterns suggest that mCherry-positive OSNs are composed of two different populations in H-$p_{(1.2kb)}$OR101-1-mCherry-inter$_{(1.4kb)}$-OR111-7^{myc}-pA injected embryos. However, it should be noted that the protoglomerular fields, such as CZ and DZ are large OB territories and will give rise to a large number of up to 120 glomeruli in the adult. Thus, the compressed nature of the embryonic map does not readily allow a good distinction of whether small changes in the exact position of transgene-expressing axons has occurred. Therefore, from this analysis it cannot be concluded that a second OR111-7-expressing ciliated OSN population exists and that the endogenous OR111-7 glomerulus can be revealed.

A quantification of axons was also performed for the H-$p_{(1.2kb)}$OR101-1-mCherry-inter$_{(1.4kb)}$-OR101-1-pA construct similar to the quantification described above. In 23 transgenic embryos, a total of 548 mCherry-labeled axons could be detected in the OB, thus, on average 23.8 ± 2.1 mCherry-positive axons per embryo. Of those, 210 (or 38.8%) axons targeted midline glomeruli. The second largest group, 31.6% (173/548 axons) of axons projected to CZ, while 70 axons (12.8%) converged onto DZ, 50 axons (9.1%_ converged onto LG3, 34 axons (10%) targeted LG1, 2, and 4, 3 axons (0.5%) projected to MG, and 8 (1.4%) axons terminated in VM (Figure 4.36). When the data was normalized by excluding axons projecting to midline glomeruli, the axonal distribution pattern was again identical to H-$p_{(1.2kb)}$OR101-1-EYFP-pA injection: 51.2% vs. 56.2%, 20.7% vs. 17.7%, 14.8% vs. 17.4%, 10% vs. 6.2% for CZ, DZ, LG3 and LG1, 2 and 4, respectively (Figure 4.37).

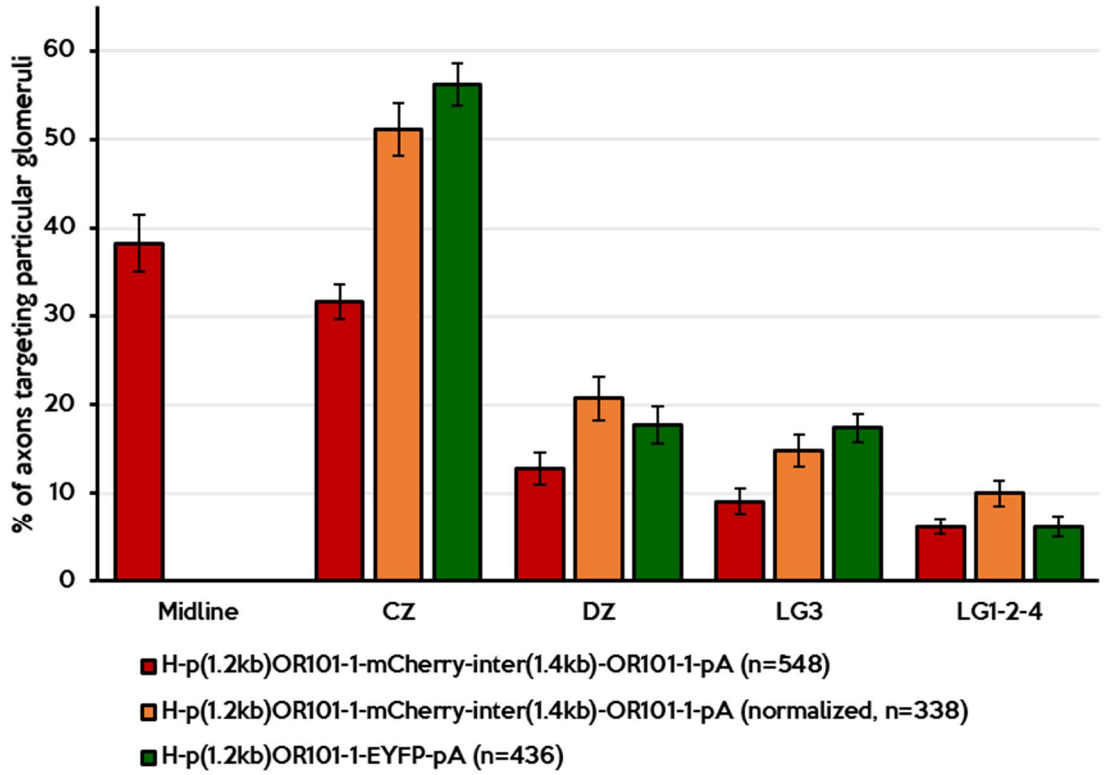

Figure 4.38. Percentage of axons targeting specified glomeruli after H-$p_{(1.2kb)}$OR101-1-mCherry-$inter_{(1.4kb)}$-OR101-1-pA injection.

4.2.7. Myc-tag Antibody Staining

A myc-tag was included in the H-$p_{(1.2kb)}$OR101-1-mCherry-$inter_{(1.4kb)}$-OR111-7^{myc}-pA construct to be able to follow OR111-7 protein expression using immunohistochemistry against the myc epitope. Staining of OR111-7^{myc} may reveal the identity of axons and OSNs that have been successfully transformed.

First, we tried to understand whether the myc-tagged OR111-7 protein can be detected in axons converging on the midline glomeruli. Whole mount antibody staining with an anti-myc antibody was performed on4 dpf embryos. mCherry expression in cell bodies and axons of transgenic OSNs could be detected by their autofluorescence after immunohistochemical procedures. However, no specific labeling for the myc-tag could be detected in axons or cell bodies of OSNs, probably due to low tissue penetrance of the antibody in whole-mount

stainings. To overcome this problem, different fixation regimes and permeabilization protocols were used but to no avail. Therefore, tissue section through the OE of 4 dpf embryos were subjected to anti-myc immunohistochemistry. On tissue sections, myc-tagged OSNs could be successfully visualized (Figure 4.38a; Figure 4.38b). In total, 12 mCherry-positive cells and 5 Anti-Myc-tag labeled cells could be identified on the sections of 6 embryos. Colocalization of mCherry was detected in all 5 cells, while 41.7% mCherry-positive OSNs costained for OR111-7^{myc}. Unfortunately, on tissue sections no mCherry-positive axons could be found. Thus, it remains unresolved at this point whether the midline axons are indeed OR111-7-positive, whether they are the only OR111-7-positive population or if other axons with transformed OR111-7 identity target other parts of the OB.

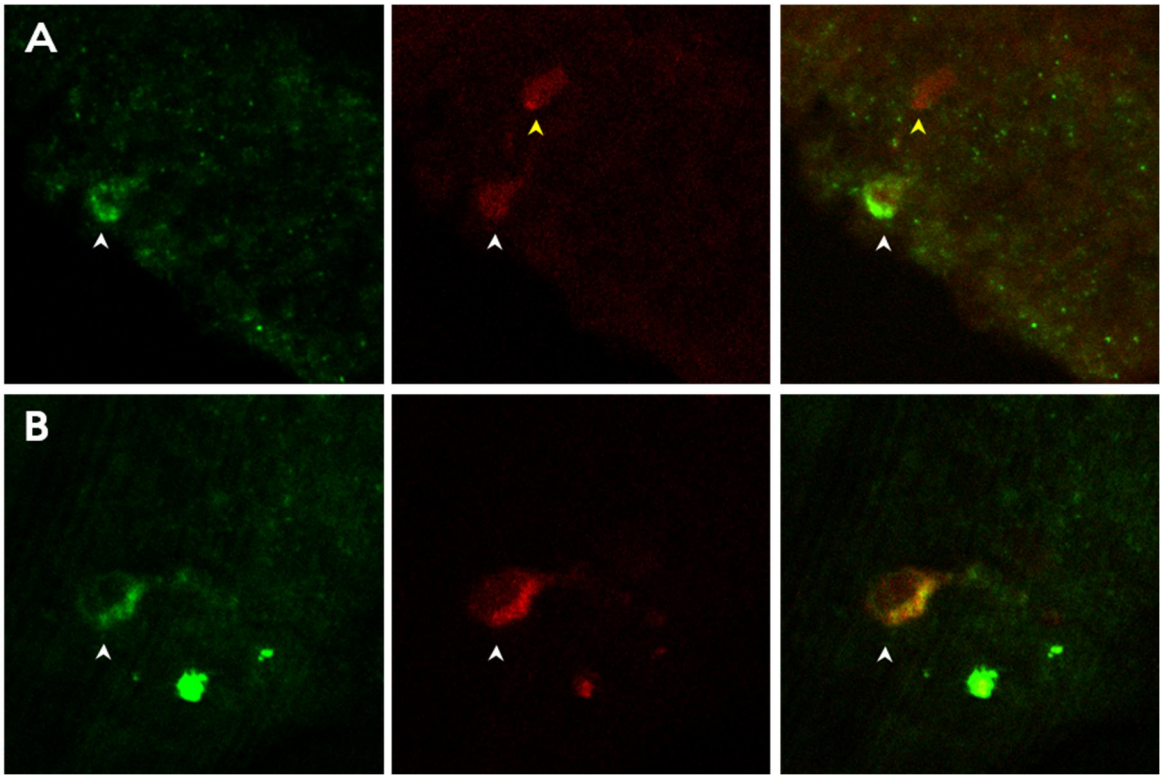

Figure 4.40. Antibody staining against Myc-tag to OE sections of H-p$_{(1.2kb)}$OR101-1-mCherry-inter$_{(1.4kb)}$-OR111-7^{myc}-pA injected embryos (A) Confocal z-stacks of an OE. (B) Close-up single confocal optical sections of a double labeled OSN.

In summary, the addition of an OR coding sequence in bi-cistronic constructs resulted in reporter gene-positive cells which always colabeled for the OR when probed by in situ hybridization. In order to expand the number of transgene-expressing OSNs the mouse H-enhancer was included in transgenic construct and to detect OR expression a myc-tag was fused in frame to the OR111-7 coding sequence. Overexpression of the OR expression constructs resulted in convergence of transgenic axons at low cell density and in novel dorsomedial glomeruli when expressed with the H-enhancer. The midline glomeruli are novel structures, OMP-negative and exclusively formed by mCherry-positive axons. Yet, they are stable over the first 8 days of embryonic development, suggesting that the axons make functional connections in the OB. Thus, the bi-cistronic approach successfully transforms some OSNs with a new OR identity, the identity expressed from the construct. Depending on the transformed cell population, axons my target the appropriate endogenous glomerulus or form novel glomerulus-like structures in the OB.

5. DISCUSSION

One fundamental feature of the mammalian olfactory system is the expression of a single OR from a large and diverse genomic repertoire in every single OSN (Malnic *et al.,* 1999), referred as the one receptor – one neuron rule (Mombaerts, 2004). The OR expression is also shown to be monoallelic (Chess *et al.,* 1994; Ishii *et al.,* 2001). Moreover, apart from their primary function of recognizing odorants, ORs appear to have a role in the regulation of monogenic and monoallelic expression: functional OR proteins initiate a negative feedback signal (Serizawa *et al.,* 2003) which is received by elements that reside in OR coding sequences (Nguyen *et al.,* 2007). Furthermore, OR proteins are also involved in the second key feature of the olfactory system which is the convergence of like axons to target glomeruli. The OR protein is present on axons and axon terminals of OSNs and act as a determinant during the formation of glomeruli in OB (Barnea *et al.,* 2004; Mombaerts, 2006). Thus, its critical role in two key features of the olfactory system makes *in vivo* investigation of ORs and their expression pattern crucial. However, the critical roles of ORs in two key features of the olfactory system renders the *in vivo* visualization of OR proteins a difficult task. First, the use of OR promoters in transgenes abolish the expression of endogenous ORs because of monogenic and monoallelic expression thus can not reveal the expression of a specific OR. Second, the instructive role of ORs in axonal targeting makes the use of OR-reporter fusion proteins problematic. The fused protein probably interferes with the OR-mediated homophilic and heterophilic interactions of axons and alter the axonal identity of OSNs resulting in formation of ectopic glomeruli. The wiring of OSNs is also shown to be activity-dependent (Imai *et al.,* 2006; Nakashima *et al.,* 2013) and the fusion protein may have an impact on the activity of ORs. Hence, the OR proteins cannot be visualized through fusion proteins without altering their axonal trajectories.

One way to overcome these difficulties and maintain the natural expression pattern of ORs is to coexpress a reporter gene along with an OR protein in bi-cistronic messages using an IRES sequence. Pioneered in 1996, this strategy is utilized to successfully coexpress a mouse OR gene (P2) and a marker protein by an IRES (lacZ; Mombaerts *et al.,* 1996). The experimental design later became the standard approach in the field and it has been used in at least fourteen other mouse OR genes: M71, M72, P3, P4, M50, I7, MOR23, mOR37A,

mOR37B, mOR37C, M5, MOR28, SR1, and MOL2.3 (Serizawa *et al*., 2000; Strotmann *et al*., 2000; Zheng *et al*., 2000; Potter *et al*., 2001; Zou *et al*., 2001; Bozza *et al*., 2002; Treloar *et al*., 2002; Vassalli *et al*., 2002; Weber *et al*., 2002; Cuthforth *et al*., 2003; Feinstein & Mombaerts 2004; Feinstein *et al*., 2004; Shykind et al. 2004). This strategy was instrumental in identifying and studying aspects of olfactory function, such as zonal expression of ORs, their role in axonal convergence, and to elucidate their ligand spectrum (refer to Sections 1.3.3. and 1.5.2. for further details).

Nevertheless, attempts to adopt the OR-IRES-marker strategy to visualize specific subpopulations of OSNs in the zebrafish olfactory system have failed (Sato *et al*., 2007). Although IRES sequences of viral origin are reported to drive two fluorescent proteins in various tissues other than the OE in zebrafish (Fahrenkrug *et al*., 1999), the level of EMCV IRES driven proteins was demonstrated to be low (Kwan *et al*., 2007). The underlying reason behind this failure may be the differential efficiency of viral IRES sequences to initiate translation in different species or their temperature dependence. In order to bypass this problem, several approaches have been applied in various studies.

A method to visualize the expression of a specific protein *in vivo* is the insertion of self-cleaving peptides of the 2A-family between the coding regions of two proteins in same orientation to generate two individual proteins from a single open reading frame (Provost *et al*., 2007). Thus, by replacing the IRES with a self-cleaving peptide in OR-IRES-Marker strategy, two independent proteins could be translated while keeping the natural expression pattern of ORs intact. A member of the self-cleaving peptides family, T2A, was previously used in our laboratory in order to coexpress a fluorescrent protein with an OR gene in OSNs. The self-cleavage efficiency of T2A is confirmed after observing the colocalization of two reporter genes in transgenic embryos that are injected with constructs comprising ‘mCherry-T2A-EYFP’ complex. Nevertheless, when the first reporter gene is replaced with an OR coding sequence, transgenic expression is totally diminished in injected embryos. A negative feedback mechanism is shown to be available in OSNs to ensure that a single functional OR allele is expressed and the feedback mechanism is initiated by OR proteins (Serizawa *et al*., 2003; Lewcock and Reed, 2004; Shykind *et al*., 2004). Critically, transgenic ORs are inhibited by the negative feedback signal, even if they are driven under the control of

regulatory sequences that are unrelated with the olfactory system (Nguyen *et al.,* 2007); proving that the negative feedback signal initiated by OR proteins is received by the elements in OR coding sequences. For this reason, the presence of an OR coding sequence in the OR-T2A-Marker construct may have suppressed the transgenic expression. Nishizumi *et al* (2007) reported that an OR gene tagged by direct fusion of a reporter gene is able to be expressed with the help of H region in 50-60% of injected embryos. The construct that could drive OR expression also contains 1.7 and 7.3 kb long 5' and 3' flanking sequences of that specific OR, respectively. Comparatively, in order to avoid the negative feedback signal in OR-T2A-Marker approach, 530 bp downstream region of OR111-7 gene consisting complete 3' untranslated region (UTR) is cloned directly downstream of OR-T2A-Marker complex. Similar to 1.7 and 7.3 kb sequences used by Nishizumi *et al.*, within that 503 bp, regulatory elements may exist which blocks the negative feedback signal and results in stable transgenic expression. Upon the injection of OR-T2A-Marker-3'UTR construct transgenic OSNs are detected. However, the number of reporter gene-positive OSNs were too low compared with the constructs that comprises the same promoter/enhancer regions and lack OR coding sequences (Tastekin, 2012). In conclusion, the impact of negative feedback signal on the OR coding sequence cannot be bypassed and the modification of OR-IRES-Marker approach with the self-cleaving peptide T2A is unable to visualize the expression of a specific OR gene in a subpopulation of OSNs in the zebrafish olfactory system.

A study in 2012 used an alternative strategy to visualize a transgenic OR gene in a subpopulation of OSNs *in vivo*. In this study, they have adopted the Tol2-mediated Gal4-UAS system which is shown to be feasible in in zebrafish (Asakawa and Kawakami, 2009) and combined it with the OR-IRES-Marker strategy. Thus, they generated a transgenic line where the expression of an OR (OR111-7) is linked by an IRES sequence to the simultaneous expression of the transactivating factor Gal4 and another transgenic line where its consensus UAS (upstream activating sequence) binding site drives a reporter gene (Cistrine). Thus, in the OE of double-transgenic larvae OR111-7 transgene expressing neurons should also be cistrine-positive. However, there are few experimental considerations. Primarily, there is no direct evidence that the transgenic OR protein is introduced to neurons. Thus, OR111-7 transgene may not be present in reporter gene-positive OSNs, or could be found only in a minority of reporter gene expressing neurons. The indirect evidence of transgenic OR

presence is the innervation of reporter gene-positive neurons to the CZ. However, a fraction of neurons also converged onto one of the lateral glomeruli which is not innervated by ciliated OSNs. Moreover, the CZ is a major zone in embryonic OB which is packed with a series of at least 5 protoglomeruli (Dynes and Ngai, 1998). Yet, the reporter gene-positive neurons are not localized to any specific subcompartment within the zone and their axons terminals seems to be scattered throughout the whole extent of the CZ. Therefore, the axonal projection pattern does not provide sufficient evidence to conclude that cistrine-positive OSNs only express transgenic OR111-7 gene and converged onto OR111-7 specific glomeruli. For instance when we investigated the OB of Tg(OMP:tauGFP) line at 4dpf (Figure 4.2.4.2) more than half of tauGFP-positive OSNs converged onto protoglomeruli located within the CZ, and these neurons should theoretically represent more than half of the OR repertoire, which is at least 80 in the zebrafish genome (Alioto and Ngai, 2005; Niimura and Nei, 2005).

Furthermore, scattered pattern of reporter gene-positive neurons within the CZ together with the penetrance of axons to microvillous-specific glomeruli suggests that the overall detected axonal projection pattern is not unique to a single OR but represents a heterogeneous set of ORs that are selected in the second OR gene choice. In Section 4.2.4.4, embryonic OBs of Tg(pOR101-1:EYFP) line is investigated in detail. In this transgenic line the presence of a reporter gene instead of an OR forces the cells where pOR101-1 drives expression to undergo a second round of OR gene selection. The set of available ORs for the second choice of OR genes is shown to be restricted and subfamily specific (Sato *et al.*, 2007). Since the OR101-1 gene is the only member of Class II ORs and OR101 subfamily (Tınaztepe, 2009); theoretically, the selected OR in the second round of selection could only be the endogenous OR101-1 gene. Correspondingly, EYFP-positive cells form a small glomerulus at the CZ in each half of the OB (Figure 4.30 & 4.31). Nevertheless, its specificity for OR101-1 gene could not be confirmed due to the inefficiency of visualizing axons by *in situ* hybridizations and lack of a specific antibody against OR101-1 protein. On the other hand, upon the injection of Hregion-pOR101-1-EYFP-pA construct in Section 4.2.4.1, reporter gene-positive OSNs not only expanded to a larger population in the OE, but their axons also innervate multiple glomeruli located in various regions of embryonic OB (Figure 4.23). Importantly, EYFP-positive axons innervate every region in the embryonic

glomerular map that is identified in Section 4.2.1 including CZ, DZ, LG3, LG1-2-4, MG and VM. Existence of reporter gene-positive axons in every region of the OB represents the heterogeneity and diversity in OR gene expression following second choice. This could be explained by two alternative scenarios. First, in OSNs where pOR101-1 drives EYFP expression, the set of ORs available for the second OR gene choice may comprise more than one OR (endogenous OR101-1) in the initial experiments and became evident only when it is enhanced by the H region. Second, the impact of H region may also resulted in the expansion of the set of ORs for selection during the second OR gene choice. Considering the highly scattered axonal projection pattern of H-pOR101-1-EYFP-pA injected embryos, this expansion may expanded this set even to the whole OR repertoire. Finally, the quantification of axons revealed that CZ is the region which is innervated by the largest fraction of axons (56.2%). The impact of the enhancer also resulted with the projection of neurons to microvillous-specific glomeruli (LG1-2-4; 6.2%). As a result, the impact of H region may expand the set of ORs selectable for the second OR gene choice, and the set of OSNs that OR101-1 promoter is active; even in these cases most of the axons converged onto the CZ.

In a study in 2007, the insertion of H region to expand the expression pattern of OR111-1 gene generated a similar case (Nishizumi et al 2007). When a transgenic construct comprising a direct fusion of OR111-1 coding sequence with a reporter gene along with 10 kb of flanking sequences is injected into zebrafish embryos, transgenic expression could only be detected in 4% of the embryos with the expressivity of a few reporter gene-positive OSNs. But after the addition of H region to the injection construct transgene expression is observed in 50-60% of the embryos while the number of OSNs increased to 60-70 cells per embryo. The increased expressivity of the transgenic construct resulted in a visible pattern of axonal trajectories. In this pattern, it could be seen that most of the axons projected onto CZ and a few penetrate into VM without entering the OB. The distribution of axons is not specific to a subcompartment within the CZ in parallel with the ones that are detected in cistrine-positive neurons by Lakhina *et al* (2012). Although the transgenic construct contains an OR111-1-EYFP fusion protein, a fraction of neurons should comprise a particular level of the fusion protein at which EYFP fluorescence reaches the threshold of detection but OR proteins does not accumulate in sufficient amounts to initiate negative feedback signal and

form an axonal identity specific for OR111-1. These neurons must undergo another round of OR gene selection and according to the hierarchical regulation of OR gene choice (Sato *et al.,* 2007), the selectable OR set for the second choice of these neurons should only comprise ORs of OR111 subfamily which includes 11 OR genes. Consequently, the EYFP-positive neurons detected in Nishizumi *et al.* (2007) should not necessarily positive for the OR111-transgene but also includes population of neurons which undergo second OR gene choice. Since the second choice set is limited to 11 ORs, the axonal projection pattern only consists neurons that converged onto various protoglomeruli in the CZ.

The scenario for cistrine-positive neurons in Lakhina paper might be very similar. In that study, the enhancer E15 is included to the transgenic constructs instead of H region. E15 is identified by Nishizumi *et al* (2007); and when two reports are compared it has a similar impact with the H region. H region is shown to elevate expression rate from 4% to 50-60% while increasing the number of reporter gene-positive cells from few cells to 60-70 cells per transgenic embryo (Nishizumi *et al.,* 2007). The enhancer E15 is also shown to increase EYFP expression rate from 0% to 50% in BAC injected embryos (Nishizumi *et al.,* 2007) while producing 27 reporter gene-positive neurons in each nose (Lakhina *et al.,* 2012). The initial activity of pOR111-7 is previously demonstrated to be 3 cells per embryo in our lab (Tastekin, 2012). In summary, the impact of E15 enhancer on OR gene promoters is comparable to H region's effect.

On the other hand, a BAC transgenic line was previously generated where OR111-7 is replaced by YFP by Sato *et al* (2007). In parallel with the Tg(pOR101-1:EYFP) line used in Section 4.2.4.4, these YFP-positive neurons are also bound to undergo second OR gene choice. These neurons can only select 11 ORs from the OR111 subfamily as second choice. And YFP-positive axons that should contain one of those 11 genes are shown to project their axons within the CZ (Sato *et al.,* 2007). Thus, the distribution of neurons that represents the restricted second choice of OR set for OR111-7 is also confined to the CZ. Consequently, if the YFP-positive neurons detected by Sato *et al.* are enhanced with an enhancer (H region or E15), the expected result would be again convergence of axons onto CZ but with an increased number of visible axons. Hence, the cistrine-positive axons converging onto the

CZ that are detected by Lakhina *et al* (2012) probably contain a mixture OSNs that express various ORs among the OR111 family. And the fraction of OR111-7 transgene expressing axons cannot be directly differentiated. Next, cistrine-positive axons that converged onto the lateral glomeruli is detected in 60% of the embryos (Lakhina *et al.*, 2012) which forms a similar rate with the axons that project their axons to OMP-negative lateral glomeruli (LG1-2-4) which is detected in 72% of the embryos in Section 4.2.6. Therefore, those axons probably occur due to the impact of E15 or H enhancer, and their OR identity is also not known.

Another disadvantage of the system used by Lakhina *et al.* (2012), is the transiency of the reporter gene-positive OSNs. First of all, in order to combine the Gal4-UAS system with OR-IRES-Marker strategy transgenic lines should be formed. And even in transgenic lines where the transgenic constructs are integrated to the zebrafish genome, reporter gene-positive OSNs are shown to be transient. The average number of OSNs detected per nose at 3dpf is 27 whereas it decreases to 4 cells by 9dpf (Lakhina *et al.*, 2012). Because of the anatomy of zebrafish embryos, and the early formation of stereotyped glomerular map axonal targeting analyses are performed around 3 or 4 dpf, so the decrease in the number of labeled axons might not cause a problem by 9 dpf. However, the innervation to the correct glomeruli and formation of functional connections within the OB may enhance axon's stability and miswired axons may not be retained in the system (Mombaerts, 2006). Thus, the transiency of reporter gene-positive axons might imply that those neurons do not contain sufficient amounts of OR proteins to form functional connections in the OB and discarded through time. The failure at the formation of stable connections in the OB leads to uncertainty of the axonal identity of those axons and specificity of their glomerular targets.

Consequently, considering i) the scattered pattern of axonal projections in the CZ ii) the innervation to OMP-negative glomeruli in 60% of embryos iii) the transient nature of reporter gene-positive OSNs iv) the similarity of axonal projection pattern detected by Nishizumi *et al* (2007); OR111-7 transgene expressing OSNs may constitute only a minority of the cistrine-positive axons and the remaining population may represent OSNs that undergo second OR gene choice from a restricted set of ORs (OR111 subfamily) similar to

an enhanced version of OR111-7/YFP replaced axons detected by Sato *et al* (2007). Thus, the combination of OR-IRES-Marker strategy with the Gal4:UAS system cannot efficiently tag a given OR in a subpopulation of neurons and visualize its axonal projections.

A recent report tried to express a fusion of OR111-1 and GFP genes under the control of OMP promoter in injected zebrafish embryos (Ferreira *et al.*, 2014). In a previous study, the use of OMP promoter which could efficiently drive non-OR reporter genes could not generate transgenic OR expression in OSNs in the mouse olfactory system (Nguyen *et al.*, 2007). Nguyen *et al* (2007) concluded that this failure is the result of a negative feedback signal which limits OR expression through receptor-promoter interactions and they have tried to overcome the suppression by separating the promoter from the OR coding sequence. On the other hand, in order to overcome the negative feedback signal Ferreira *et al* (2014) included the 3' UTR of OR111-1 gene into injection construct. The 3' UTR of OR111-1 gene may contain regulatory elements which helps the transgenic expression to escape negative feedback signal. The same 3' UTR was also available in the 11 kb construct that Nishizumi *et al* used to drive OR111-1-EYFP fusion (2007). Moreover, these regulatory elements are probably not specific for the 3' UTR of OR111-1 gene but exists in other 3' UTR regions of OR genes. For instance transgenic constructs including OR111-7 coding sequence along with 3' UTR of OR111-7 gene also resulted in reporter gene-positive OSNs (Lakhina *et al.,* 2012; Tastekin, 2012). In spite of escaping the negative feedback signal and detecting reporter gene-positive OSNs, the presence of transgenic ORs is not directly known in this approach, either. The indirect evidence stems from the decreased number of endogenous OR-positive OSNs detected by *in situ* hybridizations between injected and control embryos. 12-15% decrease in OR103-1, OR103-2 or OR111-6-positive cells suggest that OMP:OR-GFP construct introduced transgenic ORs to a subpopulation of OSNs, thereby, resulted in smaller number of OSNs for the rest of the repertoire. Moreover, when double *in situ* hybridization is performed targeting the reporter gene and a number of endogenous ORs, the proportion of double-positive OSNs tend to decrease in OMP:OR-GFP injected embryos compared with the control group (Ferreira *et al.*, 2014). Since the reporter gene is targeted instead of OR 111-1 coding sequence in double *in situ* hybridizations, the existence of OR111-1 transgene in embryos is still unclear. Another problem with the method is that only cell bodies of OSNs are depicted in the figures and the visibility of axons

is unclear. Additionally, since a fusion protein is used, the glomerular targets of the axons may also be disrupted. In conclusion, considering the lack of direct evidence for OR111-1 transgene and the occurrences of double labeling between reporter gene-positive OSNs and endogenous ORs, the approach conducted by Ferreira *et al.* (2014) cannot tag OSN subpopulations that express a specific OR gene in vivo and is not suitable for the investigation of OR's instructive role at axonal targeting due to possible disruptions by fusion proteins.

In this study, we also propose an alternative model to OR-IRES-Marker strategy. As previously mentioned, due to differential efficiency of viral IRES sequences to initiate translation in different species or due to their temperature dependence attempts of employing OR-IRES-Marker strategy have failed in zebrafish olfactory system (Sato *et al.,* 2007). However, the utilization of cellular IRES sequences that are derived from the zebrafish genome may bypass this caveat. In order to address this problem, we tried to use OR103-1/5 intergenic regions' ability of bi-cistronic translation within the OR-IRES-Marker experimental design. In this context the co-expression ability of the intergenic region which is validated in Section 4.1 will be used as a molecular tool to introduce transgenic OR proteins to a subpopulation of OSNs in the zebrafish olfactory system. Critically, there is a difference with the original OR-IRES-Marker strategy and its modification with the intergenic region: the order of the OR and reporter protein in the bi-cistronic message. We tried to drive the bi-cistronic message that contains the OR and the reporter gene under the control of pOR101-1, and to reach a significant number of transgenic OSNs per embryo we also cloned the H region directly upstream of the promoter in Section 4.2.3. H region expands the expression of pOR101-1 to a larger subset of neurons. For instance, throughout the study, the average number of reporter gene-positive OSNs is 6.5 ± 0.4, 5.3 ± 1.1, 4.1 ± 0.5 and 7 ± 0.6, in various constructs using only pOR101-1 as the main promoter. On the other hand, pOR101-1 is able to drive transgenic expression in 52.8 ± 7.0, 35.8 ± 2.1 and 38.8 ± 5.8 cells per embryo under the influence of the H region. This drastic impact might also affect the intrinsic promoter activity within the intergenic region which produces 3.5 ± 0.8 cells per embryo. Thus, utilization of the intergenic region in OR-IntergenicRegion-Marker complex will generate a significant number of OSNs that is only marker positive in each injected embryo. Distinguishing these neurons within the whole population of marker-positive OSNs

would cause another difficulty. Instead, in the Marker-IntergenicRegion-OR complex, the possible impact of the H region on the intergenic region is neglected because neurons that contain monocistronic message originating from the intergenic region are not visualized; thus, they are excluded from the axon quantification data.

Previously while using the OR-T2A-Marker complex, transgenic expression was inhibited by the negative feedback signal (Tastekin, 2012). However, the presence of transgenic protein in reporter gene-positive OSNs is confirmed in our case. There are two possibilities that could lead to these results. The first explanation is the presence of 1.4 kb region in the constructs (OR103-1/5 intergenic sequence) which constitutes the entire sequence between two OR genes. The negative feedback signal that inhibits the expression of transgenic ORs are shown to be received by elements residing in OR coding sequences (Nguyen *et al.*, 2007), and the signal could be bypassed by the addition of 3' UTR sequences of OR genes into the transgenic constructs (Nishiumi *et al.*, 2007; Lakhina *et al.*, 2012; Tastekin, 2012; Ferreira *et al.*, 2014). Along with its bi-cistronic translation ability, the intergenic region also possess 3' UTR of the OR103-1 gene which could generate a similar effect. Contrary to other studies, the 3' UTR is located upstream of OR coding sequence in Marker-IntergenicRegion-OR context. Still, if the 3' UTR is efficient when located 1.5 kb downstream of OR111-7 gene (IRES and GAL4 gene; Lakhina *et al.*, 2012); it may exert the same impact on OR coding sequence when located 1.4 kb upstream of the OR coding sequence. Moreover, OR103-1 gene is reported to be more resistant to suppression initiated by other receptors (Ferreira, 2007), and this resistance may be related with some regulatory elements located in its 3' UTR. Thus, the presence of 3' UTR of OR103-1 gene in the intergenic region might have resulted in transgenic OR expression in injected embryos by helping it escape the negative feedback signal. Another possibility of bypassing the negative feedback signal is the presence of the OR coding sequence in the second cistron in our bi-cistronic constructs. It is shown that OR expression is limited by receptor-promoter interactions and regardless of the nature of the promoter that drives their expression (Nguyen *et al.*, 2007). This inhibition may act on promoters that is directly upstream of the OR coding sequence or in close proximity. Thus, the negative feedback signal received by the OR coding sequences in Marker-inter$_{(1.4kb)}$-OR complex may only inhibit the intrinsic promoter activity within the intergenic region. Hence, the main promoter that drives the bi-cistronic

message is not affected by the inhibitory signals which results in the production of transgenic ORs in reporter gene-positive OSNs through bi-cistronic translation. Consequently, through the use of bi-cistronic constructs including the intergenic region, the inhibition problem faced in OR-T2A-Marker constructs is eliminated.

The introduction of transgenic ORs is confirmed in Section 4.2.7 using Myc-tag antibody staining. Further, in Section 4.2.6, two different axonal populations were detected upon the injection of Hregion-pOR101-$1_{(1.2kb)}$-mCherry-$inter_{(1.4kb)}$-$OR111\text{-}7^{myc}$ or Hregion-pOR101-$1_{(1.2kb)}$-mCherry-$inter_{(1.4kb)}$-OR101-1 constructs. Since the Myc-tag antibody staining protocols could not label cells in whole mount embryos but only in embryonic OB sections, we cannot differentiate which population of axons consist the Myc tagged transgenic OR protein. However, the generation of a novel phenotype by one of the populations through converging onto the midline glomeruli implies that these neurons consist a novel axonal identity. The lack of those axons in previous injection results even in constructs that contains the same enhancer and promoter sequence together with the need of a novel axonal identity of the axonal population indirectly confirms that transgenic ORs revealed by anti-Myc-tag staining should be in the axons that create the phenotype. This novel axonal target is however, is not specific to OR111-7 or OR101-1; because it is detected in both Hregion-pOR101-$1_{(1.2kb)}$-mCherry-$inter_{(1.4kb)}$-$OR111\text{-}7^{myc}$ and Hregion-pOR101-$1_{(1.2kb)}$-mCherry-$inter_{(1.4kb)}$-OR101-1 injected embryos. Hence, it should be specific for transgenic ORs that is present in reporter gene-positive OSNs. The generation of different glomeruli between transgenic and endogenous versions of a single OR is previously shown (Wang *et al.,* 1998; Bozza *et al.,* 2002; Feinstein *et al.,* 2004). Moreover, the level of expression for the OR is demonstrated to be another determinant of the axonal identity. Upon decreasing the levels of expression by the insertion of an IRES sequence directly upstream of an OR, the glomerular position specific for M71 gene shifted to a more anterior and ventral location (Firestein *et al.,* 2004). A similar case might have happened in the zebrafish olfactory system. In Tg(pOR101-1:EYFP) line the EYFP-positive glomeruli is located in the CZ and Lakhina *et al* (2012) also demonstrated that OR111-7 transgene expressing neurons converged onto CZ. Thus, altering the expression levels of transgenic OR101-1 and OR111-7 genes by using bi-cistronic translation from the intergenic region, a shift from CZ to midline glomeruli may have happened in axonal targeting in parallel with the shift detected

by Firestein *et al* in the mouse olfactory system (2004). Finally, in a review in 2006, an alternative axonal wiring model is proposed (Mombaerts, 2006). This model favors self-sorting of axons by OR-mediated homophilic and heterophilic interactions between axons over the existence of predetermined targets along the OB to which axons are guided. In that case, axons became the targets themselves and accordingly, OSNs axons do not converge onto a glomerulus but coalesce into a glomerulus. The outcome of this model is the dependence of the glomerular array in the OB to the expressed OR repertoire of an organism. In parallel to the self-sorting model, Hregion-pOR101-1$_{(1.2kb)}$-mCherry-inter$_{(1.4kb)}$-OR111-7^{myc} and Hregion-pOR101-1$_{(1.2kb)}$-mCherry-inter$_{(1.4kb)}$-OR101-1 constructs introduced a new transgenic OR to the OR repertoires of the injected embryos and this addition may have resulted in the formation of novel glomeruli which are the midline glomeruli in our case.

When the mCherry-positive axons are quantified in Section 4.2.6, it is found that the axons converging onto the midline glomeruli form 48.5% and 38.5% of the whole axonal population in Hregion-pOR101-1$_{(1.2kb)}$-mCherry-inter$_{(1.4kb)}$-OR111-7^{myc} and Hregion-pOR101-1$_{(1.2kb)}$-mCherry-inter$_{(1.4kb)}$-OR101-1 injected embryos, respectively. As previously stated, these axons should express OR111-7 transgene through bi-cistronic translation from the intergenic region. The co-translation efficiency of reporter genes -mCherry and GFP- is demonstrated to be around 73.8-86.8% in Section 4.1.2. However, this ratio dropped to 38.5-48.5% upon the presence of an OR coding sequence in the second cistron. First explanation of the detected decrease may be the negative feedback signal that is received by specific sequences within the OR coding sequence (Nguyen *et al.,* 2007; Tastekin, 2012). As mentioned above, the presence of 3' UTR of OR103-1 gene may helped our transgenic constructs to escape the negative feedback signal. Nonetheless, the impact of the suppression may have a gradual effect instead of working with an on / off mechanism. Thus, transgenic constructs with the intergenic region may escape from the negative feedback signal only to some extent, and cannot reach the co-translation efficiencies achieved with two reporter genes. Another explanation of the difference between 78.8-86.8% double expression rates of reporter genes and 40% of axons that converged onto the novel midline glomeruli is the differential amounts of protein levels that is sufficient for the detection of GFP fluorescence and the instruction of axons by ORs. The proteins that are translated from the second cistron, GFP and transgenic ORs, are visualized through direct and indirect methods, respectively.

For an OSN to be classified as GFP-positive detection of GFP fluorescence is sufficient whereas in order to define an OSN as transgenic OR-positive, its presence should have an impact on the axonal trajectory. These two levels may differ in terms required amounts of protein. For instance, higher amounts of transgenic OR proteins should be accumulated to act as an axonal determinant. In order to address this problem we investigated the signal intensity levels of GFP fluorescence in bi-cistronic constructs. The double expression rates among mCherry-positive cell were 86.8% and 82.1% for pOMP-mCherry-IntergenicRegion-GFP-pA and pOR101-1-mCherry-IntergenicRegion-GFP-pA constructs, respectively. In total, these constructs produced 321 and 252 GFP-positive cells. The signal intensity of GFP and mCherry were also scored while counting the number of reporter gene-positive cells per embryo for every transgenic construct. According to the signal intensity scoring data, pOMP-mCherry-IntergenicRegion-GFP-pA generated 64, 84 and 173 cells that are strong, intermediate and weak GFP-positive, respectively. We have decided to exclude the weak GFP-positive cells from the double expression calculations which corresponds to the neurons that comprise insufficient levels of transgenic ORs to guide the axons. All of the mCherry-positive cells regardless of their signal intensity are included to the new double expression calculations because they are also visible in the Hregion-pOR101-$1_{(1.2kb)}$-mCherry-$inter_{(1.4kb)}$-OR111-7^{myc} & Hregion-pOR101-$1_{(1.2kb)}$-mCherry-$inter_{(1.4kb)}$-OR101-1 injection results. The new double expression rate became 40.7% for pOMP-mCherry-IntergenicRegion-GFP-pA construct. When the same strategy is employed to pOR101-1-mCherry-IntergenicRegion-GFP-pA construct, 141 weak GFP-positive OSNs are excluded from the data and the new double expression rate is calculated as 39.0%. Critically, upon the exclusion of weak GFP-positive OSNs from the calculations, double expression rates of dropped to 39.0-40.7% which is in range with the percentage of axons that converged onto the midline glomerulus in Hregion-pOR101-$1_{(1.2kb)}$-mCherry-$inter_{(1.4kb)}$-OR111-7^{myc} and Hregion-pOR101-$1_{(1.2kb)}$-mCherry-$inter_{(1.4kb)}$-OR101-1 injected embryos: 48.5% and 38.5% respectively.

The 38.5-48.5% rate may seem low when compared with the double expression rates of reporter genes; but it is efficient in terms of bi-cistronic translation and most importantly, it provides a method to introduce transgenic ORs into OSNs in the zebrafish olfactory system. In the OR-IRES-Marker strategy which plays an important role at identifying and

studying aspects of olfactory function, translation from the IRES sequences are demonstrated to be less efficient. In fact, in a study the IRES sequence is used to reduce the expression levels of M71 gene (Firestein *et al.,* 2004). Through translation from an IRES, the protein levels are shown to be reduced by a factor of tenfold which is deduced by reporter gene fluorescence levels. Thus, even with 10% efficiency, IRES sequences became valuable tools in the mouse olfactory system. On the other hand, in the zebrafish olfactory system efficiency of the IRES sequences are even lower. In the report where EMCV IRES is demonstrated to be functional in zebrafish, it is asserted that the second cistron is clearly translated far less efficiently than the first cistron (Kwan *et al.,* 2007). For instance, when mCherry is used as the reporter gene in the second cistron it could not reach to detectable expression levels. Additionally, the threshold needed for transgenic ORs to instruct axonal targeting could be higher than the one which is required for reporter genes to be detected. Consequently, by generating a novel phenotype in 40% of the reporter gene-positive axons, the efficiency of translation from the intergenic region seems sufficient to introduce transgenic OR proteins into OSNs and instruct them to a novel axonal target.

Furthermore, the comparison of luminescence levels between vectors that contain EMVC IRES and the intergenic region may also be informative about the efficiency of translation from the intergenic region. In Section 4.1.1 the ratio of firefly over renilla luciferases are calculated to assess the IRES activity within the intergenic region, and as a positive control the same experiments are also performed with EMCV IRES sequence. Compared with pRF vector, EMCV IRES resulted in 29.2 ± 6.1 fold increase in Fluc/Rluc ratio whereas the intergenic region provides a 116.5 ± 7.2 fold increase (Figure 4.1). When the SV40 promoter is removed from the constructs to elucidate the contribution of intrinsic promoter activities of the inserts Fluc/Rluc ratios dropped to 53.9 ± 4.5 and 4.2 ± 2.6 for the intergenic region and EMCV, respectively (Figure 4.2). Thus, the difference between the calculated Fluc/Rluc ratios of intact vectors and promoterless vectors are reasoned to be the contribution of IRES activity within the inserts. These differences constitute 62.6 and 25 fold increase for the intergenic region and EMCV sequence, respectively; and indirectly confirms the higher translation efficiency of the intergenic region. However, these calculations are based on luciferase activity detected in transfected HeLa cells and their efficiencies may differ in the zebrafish olfactory system.

The final consideration is the confirmation of the intergenic region on RNA level. We have proposed an alternative method to introduce transgenic OR proteins into subsets of OSNs through bi-cistronic translation. For the translation of second cistron, the transcribed bi-cistronic message should include the intergenic region. We have tried to confirm the intergenic region's existence on RNA level by several direct and indirect approaches. First evidence arise from RT-PCRs that use OE derived cDNA as a template. Using primers that target coding sequences of OR103-1 and OR103-5, a 1.9kb fragment is tried to be amplified which spans all of the intergenic region. In RT-PCR results two specific bands were detected which corresponds to 1906 bp and 1788 bp size (Atasoy, 2011). On single faint band is also detected in –RT negative control reaction which suggests genomic contamination. However, the higher intensity of observed bands in +RT reactions and existence of multiple bands which corresponds to variant of transcripts where 118 bp intron is spliced out indicates that these bands are specific for RNA; confirming that the intergenic region exists on RNA level. We have also performed another RT-PCR reaction with OE derived cDNA templates targeting 600 bp region within the intergenic region. The targeted fragment could be detected both in +RT and –RT reactions. Still, the intensity of the +RT experiment was much higher than the negative control, suggesting that the targeted fragment also exists in mRNA form. An indirect evidence also comes from amplification of OR103-1 gene in RT-PCR reactions which uses OR103-5 RNA derived cDNA as template and primers targeting OR103-1 gene (Atasoy, 2011). The amplified products imply that OR103-1 transcript is present as the upstream of OR103-5 gene; thus, long transcripts that spans the entire intergenic region exist. Next evidence of the intergenic region's existence on RNA level originates from *in vivo* injection results. GFP fluorescence is detected in 78.8-86.8% of mCherry-positive OSNs upon the injection bi-cistronic constructs in Section 4.1.2.3. Critically, these double expression rates could only be achieved when the reporter genes and the intergenic region exist on a single piece of DNA. The separation of reporter genes into different plasmids diminished the high double expression rates among mCherry-positive cells. Finally, when the intergenic region is replaced by another OR promoter in bi-cistronic injection constructs, GFP fluorescence is again diminished among mCherry-positive cells; suggesting that the double expression rates originate from the bi-cistronic transcripts instead of intrinsic promoter activity.

In summary, the intergenic region's ability to promote bi-cistronic translation is used as a molecular tool to introduce transgenic OR proteins to a subpopulation of OSNs. However, the transgenic expression of ORs is confined to a fraction of OSNs that is tagged with a reporter gene. In the preliminary results, the share of neurons which contains the OR111-7 transgene is found to be 41.7% using anti-Myc-tag staining. This rate is in similar range with the colabeling of reporter genes when the cells that contain low levels of protein originating from the second cistron is excluded (39-40.7%). Moreover, a similar rate is also revealed when the axons that generate a novel phenotype by converging onto the midline are quantified (38.5-48.5%); in parallel with the OR's instructive role in axon guidance. Consequently, the OR103-1/5 intergenic region is able to tag at least a fraction of OSNs that express specific OR genes *in vivo*. If two distinct axonal populations residing among reporter gene-positive OSNs could be discriminated through further investigations, the intergenic region may provide an alternative method for the adoption of OR-IRES-Marker strategy to the zebrafish olfactory system.

APPENDIX A: EQUIPMENT

Table 6.1. Equipment.

4 °C Room	Birikim Elektrik, Turkey
Autoclaves	Astell Scientific, UK
Centrifuge	Eppendorf, Germany (5417R)
Confocal Microscope	Leica SP5-AOBS, USA
Electronic Balance	Sartorius, Germany (TE412)
Electrophoresis Supplies	Bio-Rad Labs, USA (ReadySub-Cell GT Cells)
Fluorescence Microscope	Leica Microsystems, USA (MZ16FA)
Freezer 1 -20 °C	Arçelik, Turkey
Freezer 2 -80 °C	Thermo Electron Corp., USA (Farma 723)
Gel Documentation	Bio-Rad Labs, USA (GelDoc XR)
Glass Bottles	Isolab, Germany
Incubator 1	Weiss Gallenkamp, UK
Incubator 2	Nuve, Turkey
Incubating Shaker	Thermo Electron Corp., USA
Micropipetters	Eppendorf, Germany (Research)
Microwave Oven	Vestel, Turkey
Microinjector	Eppendorf, Germany (FemtoJet)
Luminometer	Fluroskan Ascent Fl (Thermo Scientific)
Refrigerator	Arçelik, Turkey
Softwares	Vector NTI (Invitrogen, USA)
Thermal Cyclers	Bio-Rad Labs, USA (C1000)
Vortex	Scientific Industries, USA

APPENDIX B: SUPPLIES

Table 6.2. List of Supplies.

1 kb DNA Ladder	New England Biolabs, U.S.A. (N3232)
100 bp DNA Ladder	New England Biolabs, U.S.A. (N3231)
5X GoTaq Flexi Buffer	Clontech, U.S.A. (639201)
Advantage 2 Polymerase Mix	Promega, U.S.A. (M890A)
BamHI	New England Biolabs, U.S.A. (R0136 L)
Bovine Serum Albumin	New England Biolabs, U.S.A. (B9001)
DMEM / F12 medium	Gibco, U.S.A. (11880).
EcoRI	New England Biolabs, U.S.A. (R0101 M)
EcoRV	New England Biolabs, U.S.A. (R0195 L)
Ethanol Absolute	Sigma-Aldrich, U.S.A. (34870)
Ethidium Bromide	Sigma Life Sciences, U.S.A. (E1510-1 ml)
EDTA Disodium Salt	Sigma-Aldrich., U.S.A. (E5134 - 1 kg).
Glycerol	Sigma-Aldrich, U.S.A. (G5516-500 ml)
GoTaq Flexi DNA Polymerase	Promega, U.S.A. (M830B)
KpnI	New England Biolabs, U.S.A. (R0558 L)
LB Agar	Sigma Life Sciences, U.S.A. (SL08394)
LB Broth	Sigma-Aldrich, U.S.A. (L7658- 1 kg)
Magnesium Chloride, 25 mM	Promega, U.S.A. (A3511)
Magnesium Sulfate	Sigma-Aldrich, U.S.A. (M7506)
NcoI	New England Biolabs, U.S.A. (R0193 L)
NotI	New England Biolabs, U.S.A. (R0189 L)
pGEM®-T Easy Vector System	Promega, U.S.A. (A1360)

Table 6.2. List of Supplies (cont.).

Potassium Chloride	Sigma-Aldrich, U.S.A. (P9541)
PstI	New England Biolabs, U.S.A. (R0140 L)
SalI	New England Biolabs, U.S.A. (R0138 L)
SeaKem® Agarose	Cambrex, U.S.A. (50004)
Sodium Acetate	Sigma-Aldrich, U.S.A. (S8625)
Sodium Chloride	Sigma-Aldrich, U.S.A. (S7653 - 1 kg)
Sodium Hydroxide	Sigma-Aldrich, U.S.A. (S8045 - 1 kg)
SpeI	New England Biolabs, U.S.A (R0133 L)
SphI	New England Biolabs, U.S.A (R0182 L)
T4 DNA Ligase	New England Biolabs, U.S.A (M0202L)
Trizma® Base	Sigma-Aldrich, U.S.A. (T6066)
XhoI	New England Biolabs, U.S.A. (R0146 L)
X-treme® Transfection Reagent	Roche, Germany (04709691001)

REFERENCES

Ahuja, G., B., Nia, V., Zapilko, V., Shiriagin, D., Kowatschew, Y., Oka, and S., Korsching, 2014, "Kappe Neurons, a Novel Population of Olfactory Sensory Neurons", *Scientific Reports*, Vol 4, p. 4037.

Alioto, S., and J., Ngai, 2005, "The Odorant Receptor Repertoire of Teleost Fish", *BMC Genomics*, Vol. 6, p. 173.

Alioto, S., and J., Ngai, 2006, "The Repertoire of Olfactory C Family G Protein-Coupled Receptors in Zebrafish: Candidate Chemosensory Receptors for Amino Acids", *BMC Genomics*, Vol. 7, p. 309.

Aoki, M., H., Takeuchi, A., Nakashima, H., Nishizumi, and H., Sakano, 2013, "Possible Roles of Robo1+ Ensheathing Cells in Guiding Dorsal-Zone Olfactory Sensory Neurons in Mouse", *Developmental Neurobiology*, Vol. 73, p. 11.

Argo, S., F., Weth, and S., Korsching, 2003, "Analysis of Penetrance and Expressivity During Ontogenesis Supports a Stochastic Choice of Zebrafish Odorant Receptors from Predetermined Groups of Receptor Genes", *European Journal of Neuroscience*, Vol. 17, pp. 833-843.

Baier, H., S., Rotter, and S., Korsching, 1994, "Connectional Topography in the Zebrafish Olfactory System: Random Positions but Regular Spacing of Sensory Neurons Projecting to an Individual Glomerulus", *Proceedings Of The National Academy Of Sciences Of The United States Of America*, Vol. 91, No. 24, pp. 11646-11650.

Bailey, S., A., Puche, and M., Shipley, 1999, "Development of the Olfactory Bulb: Evidence for Glia-neuron Interactions in Glomerular Formation", *Journal of Comparative Neurology*, Vol. 415, pp. 423–448.

Barnea, G., S., O'Donnell, and R., Axel, 2004, "Odorant Receptors on Axon Termini in the Brain", *Science*, Vol. 304, p. 1468.

Belluscio, L., G., Koentges, R., Axel, and C., Dulac, 1999, "A Map of Pheromone Receptor Activation in the Mammalian Brain", *Cell*, Vol. 97, No. 2, pp. 209-220.

Bert, G., R., Grepin, and M., Vadas, 2006, "Assessing IRES Activity in the HIF-1a and Other Cellular 5' UTRs", *RNA*, Vol. 12, pp. 1074-1083.

Bozza, T., P., Feinstein, C., Zheng, and P., Mombaerts, 2002, "Odorant Receptor Expression Defines Functional Units in the Mouse Olfactory System", *Journal of Neuroscience*, Vol. 22, pp. 3033–3043.

Bozza, T., A., Vassalli, S., Fuss, J., Zhang, B., Weiland, R., Pacifico, P., Feinstein, and P., Mombaerts, 2009, "Mapping of Class I and Class II Odorant Receptors to Glomerular Domains by Two Distinct Types of Olfactory Sensory Neurons in the Mouse", *Neuron*, Vol. 61, No. 2, pp. 220-233.

Braubach, R., A., Fine, and R., Croll, 2012, "Distribution and Functional Organization of Glomeruli in the Olfactory Bulbs of Zebrafish", *Zebrafish*, Vol. 2339, pp. 2317-2339.

Buck, L., and R., Axel, 1991, "A Novel Multigene Family may Encode Odorant Receptors: A Molecular Basis for Odor Recognition", *Cell*, Vol. 65, No. 1, pp. 175-87.

Buck, L., 2000, "The Molecular Architecture of Odor and Pheromone Sensing in Mammals", *Cell*, Vol. 100, No. 6, pp. 611-618.

Buck, L., 2005, "Unraveling the Sense of Smell", *Angewandte Chemie International Edition*, Vol. 44, No. 38, pp. 6128-6140.

Catania, S., A., Germana, R., Laura, and J., Vega, 2003, "The Crypt Neurons in the Olfactory Epithelium of the Adult Zebrafish Express TrkA-like Immunoreactivity", *Neuroscience Letters*, Vol. 350, pp. 5–8.

Chess, A., I., Simon, H., Cedar, and R., Axel, 1994, "Allelic Inactivation Regulates Olfactory Receptor Gene Expression", *Cell*, Vol. 78, pp. 823-834.

Cho, H., M., Lépine, W., Andrews, J., Parnavelas, and J., Cloutier, 2007, "Requirement for Slit- 1 and Robo-2 in Zonal Segregation of Olfactory Sensory Neuron Axons in the Main Olfactory Bulb", *Journal of Neuroscience*, Vol. 27, No. 34, pp. 9094-9104.

Coldwell, M., M., deSchoolmeester, G., Fraser, and A., Willis, 2001, "The p36 Isoform of BAG-1 is Translated by Internal Ribosome Entry Following Heat Shock", *Oncogene*, Vol. 20, p. 30.

Cutforth, T., L., Moring, M., Mendelsohn, and N., Shah, 2003, "Axonal Ephrin-As and Odorant Receptors: Coordinate Determination of the Olfactory Sensory Map", *Cell*, Vol. 114, pp. 311–322.

Dalton, R., D., Lyons, and S., Lomvardas, 2013, "Co-opting the Unfolded Protein Response to Elicit Olfactory Receptor Feedback", *Cell*, Vol. 155, No. 2, pp. 321-332.

Dulac, C., 1997, "Molecular Biology of Pheromone Perception in Mammals", *Cell and Developmental Biology*, Vol. 8, pp. 197-205.

Dulac, C., and R., Axel, 1995, "A Novel Family of Genes Encoding Putative Pheromone Receptors in Mammals", *Cell*, Vol. 83, pp. 195-206.

Dynes, J. L., and J., Ngai, 1998, "Pathfinding of Olfactory Neuron Axons to Stereotyped Glomerular Targets Revealed by Dynamic Imaging in Living Zebrafish Embryos", *Neuron*, Vol. 20, No. 6, pp. 1081-1091.

Eggan, K., K., Baldwin, M., Tackett, J., Osborne, J., Gogos, A., Chess, R., Axel, and R., Jaenisch, 2004, "Mice Cloned from Olfactory Sensory Neurons", *Nature*, Vol. 428, pp. 44–49.

Emes, R., S., Beatson, P., Ponting, and L., Goodstadt, 2004, "Evolution and Comparative Genomics of Odorant- and Pheromone-associated Genes in Rodents", *Genome Research*, Vol. 14, pp. 591–602.

Fahrenkrug, C., K., Clark, M., Dahlquist, and P., Hackett, 1999, "Dicistronic Gene Expression in Developing Zebrafish", *Marine Biotechnology*, Vol. 1, pp. 552- 561.

Feinstein, P., T., Bozza, I., Rodriguez, A., Vassalli and P., Mombaerts, 2004, "Axon Guidance to Glomeruli by Odorant Receptors and the ß2 Adrenergic Receptor", *Cell*, Vol. 117, pp. 833–846.

Feinstein, P., and P., Mombaerts, 2004, "A Contextual Model for Axonal Sorting into Glomeruli in the Mouse Olfactory System", *Cell*, Vol. 117, pp. 817–831.

Ferreira, T., S., Wilson, Y., Choi, and J., Ngai, 2014, "Silencing of Odorant Receptor Genes by G Protein βγ Signaling Ensures the Expression of One Odorant Receptor per Olfactory Sensory Neuron", *Neuron*, Vol. 81, No. 4, pp. 847-859.

Firestein, S., 2001, "How the Olfactory System Makes Sense of Scents", *Nature*, Vol. 413, No. 6852, pp. 211-218.

Freitag, J., J., Krieger, J., Strotmann, and H., Breer, 1995, "Two Classes of Olfactory Receptors in Xenopus Laevis", *Neuron*, Vol. 15, pp. 1383–1392.

Freitag, J., G., Ludwig, I., Andreini, P., Rossler, and H., Breer, 1998, "Olfactory Receptors in Aquatic and Terrestrial Vertebrates", *Journal of Comparative Physiology*, Vol. 183, pp. 635–650.

Fuss, S., M., Omura, and P., Mombaerts, 2007, "Local and Cis Effects of the H Element on Expression of Odorant Receptor Genes in Mouse", *Cell*, Vol. 130, No. 2, pp. 373-438.

Germana, A., G., Montalbano, R., Laura, and J., Vega, 2004, “S100 Protein-like Immunoreactivity in the Crypt Olfactory Neurons of the Adult Zebrafish”, *Neuroscience Letters*, Vol. 371, pp. 196–198.

Ghattas, R., J., Sanes, and J., Majors, 1991, “The Encephalomyocarditis Virus Internal Ribosome Entry Site Allows Efficient Coexpression of Two Genes from a Recombinant Provirus in Cultured Cells and in Embryos", *Molecular and Cellular Biology*, Vol. 11, No. 12, pp. 5848-5859.

Glusman, G., I., Yanai, I., Rubin, and D., Lancet, 2001, “The Complete Human Olfactory Subgenome”, *Genome Research*, Vol. 11, pp. 685–702.

Grus W., P., Shi, P., Zhang, and J., Zhang, 2005, “Dramatic Variation of the Vomeronasal Pheromone Receptor Gene Repertoire among Five Orders of Placental and Marsupial Mammals”, *Proceedings of the National Academy of Science*, Vol. 102, pp. 5767–5772.

Grus, W., P., Shi, and J., Zhang, 2007, “Largest Vertebrate Vomeronasal Type 1 Receptor Gene Repertoire in the Semiaquatic Platypus”, *Molecular Biology and Evolution*, Vol. 24, pp. 2153–2157.

Hamdani, H., G., Alexander, and B., Doving, 2001, “Projection of Sensory Neurons with Microvilli to the Lateral Olfactory Tract Indicates Their Participation in Feeding Behaviour in Crucian Carp”, *Chemical Senses*, Vol. 26, pp. 1139–1144.

Hamdani, H., and B., Døving, 2007, “The Functional Organization of the Fish Olfactory System”, *Progress In Neurobiology*, Vol. 82, pp. 80-86.

Hansen, A., S., Rolen, K., Anderson, Y., Morita, J., Caprio, and T., Finger, 2003, “Correlation between Olfactory Receptor Cell Type and Function in the Channel Catfish”, *Journal of Neuroscience*, Vol. 23, No. 28, pp. 9328-9339.

Hansen, A., and E., Zeiske, 1998, “The Peripheral Olfactory Organ of the Zebrafish, Danio Rerio: An Ultrastructural Study”, *Chemical Senses*, Vol. 23, No. 1, pp. 39-48.

Hashiguchi, Y., and M., Nishida, 2006, “Evolution and Origin of Vomeronasal-type Odorant Receptor Gene Repertoire in Fishes”, *BMC Evolution and Biology*, Vol. 6, p. 76.

Hashiguchi, Y., and M., Nishida, 2007, “Evolution of Trace Amine Associated Receptor (TAAR) Gene Family in Vertebrates: Lineage-Specific Expansions and Degradations of a Second Class of Vertebrate Chemosensory Receptors Expressed in the Olfactory Epithelium”, *Molecular Biology and Evolution*, Vol. 24, No. 9, pp. 2099-2107.

Hellen, C., and P., Sarnow, 2001, “Internal Ribosome Entry Sites in Eukaryotic mRNA Molecules”, *Genes and Development*, Vol. 15, No. 13, pp. 1593-1612.

Hirota, J., and P., Mombaerts, 2004, “The LIM-Homeodomain Protein Lhx2 is Required for Complete Development of Mouse Olfactory Sensory Neurons”, *Proceedings of the National Academy of Sciences*, Vol. 101, No. 23, pp. 8751-8755.

Hirota, J., M., Omura, and P., Mombaerts, 2007, “Differential Impact of Lhx2 Deficiency on Expression of Class I and Class II Odorant Receptor Genes in Mouse”, *Molecular and Cellular Neurosciences*, Vol. 34, No. 4, pp. 679-688.

Holcik, M., and N., Sonenberg, 2005, “Translational Control in Stress and Apoptosis", *Nature Reviews Molecular Cell Biology*, Vol. 6, No. 4, pp. 318-327.

Hoppe, R., H., Breerand, and J., Strotmann, 2006, “Promoter Motifs of Olfactory Receptor Genes Expressed in Distinct Topographic Patterns”, *Genomics*, Vol. 87, No. 6, pp. 711-723.

Imai, T., M., Suzuki, and H., Sakano, 2006, “Odorant Receptor-Derived Camp Signals Direct Axonal Targeting”, *Science*, Vol. 314, No. 5799, pp. 657-661.

Ishii, T., S., Serizawa, A., Kohda, H., Nakatani, T., Shiroishi, K., Okumura, Y., Iwakura, F., Nagawa, A., Tsuboi and H., Sakano, 2001, "Monoallelic Expresion of the Odorant Receptor Gene and Axonal Projection of Olfactory Sensory Neurons", *Genes to Cells*, Vol. 6, pp. 71-78.

Iwema, C., and J., Schwob, 2003, "Odorant Receptor Expression as a Function of Neuronal Maturity in the Adult Rodent Olfactory System", *Journal of Comparative Neurology*, Vol. 459, No., 3, pp. 209-222.

Jung, D., and F., Alt, 2004, "Unraveling V(D)J Recombination: Insights into Gene Regulation", *Cell*, Vol. 116, No. 2, pp. 299-311.

Kajiya K., K., Inaki M., Tanaka and K., Touhara, 2001, "Molecular Bases of Odor Discrimination: Reconstitution of Olfactory Receptors that Recognize Overlapping Sets of Odorants", *Journal of Neuroscience*, Vol. 21, pp. 6018-6025.

Khan, M., E., Vaes, and P., Mombaerts, 2011, "Regulation of the Probability of Mouse Odorant Receptor Gene Choice", *Cell*, Vol. 147, No. 4, pp. 907-921.

Kim, S., and H., Martinson, 2003, "Poly (A)-dependent Transcription Termination", *Journal of Biological Chemistry*, Vol. 278, No. 4), pp. 41691-41701.

Kobayakawa, K., R., Kobayakawa, H., Matsumoto, K., Mori and H., Sakano, 2007, "Innate versus Learned Odour Processing in the Mouse Olfactory Bulb", *Nature*, Vol. 450, pp. 503–508.

Kolterud, A., M., Alenius, L., Carlsson, and S., Bohm, 2004, "The Lim Homeobox Gene Lhx2 is Required for Olfactory Sensory Neuron Identity", *Development*, Vol. 131, pp. 5319–5326.

Korsching, S., 2009, "The Molecular Evolution of Teleost Olfactory Receptor Gene Families", *Chemosensory Systems in Mammals, Fishes, and Insects*, pp. 221-238.

Kozak, M., 1991, “Structural Features in Eukaryotic mRNAs that Modulate the Initiation of Translation”, *Journal of Biology and Chemistry*, Vol. 266, No. 30, pp. 19867-19870.

Kubick, S., J., Strotmann, I., Andreini, and H., Breer, 1997, “Subfamily of Olfactory Receptors Characterized by Unique Structural Features and Expression Patterns”, *Journal of Neurochemistry*, Vol. 69, No.2, pp. 465-475.

Kwan, M., E., Fujimoto, C., Grabher, B., Mangum, and C., Chien, 2007, “The Tol2kit: A Multisite Gateway-based Construction Kit for Tol2 Transposon Transgenesis Constructs”, *Developmental Dynamics*, Vol. 236, No. 1, pp. 3088-3099.

Lakhina, V., C., Marcaccio, X., Shao, E., Lush, and J. Raper, 2012, “Netrin/DCC Signaling Guides Olfactory Sensory Axons to their Correct Location in the Olfactory Bulb”, *Journal of Neuroscience*, Vol. 13, pp. 4440-4456.

Laska, M., A., Seibt, and A., Weber, 2000, “Microsmatic Primates Revisited: Olfactory Sensitivity in the Squirrel Monkey”, *Chemical Senses,* Vol. 25, pp. 47–53.

Lekven, C., C., Thorpe, J., Waxman, and T., Moon, 2001, “Zebrafish Wnt8 Encodes Two Wnt8 Proteins on a Bicistronic Transcript and is Required for Mesoderm and Neuroectoderm Patterning”, *Developmental Cell,* Vol. 1, No. 1, pp. 103-114.

Lewcock, J. W., and R. R., Reed, 2004, “A Feedback Mechanism Regulates Monoallelic Odorant Receptor Expression”, *Proceedings of the National Academy of Sciences,* Vol. 101, No. 4, pp. 1069-1074.

Li, J., J., Mack, M., Souren, E., Yaksi, S., Higashijima, M., Mione, J., Fetcho, and R. W., Friedrich, 2005, “Early Development of Functional Spatial Maps in the Zebrafish Olfactory Bulb”, *Journal of Neuroscience*, Vol. 25, No. 24, pp. 5784-5795.

Li, J., T., Ishii, P., Feinstein, and P., Mombaerts, 2004, “Odorant Receptor Gene Choice is Reset by Nuclear Transfer from Mouse Olfactory Sensory Neurons”, *Nature*, Vol. 428, No. 425, pp. 393-399.

Liberles, S. D., and L., Buck, 2006, “A Second Class of Chemosensory Receptors in the Olfactory Epithelium”, *Nature*, Vol. 442, No. 7103, pp. 645-650.

Liu A., and X., Zhang, 2003, “Motif-based Construction of a Functional Map for Mammalian Olfactory Receptors”, *Genomics*, Vol. 81, pp. 443-456.

Lomvardas, S., G., Barnea, D., Pisapia, M., Mendelsohn, J., Kirkland, and R., Axel, 2006, “Interchromosomal Interactions and Olfactory Receptor Choice”, *Cell*, Vol. 126, No. 2, pp. 403-413.

Lyons, D., W., Allen, G., Barnea, and S. Lomvardas, 2013, “An Epigenetic Trap Stabilizes Singular Olfactory Receptor Expression”, *Cell*, Vol. 154, pp. 325-336.

Malnic, B., J., Hirono, T., Sato and L., Buck, 1999, “Combinatorial Receptor Codes for Odors”, *Cell*, Vol. 96, No. 5, pp. 713-723.

Malnic, B., D., Gonzalez-Kristeller, and L., Gutiyama, 2010, “7 Odorant Receptors”, *Neurobiology of Olfaction*, Vol. 12, p. 181.

Maresh, A., D., Gil, M., Whitman, and C., Greer, 2008, “Principles of Glomerular Organization in the Human Olfactory Bulb-implications for Odor Processing”, *Plos One*, Vol. 3, e2640.

Matsunami, H., and L., Buck, 1997, “A Multigene Family Encoding a Diverse Array of Putative Pheromone Receptors in Mammals”, *Cell*, Vol. 90, pp. 775–784.

McIntyre, J. C., S. C., Bose, A., Stromberg, and T. S., McClintock, 2008, “Emx2 Stimulates Odorant Receptor Gene Expression”, *Chemical Senses*, Vol. 33, No. 9, pp. 825-837.

Michaloski, J. S., P. A., Galante, and B., Malnic, 2006, “Identification of Potential Regulatory Motifs in Odorant Receptor Genes by Analysis of Promoter Sequences”, *Genome Research*, Vol. 16, No. 9, pp. 1091-1098.

Miyamichi, K., S., Serizawa, H., Kimura, and H., Sakano, 2005, "Continuous and Overlapping Expression Domains of Odorant Receptor Genes in the Olfactory Epithelium Determine the Dorsal/Ventral Positioning of Glomeruli in The Olfactory Bulb", *Journal of Neuroscience*, Vol. 25, No. 14, pp. 3586-3592.

Miyasaka, N., H., Knaut, and Y., Yoshihara, 2007, "Cxcl12/Cxcr4 Chemokine Signaling is Required for Placode Assembly and Sensory Axon Pathfinding in the Zebrafish Olfactory System", *Development*, Vol. 134, pp. 2459–2468.

Miyasaka, N., Y., Sato, H., Okamoto and Y., Yoshihara, 2005, "Robo2 is Required for Establishment of a Precise Glomerular Map in the Zebrafish Olfactory System", *Development*, Vol. 132, pp. 1283–1293.

Mokrejs, M., V., Vopalensky, O., Kolenaty, T., Masek, Z., Feketova, P., Sekyrova, and M., Pospisek, 2006, "IRESite: the Database of Experimentally Verified IRES", *Nucleic Acids Research*, Vol. 34, pp. 125-130.

Mombaerts, P., 2006, "Axonal Wiring in the Mouse Olfactory System", *Annual Reviews Cell and Developmental Biology*, Vol. 22, pp. 713-737.

Mombaerts, P., F., Wang, C., Dulac, S., Chao, A., Nemes, M., Mendelsohn, J., Edmondson, and R., Axel, 1996, "Visualizing an Olfactory Sensory Map", *Cell*, Vol. 87, pp. 675–686.

Nagawa, F., S., Yoshihara, A., Tsuboi, S., Serizawa and H., Sakano, 2002, "Genomic Analysis of the Murine Odorant Receptor MOR28 Cluster: a Possible Role of Gene Conversion in Maintaining the Olfactory Map", *Gene*, Vol. 292, pp. 73–80.

Nakashima, A., H., Takeuchi, T., Imai, and H., Sakano, 2013, "Agonist-independent GPCR Activity Regulates Anterior-posterior Targeting of Olfactory Sensory Neurons", *Cell*, Vol. 154, pp. 1314–1325.

Ngai, J., M., Dowling, L., Buck, R., Axel and A., Chess, 1993, "The Family of Genes Encoding Odorant Receptors in the Channel Catfish", *Cell*, Vol. 72, No. 5, pp. 657-666.

Nguyen, M. Q., Z., Zhou, C. A., Marks, N. J. P., Ryba, and L., Belluscio, 2007, "Prominent Roles for Odorant Receptor Coding Sequences in Allelic Exclusion", *Cell*, Vol. 131, No. 5, pp. 1009-1017.

Niimura, Y., and M., Nei, 2005, "Evolutionary Dynamics of Olfactory Receptor Genes in Fishes and Tetrapods", *Proceedings of the National Academy of Sciences of the United States of America*, Vol. 102, No. 17, pp. 6039-6044.

Niimura Y., and M., Nei, 2006, "Evolutionary Dynamics of Olfactory and Other Chemosensory Receptor Genes in Vertebrates", *Journal of Human Genetics*, Vol. 51, pp. 505–517.

Niimura, Y., and M., Nei, 2007, "Extensive Gains and Losses of Olfactory Receptor Genes in Mammalian Evolution", *Plos One*, Vol. 8, e708.

Nishizumi, H., K., Kumasaka, , A., Nakashima, and H., Sakano, 2007, "Deletion of the Core-H Region in Mice Abolishes the Expression of Three Proximal Odorant Receptor Genes in Cis", *Proceedings of the National Academy of Sciences of the United States of America*, Vol. 104, No. 50, pp. 20067-20072.

Norlin, E. M., and A., Berghard, 2001a, "Spatially Restricted Expression of Regulators of G-Protein Signaling in Primary Olfactory Neurons", *Molecular and Cellular Neurosciences*, Vol. 17, No. 5, pp. 872-882.

Norlin, E. M., M., Alenius, F., Gussing, M., Hägglund, V., Vedin, and S., Bohm, 2001b, "Evidence for Gradients of Gene Expression Correlating with Zonal Topography of the Olfactory Sensory Map", *Molecular and Cellular Neurosciences*, Vol. 18, No. 3, pp. 283-295.

Oka, Y., K., Kobayakawa, H., Nishizumi, K., Miyamichi, S., Hirose, A., Tsuboi, and H., Sakano, 2003, "O-MACS, a Novel Member of the Medium-Chain Acyl-Coa Synthetase Family, Specifically Expressed in the Olfactory Epithelium in a Zone-Specific Manner", *European Journal of Biochemistry*, Vol. 270, No. 9, pp. 1995-2004.

Oka, Y., L. R., Saraiva, and S., Korsching, 2011, "Crypt Neurons Express a Single V1R-Related Ora Gene", *Chemical Senses*, Vol.37, No. 3, pp. 1-9.

Olender, T., and T., Fuchs, 2004, "The Canine Olfactory Subgenome", *Genomics*, Vol. 83, No. 3, pp. 361-372.

Omura, M., X., Grosmaitre, M., Ma, and P., Mombaerts, 2013, "The β2-adrenergic receptor as a Surrogate Odorant Receptor in Mouse Olfactory Sensory Neurons", *Molecular and Cellular Neurosciences*, Vol. 58, pp. 1–10.

Plessy, C., G., Pascarella, N., Bertin, S., Gustincich, and P., Carninci, 2012, "Promoter Architecture of Mouse Olfactory Receptor Genes", *Genome Research*, Vol. 22, No. 3, pp. 486-497.

Potter, S., C., Zheng, S., Koos, P., Feinstein, and P., Mombaerts, 2001, "Structure and Emergence of Specific Olfactory Glomeruli in the Mouse", *Journal of Neuroscience*, Vol. 21, pp. 9713–9723.

Provost, E., J., Rhee, and S., Leach, 2007, "Viral 2A Peptides Allow Expression of Multiple Proteins from a Single ORF in Transgenic Zebrafish Embryos", *Genesis*, Vol. 45, No. 10, pp. 625-629.

Qasba, P., and R. R., Reed, 1998, "Tissue and Zonal-Specific Expression of an Olfactory Receptor Transgene", *Journal of Neuroscience*, Vol. 18, No. 1, pp. 227-236.

Rawson, N. E., J., Eberwine, R., Dotson, J., Jackson, P., Ulrich, and D., Restrepo, 2000, "Expression of mRNAs Encoding for two Different Olfactory Receptors in a Subset

of Olfactory Receptor Neurons", *Journal of Neurochemistry*, Vol. 75, No. 1, pp. 185-195.

Ressler, K. J., S. L., Sullivan, and L., Buck, 1993, "A Zonal Organization of Odorant Receptor Gene Expression in the Olfactory Epithelium", *Cell*, Vol. 73, No. 3, pp. 597-609.

Rothman, A., P., Feinstein, J., Hirota, and P., Mombaerts, 2005, "The Promoter of the Mouse Odorant Receptor Gene M71," *Molecular and Cellular Neurosciences*, Vol. 28, No. 3, pp. 535-546.

Royal S., and J., Key, 1999, "Development of P2 Olfactory Glomeruli in P2-IRES-tau-LacZ Transgenic Mice", *Journal of Neuroscience*, Vol. 19, pp. 9856-9864.

Saraiva, L. R., and S., Korsching, 2007, "A Novel Olfactory Receptor Gene Family in Teleost Fish", *Genome Research*, Vol. 17, No. 10, pp. 1448-1457.

Sato, Y., N., Miyasaka, and Y., Yoshihara, 2005, "Mutually Exclusive Glomerular Innervation by Two Distinct Types of Olfactory Sensory Neurons Revealed in Transgenic Zebrafish", *Journal of Neuroscience*, Vol. 25, No. 20, pp. 4889-4897.

Sato, Y., N., Miyasaka, and Y., Yoshihara, 2007, "Hierarchical Regulation of Odorant Receptor Gene Choice and Subsequent Axonal Projection of Olfactory Sensory Neurons in Zebrafish", *Journal of Neuroscience*, Vol. 27, No. 7, pp. 1606-1615.

Serizawa, S., T., Ishii, A., Tsuboi, and F., Nagawa, 2000, "Mutually Exclusive Expression of Odorant Receptor Transgenes", *National Neuroscience*, Vol. 3, pp. 687–693.

Serizawa, S., K., Miyamichi, H., Nakatani, M., Suzuki, M., Saito, Y., Yoshihara, and H., Sakano, 2003, "A Negative Feedback Regulation Ensures the One Receptor – One Olfactory Neuron Rule in Mouse", *Science*, Vol. 302, pp. 2088-2094.

Serizawa, S., K., Miyamichi, H., Takeuchi, Y., Yamagishi, M., Suzuki, and H., Sakano, 2006, "A Neuronal Identity Code for the Odorant Receptor-Specific and Activity-Dependent Axon Sorting", *Cell*, Vol. 127, No. 5, pp. 1057-1069.

Shepherd, G., 2004, "The Human Sense of Smell: Are We Better Than We Think?", *Plos Biology*, Vol. 2, e146.

Shi, P., and J., Zhang, 2007, "Comparative Genomic Analysis Identifies an Evolutionary Shift of Vomeronasal Receptor Gene Repertoires in the Vertebrate Transition from Water to Land", *Genome Research*, Vol. 17, pp. 166-174.

Shi, P., and J., Zhang, 2009, "Extraordinary Diversity of Chemosensory Receptor Gene Repertoires Among Vertebrates", *Chemosensory Systems in Mammals, Fishes, and Insects*, pp. 57-75.

Shykind, M., S., Rohani, S., O'Donnell, and M., Mendelsohn, 2004, "Gene Switching and the Stability of Odorant Receptor Gene Choice", *Cell*, Vol. 117, pp. 801–815.

Song, H. G., Y., Bae, and C., Moon, 2008, "First Contact to Odors: Our Current Knowledge About Odorant Receptor", *Sensors*, Vol. 8, No. 10, pp. 6303-6320.

Spriggs, K. A., M., Bushell, and A. E., Willis, 2010, "Translational Regulation of Gene Expression During Conditions of Cell Stress", *Molecular Cell*, Vol. 40, No. 2, pp. 228-237.

Strotmann, J., S., Conzelmann, and P., Mombaerts, 2000, "Local Permutations in the Glomerular Array of the Mouse Olfactory Bulb", *Journal of Neuroscience*, Vol. 20, pp. 6927–6938.

Strotmann, J., I., Wanner, T., Helfrich, A., Beckand, and H., Breer, 1994, "Rostro-Caudal Patterning of Receptor-Expressing Olfactory Neurones in the Rat Nasal Cavity", *Cell and Tissue Research*, Vol. 278, No. 1, pp. 11-20.

Takeuchi, H., K., Inokuchi, M., Aoki, F., Suto, A., Tsuboi, I., Matsuda, M., Suzuki, A., Aiba, S., Serizawa, Y., Yoshihara, H., Fujisawa, and H., Sakano, 2010, "Sequential Arrival and Graded Secretion of Sema3F by Olfactory Neuron Axons Specify Map Topography at the Bulb", *Cell*, Vol. 141, No. 6, pp. 1056-1067.

Thomas, W., and R., Köster, 2013, "Genetic Tools for Multicolor Imaging in Zebrafish Larvae", *Methods*, Vol. 62, pp. 279-291.

Thommesen, G., 1983, "Morphology, Distribution, and Specificity of Olfactory Receptor Cells in Salmonid Fishes", *Acta Physiologica Scandinavica*, Vol. 117, pp. 241-249.

Thompson, S. R., 2012, "So You Want to Know if Your Message Has an IRES?", *Wiley Interdisciplinary Reviews: RNA*, Vol. 3, No. 5, pp. 697-705.

Tian, H., and M., Ma, 2008 "Differential Development of Odorant Receptor Expression Patterns in the Olfactory Epithelium: A Quantitative Analysis in the Mouse Septal Organ", *Developmental Neurobiology*, Vol. 68, No. 4, pp. 476-486.

Tonegawa, S., 1983, "Somatic Generation of Antibody Diversity", *Nature*, Vol. 302, No. 5909, pp. 557-640.

Touhara, K., S., Sengoku, and T., Haga, 2000, "Functional Identification and Reconstitution of an Odorant Receptor in Single Olfactory Neurons", *Proceedings of the National Academy of Science*, Vol. 96, pp. 4040–4045.

Treloar, H., P., Feinstein, P., Mombaerts, and C. Greer, 2002, "Specificity of Glomerular Targeting by Olfactory Sensory Axons", *Journal of Neuroscience*, Vol. 22, pp. 2469–2477.

Trinklein, T., S., Aldred, S., Hartman, and R., Myers, 2004, "An Abundance of Bidirectional Promoters in the Human Genome", *Genome Research*, Vol. 14, No. 1, pp. 62-66.

Tsuboi, A., S., Yoshihara, N., Yamazaki, and H., Sakano, 1999, "Olfactory Neurons Expressing Closely Linked and Homologous Odorant Receptor Genes Tend to Project their Axons to Neighboring Glomeruli on the Olfactory Bulb", *Journal of Neuroscience*, Vol. 19, No. 19, pp. 8409-8418.

Ul-Hussain, M., G., Zoidl, J., Klooster, M., Kamermans, and R., Dermietzel, 2002 "Ires Mediated Translation of the Carboxy-Terminal Domain of the Horizontal Cell Specific Connexin Cx55.5 in Vivo and in Vitro", *BMC Molecular Biology*, Vol. 9, p. 52.

Vassalli, A., A., Rothman, P., Feinstein and P., Mombaerts, 2002, "Minigenes Impart Odorant Receptor-specific Axon Guidance in the Olfactory Bulb", *Neuron*, Vol. 35, pp. 681–696.

Vassalli, A., P., Feinstein, and P., Mombaerts, 2011, "Homeodomain Binding Motifs Modulate the Probability of Odorant Receptor Gene Choice in Transgenic Mice", *Molecular and Cellular Neurosciences*, Vol. 46, No. 2, pp. 381-396.

Vassar, R., S., Chao, R., Sitcheran, L., Vosshall, and R., Axel, 1994, "Topographic Organization of Sensory Projections to the Olfactory Bulb", *Cell*, Vol. 79, No. 6, pp. 981-991.

Verbeurgt, C., F., Wilkin, and P., Chatelain, 2014, "Profiling of Olfactory Receptor Gene Expression in Whole Human Olfactory Mucosa", *Plos One*, Vol. 9, No. 5, e96333.

Vopalensky, V., T., Masek, and M., Pospisek, 2008, "Firefly Luciferase Gene Contains a Cryptic Promoter", *RNA*, Vol. 14, No. 9, pp. 1720-1729.

Wagner, S., A., Gresser, T., Torello, and C., Dulac, 2006, "A Multireceptor Genetic Approach Uncovers an Ordered Integration of VNO Sensory Inputs in the Accessory Olfactory Bulb", *Neuron*, Vol. 79, pp. 697-709.

Wang, F., A., Nemes, M., Mendelsohn, and R., Axel, 1998, “Odorant Receptors Govern the Formation of a Precise Topographic Map”, *Cell*, Vol. 93, pp. 47–60.

Weber, M., U., Pehl, and J., Strotmann, 2002, “Olfactory Receptor Expressed in Ganglia of the Autonomic Nervous System”, *Journal of Neuroscience Research*, Vol. 68, pp. 176–184.

Weth, F., W., Nadler, and S., Korsching, 1996, “Nested Expression Domains for Odorant Receptors in Zebrafish Olfactory Epithelium”, *Proceedings of the National Academy of Sciences of the United States of America*, Vol. 93, No. 23, pp. 13321-13326.

Yamamoto, M., and K., Ueda, 1978, “Comparative Morphology of Fish Olfactory Epithelium”, *Journal of the Faculty of Science*, Vol. 44, pp. 1201-1206.

Yanicostas, C., E., Herbomel, A., Dipietromaria, and N., Soussi-Yanicostas, 2009, “Anosmin-1a is Required for Fasciculation and Terminal Targeting of Olfactory Sensory Neuron Axons in the Zebrafish Olfactory System”, *Molecular and Cellular Endocrinology*, Vol. 312, No. 1, pp. 53-60.

Yoshihara, Y., M., Kawasaki, A., Tamada, H., Fujita, H., Hayashi, H., Kagamiyama, and K., Mori, 1997, “OCAM: A New Member of the Neural Cell Adhesion Molecule Family Related to Zone-to-Zone Projection of Olfactory and Vomeronasal Axons”, *Journal of Neuroscience*, Vol. 17, No. 15, pp. 5830-5842.

Yoshihara, Y., 2009, “Molecular Genetic Dissection of the Zebrafish Olfactory System”, *Chemosensory Systems in Mammals, Fishes, and Insects*, Vol. 1, pp. 1– 24.

Young, J., and B., Trask, 2007, “V2R Gene Families Degenerated in Primates, Dog and Cow, but Expanded in Opossum”, *Trends Genetics*, Vol. 23, pp. 212–215.

Youngentob, S. L., J. E., Schwob, P. R., Sheeheand, and L. M., Youngentob, 1997, “Odorant Threshold Following Methyl Bromide-Induced Lesions of the Olfactory Epithelium”, *Physiology and Behavior*, Vol. 62, No. 6, pp. 1241-1252.

Zhang, X., and S., Firestein, 2002, "The Olfactory Receptor Gene Superfamily of the Mouse", *Nature Neuroscience*, Vol. 5, No. 2, pp. 124-133.

Zhang, X., 2007, "Comparative Genomics of Odorant and Pheromone Receptor Genes in Rodents", *Genomics*, Vol. 89, pp. 441-450.

Zhang, X., and S., Firestein, 2009, "Genomics of Olfactory Receptors", *Chemosensory Systems in Mammals, Fishes, and Insects*, Vol. 1, pp. 239-255.

Zhao, H., L., Ivic, and S., Firestein, 1998, "Functional Expression of a Mammalian Odorant Receptor", *Science*, Vol. 279, No. 5348, pp. 237-242.

Zheng, C., P., Feinstein, T., Bozza, and P., Mombaerts, 2000, "Peripheral Olfactory Projections are Differentially Affected in Mice Deficient in a Cyclic Nucleotide-gated Channel Subunit", *Neuron*, Vol. 26, pp. 81–91.

Zou, Z., L., Horowitz, P., Montmayeur, and L., Buck, 2001, "Genetic Tracing Reveals a Stereotyped Sensory Map in the Olfactory Cortex", *Nature*, Vol. 414, pp. 173–179.